CHAPTER ONE

INTRODUCTION

CHAPTER TWO

MATERIALS & METHODS

CHAPTER THREE

RESULTS & DISCUSSION

CHAPTER FOUR

CONCLUTION

CHAPTER FIVE

REFERENCES

1.1. Water Pollution:

Pollution is the process of making land, water, air and other parts of environment unsafe to use. Less than 3% of the water on Earth is fresh water. 1% of this is ready for human and wildlife use. The other 2% is frozen into polar ice sheets and glaciers. The remaining 97% of Earth's water, including that in the Earth's oceans is too salty to drink so it is not suitable for drinking [1]. The problems of removing pollutants from wastewater are increasing with rapid industrialization so the effect of these pollutants on marine life and on public health has invited numerous research activities. Heavy metals, dyes, oil and other salts, which are toxic to many living life and organisms, are found in the wastewater streams of many industrial processes, such as dyeing, printing, mining and metallurgical engineering, electroplating processes, etc. [2,3]. Therefore, their removal from wastewater is urgent need and this is done by application of traditional physicochemical, chemical and biological principles that divided to coagulation and flocculation, adsorption, biosorption, electrochemical techniques, etc. [4]. Among all these techniques, adsorption is the most efficient method because of its simplicity, high efficiency, easy recovery and reusability of the adsorbent [5].

1.2. Dyes:

A lot of manufacturing industries such as textile, paper and plastics industries using dyes to coloring their products and also consume great volumes of process water. Due to this, it generates a considerable amount of colored wastewater and increases the fears about toxic effect of water containing these dissolved pollutants [6]. The dying industry effluents contain high value of Biological Oxygen Demand (BOD) and Carbon Oxygen Demand (COD) and other toxic materials [7]. It was found that dyes may leads troubles in water in several ways: (i) Dyes have severe and chronic

effects on organisms depending on the dye concentration and duration of exposure to the dyes. (ii) Dyes are very visible and simple secretion effluents may cause discoloration is abnormal to the water (iii) Dyes ability to absorb/reflect of the sunlight inside the water may cause negative effects on the growth and biological activity of bacteria (iv) Dyes have synthetic origin and complex aromatic molecular structures which make them more stable and more difficult to biodegradation and photodegradation (v) The presence of dyes in water causing physical and chemical changes, consume dissolved oxygen from the stream and leads to destruction of aquatic life [8,9].

1.3. Classification of Dyes:

dyes that used in the textile industries are classified into three classes; anionic which include direct, acid and reactive dyes, cationic which include all basic dyes and non-ionic which include dispersed dyes [10].

1.3.1. Classification of dyes depending on the chemical structure:

1.3.1.1. Azo Chromophore:

Azo dyes (figure (1.1)) synthesis involves two steps; first, diazotization process which is the conversion of an aromatic amine to a diazo compound. Second, diazo coupling process which is the reaction of the diazo compound with a phenol, naphthol, aromatic amine, or a compound that has an active methylene group, to produce the corresponding azo dye [11].

Figure (1.1): Azo group.

1.3.1.2. Anthraquinone Chromophore:

Less commonly used in the textile, less variety of colors and expensive compared with azo dyes. This type of dyes have the groups =C=O and =C-C=, forming an anthraquinone complex [12] as shown in figure (1.2).

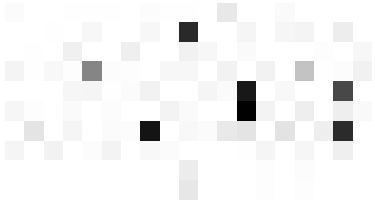

Figure (1.2): Anthraquinone group.

1.3.1.3. Indigoid Chromophore:

Indigoid dyes (figure (1.3)) were produced by processing organic precursors from plant or animal sources which are exposed to reaction conditions to yield the final indigoid dye which is extensively used to color denim [13].

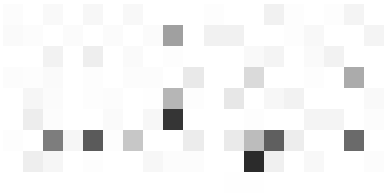

Figure (1.3): Indigo.

1.3.1.4. Polymethine and Related Chromophores:

Polymethine dyes are bode well compounds for nonlinear optical applications, such as optical limiting because of a strong and broad excited-state absorption in the visible region [14]. Within this class of dyes, a number of arylcarbenium dyes are used in the cationic, neutral and anionic dyes [15]. Figure (1.4) shows a schematic representation of the triaryl carbenium dye (Malachite green).

Figure (1.4): Malachite green, a triaryl carbenium dye.

1.3.1.5. Phthalocyanine Chromophore:

Phthalocyanines figure (1.5) are an exciting category of aromatic macrocycles with distinctive physical and chemical properties which make them appropriate for different advanced technologies like optical limiting, photodynamic therapy, organic field effect transistors and organic photovoltaic devices [16].

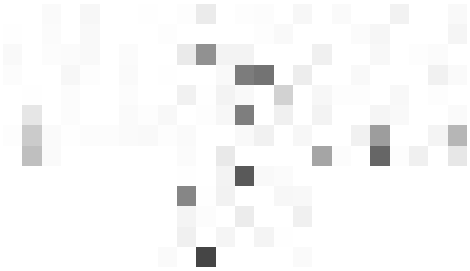

Figure (1.5): Phthalocyanine.

1.3.1.6. Sulphur Compounds and Sulphur Containing Chromophores:

Sulphur compounds formed when sulphur is heated together with aromatic compounds. Sulphur dyes are polymers with heterocyclic rings and thiophenolic sulphur [15]. Figure (1.6) represented a presumed form of sulphur dye.

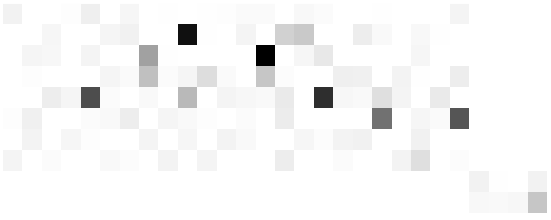

Figure (1.6): The presumed form of Sulphur dye.

1.3.1.7. Metal Complexes and Chromophores:

Metal complex dyes consist of an important class of chromophores and it been widely used in many applications such as textile dyeing and coloring polyamide fibers [17]. The metals that used in metal complex dyes are chromium, copper, iron, cobalt and nickel. The hydroxyl (-OH), carboxy (-CO2) and amino groups (-NH-) are the most important groups that used in complex formation with the metal ion [15].

1.3.2. Classification of dyes depending on dyes applications [18,19,20]:

Table (1.1): Different applications of dyes.

Dyes	Applications
Acid Dye	Water soluble anionic dyes, applied to fibers like silk, wool, nylon and modified acrylic fibers.
Basic Dye	Water soluble cationic dyes, applied to wool, silk, cotton and modified acrylic fibers.
Direct Dye	Used on cotton, paper, leather, wool, silk and nylon.
Mordant Dye	This improves the stability of the dye on the fiber such as water, light and perspiration fastness.
Vat Dye	These dyes are basically insoluble in water and not able to dyeing fibers directly.
Reactive Dye	Used to dye cellulosic fibers, wool and nylon.
Disperse Dye	Insoluble in water, applied to Polyester, polyamide, acetate, acrylic and plastics.
Azoic Dye	Insoluble azoic dye which is produced directly onto or within the fiber.
Developed Dyes	Applied to fabric and cellulosic fibers.
Solvent dyes	Applied to plastics, gasoline, varnishes lacquers,

	stains, inks, fats, oils and waxes.
Optical/Fluorescent Brighteners	Applied to leather, cotton and sports goods.
Sulphur	Applied to cellulosic fibers, cotton and rayon.
Organic pigments	Applied to cellulosic, blended fabrics, paper and cotton.
Oxidation dyes	Applied to fabric and cellulosic fibers, wool and silk.

1.4. Adsorption:

Adsorption is a surface phenomenon describes the attachment of particles (ions, atoms, and molecules) upon a change in concentration of a given substance at the interface as compared with the neighboring phases and depending on the types of surfaces that are in contact. Adsorption occurs in the following phases; liquid-gas, Liquid-liquid, solid-liquid and solid-gas [21]. Adsorbate is the substance that has been adsorbed on a surface such as dyes and metals, but adsorbent is the surface that adsorbs this substance such as silica gel, sawdust and porous clays [22]. In this process, the molecules or ions are removed from the aqueous solution by adsorption onto solid surfaces which are characterized by active and energy-rich sites that have different energies (the surface is energetically heterogeneous) so the active sites are able to interact with solutes in the adjacent aqueous phase [23]. Adsorption appears on the surface where it causes to reduce the balance of attractive forces and the surface free energy of the heterogeneous system [24]. The adsorption process may include the removal of solute molecules from the bulk solution or solid surface by a process called desorption [25]. The difference between absorption and adsorption phenomenon are that the absorption is the process in which a fluid is dissolved by a liquid or a solid (absorbent) but for

adsorption process the molecules are fixed at the surface [26]. Figure (1.7) illustrates the differences between adsorption and absorption. Decreasing in surface free energy (ΔG) is happening through the adsorption process, and decreasing in entropy (ΔS) at the surface that the adsorption take place because of losing the degree of freedom possessed before adsorption [27].

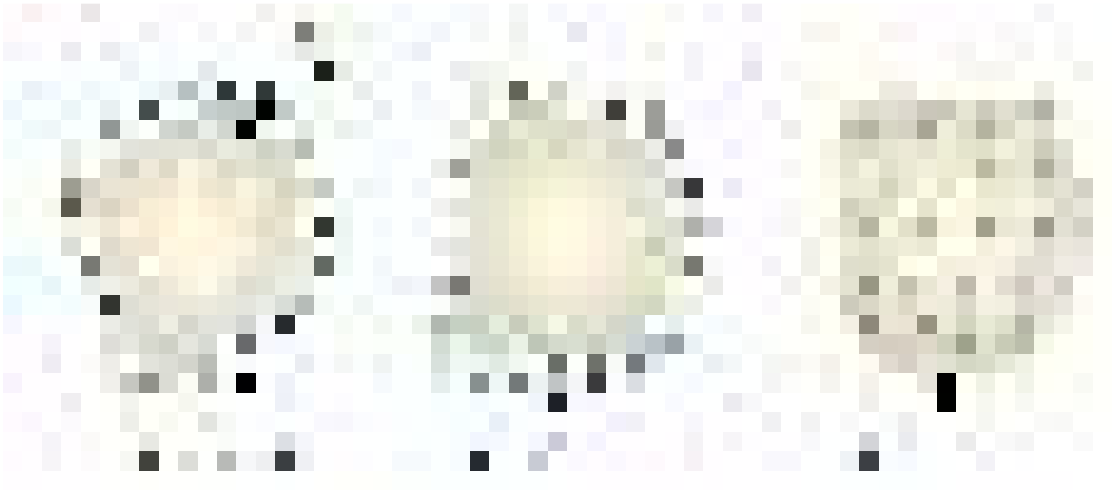

Figure (1.7): Adsorption versus absorption (illustration) [28].

1.4.1. Types of Adsorption:

The attractive forces that occur in the adsorption process of whether in gases, liquids, or vapors may be nonspecific weak force hold adsorbate and adsorbent which is called physical adsorption, or stronger specific forces hold adsorbate and adsorbent caused by the chemical bonds formation which is called chemisorption [24, 28]. The physisorption occur when Van der Waals forces, electrostatic attraction, and solvent ordering and hydrophobic force, are present the process and when the surface can take up more than one layer, it is called multimolecular but chemisorption occur when chemical bonds or electron transfer is present and the surface can take up only one layer of adsorbate, the adsorption is called unimolecular [29, 30]. For example, at liquid nitrogen temperature (77 K) nitrogen gas is adsorbed physically on iron

but at 800 K, the energy very high for physical adsorption bonds so the nitrogen is adsorbed chemically to form iron nitride. Both chemisorption and physisorption may be appears in the same time because a layer of molecules can adsorbed physically on the surface of monolayer of chemical adsorption [31]. Table (1.2) shows the main difference between chemical and physical adsorption.

Table (1.2): Differences between chemical and physical adsorption [7, 18, 28, 31].

Chemical Adsorption	Physical Adsorption
High heat of adsorption (greater than 80 $kJ.mol^{-1}$)	Low heat of adsorption (adsorption less than 40 $kJ.mol^{-1}$)
Highly specific	Non specific
Monolayer only	Monolayer or multilayer because the forces of this type act over greater distance than chemisorption.
May involve dissociation.	No dissociation of adsorbed species.
Possible over a wide range of temperature.	Only significant at relatively low temperature (below the boiling point of the adsorbate).
Activated, may be slow and irreversible which may lead to a chemical reaction.	Rapid, non-activated, reversible (the adsorbed layer can be removed by evacuating or warming to moderate temperature).
Electron transfer leading to bond formation between adsorbant and adsorbate.	No electrons transfer or shared between adsorbate and adsorbent surface although polarization of sorbate may occur.
Highly selective because it occurs	Low selective because it takes place on all

only between certain adsorptive and adsorbent species and if the chemically active surface is cleaned of previously adsorbed molecules.	surfaces if the temperature and pressure conditions are favorable.

1.4.2. Mechanism of Adsorption:

Whatever the nature of the forces, atom which is located inside the solid body is exposed to equal forces in all directions but atom which lies on solid surface is exposed to unbalanced forces so the inward pull being greater than the outward forces. Thus all adsorption phenomena (physical or chemical) are spontaneous and result in a decrease of the free energy of the system which results from the product of the surface tension and the surface area [30].

Adsorption occurs in three steps [32]:

- First, the adsorbate diffuses from the main body of the stream to the external surface of the adsorbent particle.
- Second, the adsorbate moves from the relatively small area of the external surface to the pores within each adsorbent particle. The largest amount of adsorption appears in these pores because of the large surface area.
- Final, the contaminant molecule upholds to the surface in the pores.

1.4.3. Adsorption techniques in dye removal:

There are different systems that bind the adsorbent and wastewater [33]:

1. Batch contact, are highly effective on a smaller scale of operation.

2. Fixed-bed contact, it is effectiveness for a constant dye concentration in contact with the adsorbent at all times.

3. Fluidized bed contact, have a high rate of mass transfer, the operating conditions is highly critical because of the flow rates and loading volumes.

1.4.4. Application of adsorption process:

Adsorption technology finds extensive applications both in research laboratory and in industry. Some of the important applications of adsorption are given in table (1.3).

Table (1.3): The different applications of adsorption technique.

Pollution	Adsorption is used for heavy metal and dyes removal from inorganic effluents fundamental process due to its flexibility in design depending on pH adjustment in a basic solution [34].
Catalysis	Heterogeneous catalysis includes chemical interactions between the surface of a solid and the reacting gas or liquid molecules. The catalytic cycle is generally consisting of adsorption steps, surface reaction processes, and desorption steps [35].
Soil Science	Soil is a heterogeneous mixture of several organic and inorganic compounds that may significantly effects on the herbicide behaviors. The adsorption–desorption behavior of a soil-applied herbicide is one of the most important factors governing the environment impacts such as degradation, transition, and leaching [36].

Chromatographic Analysis	Chromatography is a technique that used to separate and identify the components in the mixture. The basic principle of this technique is that components in the mixture have different tendencies to adsorb onto a surface or dissolve in a solvent [37].
Biological Science	Because of the lower treatment costs with no secondary pollution, biological treatment is one of the most economical methods compared to other physical and chemical processes. It comprises biosorption and biodegradation in either aerobic or anaerobic treatment process with microorganisms: bacteria, fungi, yeasts and algae or enzymes [38].
Medicine and pharmacology	New applications of adsorbed proteins that raising successful development of pharmacology and medicine, determining the feasibility of novel drugs and the control of drug administrations. The great problem of biocompatibility of synthetic materials for medical purposes is regulation of selective adsorption by solid surfaces mixtures of proteins [21].

1.4.5. Industrial application of adsorption:

Adsorption has an important role in the control of environmental pollution and life supporting systems. Such processes are good candidates for separation and purification because of the high reliability, energy efficiency, design flexibility, technological maturity and the ability to regenerating the exhausted adsorbent [39]. The Industrial applications of adsorption are:

1. Separation and purify of liquid and gas mixtures, bulk chemicals, isomers and air.
2. Drying gases and liquids before uploading them in industrial systems.
3. Remove unwanted materials from liquid and gas media.
4. Retrieval of chemicals from industrial and vent gases.
5. Water purification [21].

1.4.6. Factors that effect on the adsorption process:

1.4.6.1. Nature of the adsorbent:

Various types of natural materials or wastes have been used naturally or with some modifications as adsorbents because of their potential adsorption capacities, strong affinity and high loading capacity [34]. The typical properties of adsorbents that make them good are large surface area, high action exchange capacity, chemical and mechanical stability and a layered structure [40]. There are other factors that make adsorbents more effectively such as freely available, inexpensive and non-hazardous in nature, high contents of carbon or oxygen in the adsorbent, high abrasion resistance, high thermal stability and small pore diameters [22].

1.4.6.2. Nature of the adsorbate:

The chemical properties (functional groups) are the main factor that effect on adsorption equilibrium. The adsorption phenomenon of adsorbate

depends on the differences between their chemical properties, structure and interactions with the surface of adsorbent. The type and location of the active groups have a significant impact on the adsorption capacity [41].

1.4.6.3. Effect of solvent:

The distribution of an organic solute between sorbent and solvent phases results from its relative rapprochement for each phase, which is related to the nature of forces between molecules of the solute and solvent and sorbent phases. The type of interaction depends on the nature of the sorbent, hydrophobic, polar and physico-chemical characteristic of the sorbate [42]. The solvent can play an important role in a catalytic system, hydrogenation reactions, polarity and its acid–base properties. The solvent that used in hydrogenation reactions can be of use to different functions such as dissolving reactants and products, controlling the reaction rate and any exothermicity, and determine specific solvent–solute interactions that favor a higher rate and/or selectivity [43].

1.4.6.4. Effect of pH:

The particle size, surface charge, and band edge positions are strongly influenced by pH. The positive surface charge is expected at lower pH and negative surface charge is predicted at higher pH values [44]. The adsorption of such adsorbates is strongly influenced by the proton activity in the aqueous solution which is known as pH and it is influenced by the protonation/deprotonation of the adsorbate and the change of the surface charge of the adsorbent. Under certain conditions, if the surface charge density is low, the influence of the pH value on the adsorbate properties must considered, and the adsorption that depend on pH can be described by a simplified multisolute adsorption approach [23].

1.4.6.5. Effect of temperature:

The endothermic adsorption occur when the adsorption capacity increase with increasing the temperature which leads to increase the kinetic energy for adsorbing molecules on the adsorbent surface [45]. The decrease in the adsorption capacity with the rise in temperature may be attributed to the weakening of the adsorptive forces between the active sites of the adsorbent and adsorbate and the process called exothermic adsorption [46]. Thermodynamic parameters such as changes in free energy (ΔG°), enthalpy (ΔH°) and entropy (ΔS°) have been calculated at all temperatures to explain the characteristics of adsorption process [47].

1.4.6.6. Effect of ionic strength:

The relationship between ionic strength and the adsorption reactions on adsorbent surface is highly dependent upon the component adsorbed [48]. If the adsorbate is in an ionic form, increasing of ionic strength lead to increase adsorbate solubility. However, Low adsorption process might be expected unless, there are similar ions, which cause the common ion effect reducing the adsorbate solubility and increase its adsorption [49, 50].

If the adsorbent is a nonionic form, the ionic strength may lead to the occurrence of salting out process that decreases the solubility and increase the adsorption process [51].

1.4.6.7. Effect of surface area:

The pore size, pore shape and pore surface chemistry of adsorbent play an important role for selective and/or enhanced removal of specific contaminants. For adsorbing contaminants, the adsorption capacity was higher for higher surface area materials which have larger pore size due to larger pore volumes [52].

1.5. Adsorption Isotherm:

The adsorption isotherms are classified according to the adsorption of solutes in dilute solution, which relates their characteristic shapes to parameters of the solvent and any second solute. There are four classes of adsorption isotherm (S, L, H and C) as shown in figure (1.8) are accounted for by differences in relative magnitude of the activation energies adsorption of solutes and solvent except (C) isotherm is explained by penetration of substrata micro pores by solute with or without solvent, whereby new adsorption sites are opened up [53].

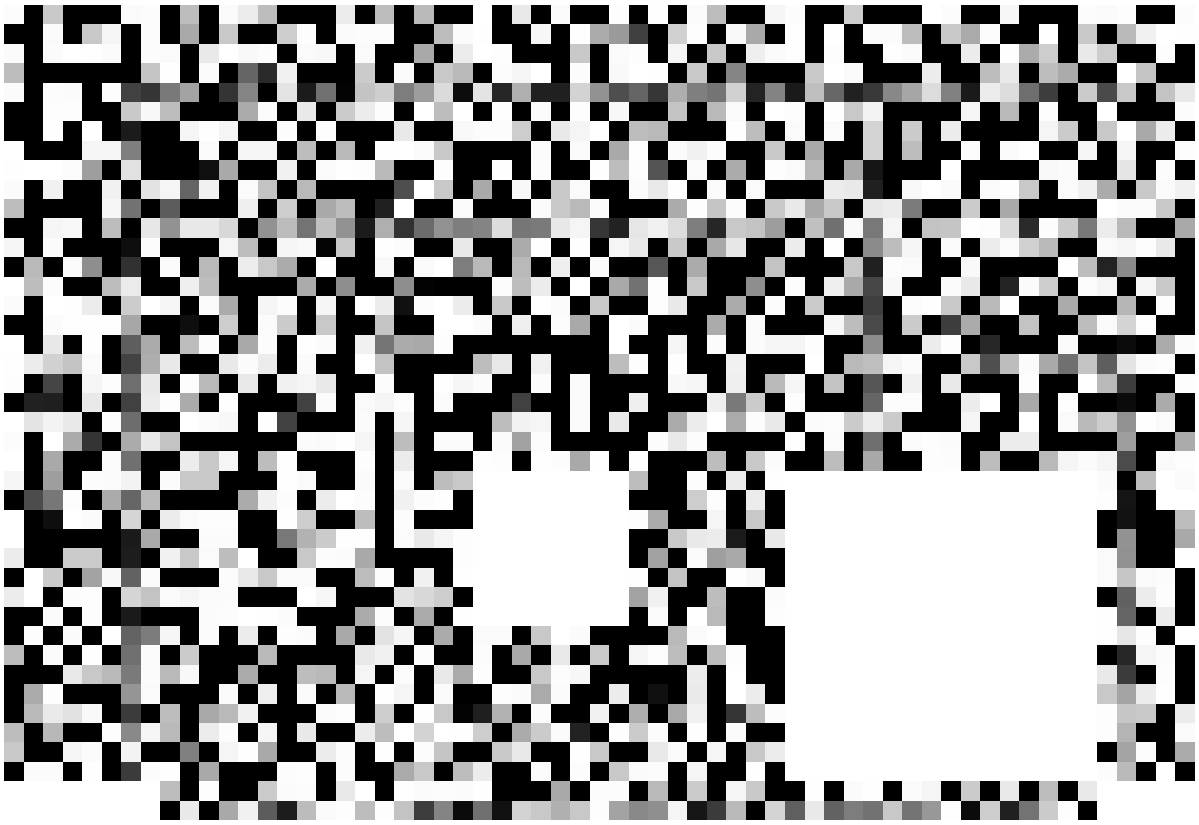

Figure (1.8): Adsorption Isotherm as in Giles Classification.

Different isotherms were observed and classified by Giles and Co-workers according to the nature of slope of the initial portion of the curve, the main classes are [54,55]:

1. **S-Curves:** refers to the vertical orientation of adsorbed molecules at the surface, there is strong intermolecular attraction within the adsorbed layer, and the adsorbate is monofunctional.
2. **L-Curves:** the normal or "Langmuir" isotherms, usually illustrates the molecules adsorbed flat on the surface, or, sometimes, of vertically oriented adsorbed ions with particularly strong intermolecular attraction, a monolayer adsorption is formed.
3. **H-Curves:** (high affinity as in the case of high molecular weight compounds like: proteins and polymer), often given by solutes adsorbed as ionic micelles and high-affinity ions exchanging with low affinity ions, this isotherm can be observed even if the solution is very dilute.
4. **C-Curves:** (constant partition), linear curves, given by solutes that penetrate into the solid more readily than does the solvent.

1.6. Theories of Adsorption:

1.6.1. The Langmuir Adsorption Isotherm:

Irving Langmuir was given the Nobel Prize in 1932 for his investigations concerning surface chemistry. According to Langmuir's isotherm of the adsorption of adsorbate onto adsorbent surface, the adsorption was described by three assumptions [56]:

1. The adsorbent surface is in contact with a solution containing an adsorbate which is strongly attracted to the surface.

2. The surface has a given number of sites where the solute molecules can be adsorbed. Each site can contract only one adsorbate molecule and all sites are equivalent and no interaction between adsorbed molecules [56,57]

3. The adsorption involves the attachment of only one layer of adsorbate to the adsorbent surface (monolayer adsorption) so the Langmuir Isotherm best describes chemisorption processes.

The Langmuir isotherm model is shown as [58]:

$$c_e/q_e = (1/(k_L . q_{max})) + (1/q_{max})\, c_e \text{--------- (1)}$$

c_e: equilibrium concentration of adsorbate in solution after adsorption (mg/L).

q_e: amount of adsorbate adsorbed per unit weight of adsorbent at equilibrium (mg/g).

q_{max}: maximum monolayer adsorption capacity (mg/g).

k_L: Langmuir constant (L/mg).

To estimate the process favorability, the dimensionless separation factor, **R_L**, was determined by:

$$R_L = 1 / (1 + k_L\, c_o) \text{ ---------- (2)}$$

Where **R_L** is the equilibrium parameter or separation factor, **c_o** is the highest initial concentration. The **R_L** indicates the biosorption to be [59]:

Unfavourable	$R_L > 1$
Linear	$R_L = 1$
Irreversible	$R_L = 0$
Favourable	$0 < R_L < 1$

1.6.2. Freundlich Adsorption Isotherm:

Herbert Max Finley Freundlich, a German physical chemist which presented an empirical adsorption isotherm for non-ideal sorption on heterogeneous surfaces and multilayer sorption [60]. In 1909, Freundlich gave a practical expression explaining the isothermal contrast of adsorption of a quantity of atoms adsorbed by unit mass of solid adsorbent with pressure [58]. It is the most significant multi-site sorption isotherm for heterogeneous surfaces. Despite the model originates from empirical expressions, it has also been derived by assuming an exponential decay energy distribution function [57].

The basic assumption of Freundlich isotherm is that if the concentration of the solute in the solution at equilibrium, c_e was raised to the power 1/n, the amount of solute adsorbed being qe, then $c_e^{1/n}q_e$ was a constant at an assumed temperature. This model widely used but it does not provide information on the monolayer biosorption capacity and it assumes neither homogeneous site energies nor limited levels of sorption [61]. The non-linear form of Freundlich equation expressed as follows:

$$q_e = K_f c_e^{1/n} \text{ ---------- (3)} \quad \text{(non-linear form)}$$

q_e: amount of adsorbate adsorbed per unit weight of adsorbent at equilibrium (mg/g).

c_e: equilibrium concentration of adsorbate in solution after adsorption (mg/L).

n: adsorption capacity

Here, **K_f** (mg/g) and **1/n** are Freundlich constants (indicators of the sorption capacity and intensity, respectively). Taking logs and rearranging of Eq. (3), it can give the linear form of Freundlich model which expressed as:

$$\log q_e = \log K_f + 1/n \log c_e \text{ ---------(4)}$$

The constants **K_f** and **1/n** can be calculated from the intercept and slope of this linear equation, respectively.

1.6.3. Dubinin-Radushkevich Adsorption Isotherm:

This isotherm was used to assessment the porosity of the adsorbent and the energy of adsorption [62]. The D-R isotherm mostly applied to explain the adsorption mechanism with a Gaussian energy distribution onto the heterogeneous surface of the adsorbent and applied to differentiate the physical and chemical adsorption of metal ions [63]. This model has successfully fitted on high solute activities and the intermediate range of concentrations [64].

$$Ln\, q_e = Ln\, q_{max} - \beta \varepsilon^2 \text{ ---------- (5)}$$

$$\varepsilon = RT\, Ln\, (1+1/c_e) \text{ ---------- (6)}$$

q_e: amount of adsorbate in the adsorbent at equilibrium(mg/g)

q_{max}: theoretical isotherm saturation capacity (mg/g)

β: Dubinin–Radushkevich isotherm constant (mol^2/kJ^2)

ε: is the Polanyi potential

R: is the gas constant (8.314 J/mol K)

T: is the absolute temperature

c_e: is the concentration of adsorbate at equilibrium time.

The constant **β** gives the mean free energy **E** of adsorption per mole of the adsorbate when it is adsorbed on the surface of the solid [63].

$$E = 1/\sqrt{2\beta} \quad \text{---------- (7)}$$

1.7. Thermodynamics of Adsorption:

The temperature in adsorption process is beneficial to define the thermodynamic parameters such as standard Gibbs free energy change ΔG◦, standard enthalpy change ΔH◦, and standard entropy change ΔS◦ [65]. The adsorption process is endothermic when ΔH>0 but if ΔH<0, the process is exothermic. Through the values of ΔG, is to know whether the interaction spontaneous or non-spontaneous [66]. The positive value of ΔS^0 resulted from the increased in randomness and the negative value resulted from decreased in randomness [67]. In aqueous phase, the temperature may have an effect on the adsorbate solubility, which effects on the adsorption interaction. If the adsorbate solubility increases with increase the temperature, the adsorbed amount decreases. Furthermore, if the adsorbate solubility decreases at increasingly high temperature, then adsorption interaction and solubility become competitive [68]. From Van't Hoff equation is calculated the standard enthalpy change ΔH^o and standard entropy change ΔS◦ of adsorption as it is shown in the following formula:

$$Ln\ K = (-\Delta H/RT) + (\Delta S/R) \text{ ---------- (8)}$$

Where,

K: equilibrium constant.

R: gas constant

T: temperature (K)

The **K** value was determined by this formula:

$$K = q_e/c_e \text{ ---------- (9)}$$

Where,

q_e: the amount adsorbed at equilibrium.

c_e: the equilibrium concentration of the solution.

The values of ΔH◦ and ΔS◦ produced from the slope and intercept of a plot of lnK against 1000/T [65].

The change in free energy can be calculated from the formula below [67]:

$$\Delta G = \Delta H - T\Delta S \text{---------- (10)}$$

1.8. Adsorption Kinetics:

To discuss the kinetic mechanism of the adsorption system, pseudo-first-order, pseudo-second-order and diffusion intraparticle models are used to fit the experimental data.

1.8.1. Pseudo-First Order Model:

In 1898, Lagergren presented a first-order rate equation to describe the kinetics of liquid-solid phase adsorption, based on the adsorption capacity and it is widely used in recent years to describe the adsorption of pollutants from wastewater in different fields [69]. Lagergren pseudo-first order kinetic model is mathematically expressed by the formula below [70]:

$$dq/dt = k_1 (q_e - q_t) \text{-------- (10)}$$

eq. (10) can be linearly presented as shown below:

$$Log\ (q_e - q_t) = Log\ q_e - k_1 t/\ 2.303 \text{ ------- (11)}$$

q_e: amounts adsorbed at equilibrium (mg/g).

q_t: amounts adsorbed at time (min).

k_1: is the adsorption rate constant of pseudo-first-order kinetic model (1/min).

The kinetic parameters of this model was calculated from the slope and intercept of the linear plots of log (qe – qt) versus t [71].

1.8.2. Pseudo-Second Order Model:

It is assumed that the adsorption capacity is proportional to the number of active sites occupied on the adsorbent and the kinetic rate law can be written as follows [72]:

$$dqt / dt = k_2 (q_e - q_t) \text{ ---------- (12)}$$

Where, **k:** is the rate constant of sorption (g/mg min).

The rearrangement of the equation gives:

$$dqt/(q_e - q_t)^2 = k\, dt \text{ -------- (13)}$$

Integrating this for the boundary conditions t=0 to t=t and qt=0 to qt=qt, the result is:

$$1/ q_e - q_t = 1/q_e + k_2 t \text{---------- (14)}$$

That is the integrated rate law for a pseudo-second order reaction and the rearrangement of the equation gives:

$$t/q_t = 1/h + 1/q_e\, t \text{ -------- (15)}$$

Where h can be regarded as the initial sorption rate.

The constants of pseudo second order model can be calculated by plotting t/qt against t.

1.8.3. Intra-Particle Diffusion Model:

Other kinetic models have been applied in the adsorption process such as intra-particle-diffusion model by Weber and Morris, which can be described as follow [73]:

$$q_t = k_D\, t^{1/2} + C \text{ --------- } (16)$$

Where,

q_t: amount of adsorbed at any time (mg/g).

k_D: is the diffusion constant (mg/g $min^{1/2}$).

$t^{1/2}$: is the square root of the time ($min^{1/2}$).

C: is the thickness of boundary layer.

The constants k_D and C can be evaluated from the slope of the linear plot of q_t versus $t^{1/2}$. If the plot passes out of the origin, then intra-particle diffusion is the rate controlling step [74] but best fit straight lines that do not pass through the origin which indicate that there is an initial boundary layer resistance. The plot of q_t against $t^{1/2}$ should be a straight line when the adsorption process follows the intra-particle diffusion process [65].

1.9. Adsorbate:

1.9.1. Bromothymol Blue BTB :

Bromothymol blue (BTB), λ_{max}=591nm, a triphenylmethane dye (3', 3"-Dibromothymolsulfonphthalein), is a pH indicator applied in physiological tissue for following the interaction of lipid with protein. It is widely used in biomedical, biological and chemical engineering applications. There are varieties of uses for BTB such as; used to determine cell walls or nuclei under the microscope, for the assessment and estimation of the pH of pools and fish tanks and to determination of carbonic acid existences in liquid [75,76]. Table (1.4) represents the chemical and physical properties of Bromothymol Blue dye.

Table (1.4): The chemical and physical properties of BTB dye.

Chemical formula	$C_{27}H_{28}Br_2O_5S$
Molar mass	624.38 $g.mol^{-1}$
λ_{max}	591 nm

Melting point	202°C
Solubility in water	Sparingly soluble in water
pH indicator	pH = bluish green
	pH > 7 yellow
	pH < 7 Blue

1.9.2. Malachite Green oxalate MGox:

Malachite Green oxalate (MGox), λ_{max}=621nm, ([4-[[4-(dimethylamino) phenyl]-phenylmethylidene] cyclohexa-2,5-dien-1-ylidene]-dimethylazanium;2-hydroxy-2-oxoacetate; oxalic acid), has been used significantly in aquaculture as a parasiticide and in food, health, textile, also used extensively for dyeing silk, wool, jute, leather, cotton and other industries. It belongs to group of tripenylmethane dyes. MGox is highly cytotoxic to mammalian cells and also acts as a liver tumor-enhancing agent. Several passively affect from the consumption of the dye because of their carcinogenic, genotoxic, mutagenic and teratogenicity properties [46, 77]. The chemical and physical properties of Malachite Green oxalate dye were presented in table (1.5).

Table (1.5): The chemical and physical properties of MGox dye.

Chemical formula	$C_{52}H_{54}N_4O_{12}$
Molar mass	927.00476 g.mol^{-1}
λ_{max}	621 nm
Melting point	159°C
Solubility	Soluble in water and alcohol
pH indicator	Green liquid 0 yellow to 2.0 green

	11.6 yellow to 14.0 colorless

1.10. Adsorbent:

There are typical requirements for the good adsorbent such as high porosity, high internal surface, high adsorption efficiency in wide range of adsorbate concentrations, thermal stability unaffected by a cyclic regeneration and low cost [39].

1.10.1. Sawdust:

Sawdust is a solid waste/by product generated in huge quantities at saw mills, usually used for its environmental friendly behavior, availability in nature and the low cost. Untreated sawdust is largely Consists of cellulose pectin; hemi-cellulose, lignin, etc and many hydroxyl groups; such as tannins or other phenolic compounds. It can be utilized as an efficient and cost effective bio-adsorbent for removing dyes from wastewater [6,78].

1.10.2. Modification of sawdust with polyaniline:

Polyaniline (PANI) is a poly aromatic amine that synthesized chemically from bronsted acidic aqueous solutions and it is considered one of the most potentially useful conducting polymers [79]. Polyaniline (PANI) exists in different forms that vary in chemical and physical properties [80]. The chemical polymerization of aniline in aqueous acidic by using oxidizing Agents, such as $(NH_4)_2S_20_8$ can explain as shown in figure (1.9).

Figure (1.9): The formation of polyaniline in acidic media.

The oxidation process is companied by the insertion of anions of acid electrolyte to maintain the charge neutrality of the final polymer product [79]. The protonation and deprotonation and various other physical and chemical properties of PANI can be due to the presence of the -NH- group. Green and Woodhead were the first to describe PANI as a chain of aniline molecules coupled head-to-tail at the para position of the aromatic ring [81]. The oxidation of monomeric aniline leads to stable polymers in at least three oxidation states can be readily converted to one another by simple redox methods as shown in figure (1.10) [82].

Figure (1.10): Various possible oxidation states of polyaniline.

Recently been using polymers such as polyaniline in water purification due to the increasing adsorption capacity of sawdust and because of their

electrical conductivity and electro negativity and it have an advantages of less sludge generation and effective in both batch and column mode systems [83,84].

1.11. Literature Review:

Hanafiah1 et al [85] Studied the acid blue 25 adsorption on base treated Shorea dasyphylla sawdust. The potential of base treated Shorea dasyphylla (BTSD) sawdust for Acid Blue 25 (AB 25) adsorption was investigated in a batch adsorption process. Various physiochemical parameters such as pH, stirring rate, dosage, concentration, contact time and temperature were studied. The adsorbent was characterized with Fourier transform infrared spectrophotometer, scanning electron microscope and Brunauer, Emmett and Teller analysis. The optimum conditions for AB 25 adsorption were pH 2, stirring rate 500 r/min, adsorbent dosage 0.10 g and contact time 60 min. The pseudo second-order model showed the best conformity to the kinetic data. The equilibrium adsorption of AB 25 was described by Freundlich and Langmuir, with the latter found to agree well with the isotherm model. The maximum monolayer adsorption capacity of BTSD was 24.39 mg/g at 300 K, estimated from the Langmuir model. Thermodynamic parameters such as Gibbs free energy, enthalpy and entropy were determined. It was found that AB 25 adsorption was spontaneous and exothermic.

Badu et al [86] studied the evaluation of adsorption of textile dyes by wood Sawdust. Dyes are usually present in trace quantities in the treated effluents of many industries. The effectiveness of adsorption for dye removal from waste waters has made it an ideal alternative to other expensive treatment methods. This study investigates sorption properties of Tectona grandis, Ceiba pentandra and Terminalia superba sawdust for the adsorption of Vat Yellow-4, Vat Red-1 and Natural dyes in water bodies. Physical parameters of the wood sawdust and textile dye such as pH and moisture content were

determined. The dye removal capacities of the various wood species were also calculated. The pH of the dyes and wood sawdust ranged from 5.93 to 9.47; and 5.06 to 8.59 respectively. The moisture content (%) also ranged from 3.00 to 4.00 with an average of 3.50. The dye removal percentage (%) by Tectona grandis, Ceiba pentandra and Terminalia superba wood sawdust were respectively found to range from 18.39 to 44.46, 9.24 to 46.65 and 12.66 to 63.56 for the adsorption of the various dye samples used. Adsorption of the textile dyes unto the selected Ghanaian wood sawdust conformed to the Type I isotherm according to the classification by IUPAC. The Freundlich model showed a better fit for the experimental data and could be attributed to the heterogeneous surface energies and exponential distribution of active sites which are characteristic of such cellulosic materials.

Kyzas et al [87] Studied the Green Adsorbents for Wastewaters. One of the most serious environmental problems is the existence of hazardous and toxic pollutants in industrial wastewaters. The major hindrance is the simultaneous existence of many/different types of pollutants as (i) dyes; (ii) heavy metals; (iii) phenols; (iv) pesticides and (v) pharmaceuticals. Adsorption is considered to be one of the most promising techniques for wastewater treatment over the last decades. The economic crisis of the 2000s led researchers to turn their interest in adsorbent materials with lower cost. In this review article, a new term will be introduced, which is called “green adsorption”. Under this term, it is meant the low-cost materials originated from: (i) agricultural sources and by-products (fruits, vegetables, foods); (ii) agricultural residues and wastes; (iii) low-cost sources from which most complex adsorbents will be produced (*i.e.*, activated carbons after pyrolysis of agricultural sources). These “green adsorbents” are expected to be inferior (regarding their adsorption capacity) to the super-adsorbents of previous literature (complex materials as modified chitosans, activated carbons, structurally-complex inorganic composite materials etc.), but their cost-potential makes them competitive. This review

is a critical approach to green adsorption, discussing many different (maybe in some occasions doubtful) topics such as: (i) adsorption capacity; (ii) kinetic modeling (given the ultimate target to scale up the batch experimental data to fixed-bed column calculations for designing/optimizing commercial processes) and (iii) critical techno-economic data of green adsorption processes in order to scale-up experiments (from lab to industry) with economic analysis and perspectives of the use of green adsorbents.

Agalya et al [88] Studied the kinetics, equilibrium on removal of ionic dyes using a novel non-conventional activated carbon. The feasibility of activated carbon prepared from Euphorbia Tirucalli wood using H_3PO_4 for the removal of Malachite Green (Cationic) and Direct Blue (Anionic) dyes was investigated. The effects of initial dye concentration, contact time, pH and temperature onto ETAC were studied. Equilibrium isotherms and kinetics were investigated and the experimental data fitted well with the Langmuir model. The maximum monolayer adsorption capacities of ETAC were found to be 181.81 mg/g and 138.88 mg/g for MG and DB respectively. The kinetic data obtained were analyzed using pseudo-first order, pseudo-second order and intra particle diffusion models. Thermodynamic parameters were evaluated and suggesting the spontaneous and endothermic nature of physisorption. Activation energy for the adsorption of MG and DB were 12.1402 kJ/mole and 28.8484 kJ/mole.

Gong et al [89 Studied the functionalization of sawdust with monosodium glutamate for enhancing malachite green removal capacity. In this paper, waste sawdust was functionalized by monosodium glutamate for improving its cationic sorption capacity. The functionalized sawdust (FS) and crude sawdust (CS) were compared for their malachite green (MG) sorption behaviors with a batch system. The effects of various experimental parameters (e.g. initial pH, sorbent dose, dye concentration, contact time, and temperature etc.) were investigated and the sorption kinetic and

thermodynamic characteristics were understood. The MG removal ratios on FS and on CS increased with increasing initial pH and came up to the maximum value beyond pH 6 for FS and pH 8 for CS, respectively. The ratio of sorbed MG kept above 95% for 250 mg/l of MG solution when 2.0 g/l or more of FS was used. The MG removal percentage decreased more on CS than on FS with increasing initial MG concentration. The isothermal data of MG sorbed on FS and on CS followed the Langmuir model. By functionalizing, the sorption capacity (Qm) of sawdust for MG was increased from 85.47 to 196.08 mg/g and the sorption equilibrium time of MG was shortened from 23 to 4.5 h. The MG sorption processes on FS and on CS followed the pseudo-second-order rate kinetics. The sorptions of MG on FS and on CS were spontaneous and exothermic processes and lower temperatures were favorable for the sorption processes.

Baserl et al [90] Studied the application of Polyaniline Nano Composite for the Adsorption of Acid Dye from Aqueous Solutions. In this research, Polyaniline coated sawdust (Polyaniline nano composite) was synthesized via direct chemical polymerization and used as an adsorbent for the removal of acid dye (Acid Violet 49) from aqueous solutions. The effect of some important parameters such as pH, initial concentration of dye, contact time and temperature on the removal efficiency was investigated in batch adsorption system. The adsorption capacity of PAC was high (96.84 %) at a pH of 3-4. The experimental data fitted well for pseudo second order model. Langmuir model is more appropriate to explain the nature of adsorption with high correlation coefficient. The Energy of activation from Arrhenius plot suggested that the adsorption of AV49 onto PAC involves physisorption mechanism.

Patil et al [91] Studied the adsorption of malachite green by polyaniline–nickel ferrite magnetic nanocomposite. This work deals with the development of an efficient method for the removal of a MG (malachite green) dye from

aqueous solution using polyaniline (PANI) – Nickel ferrite ($NiFe_2O_4$) magnetic nanocomposite. It is successfully synthesized in situ through self-polymerization of monomer aniline. Adsorptive removal studies are carried out for water soluble MG dye using PANI–Nickel ferrite magnetic nanocomposite in aqueous solution. Different parameters like dose of adsorbent, contact time, different initial conc., and pH have been studied to optimize reaction condition. It is concluded that adsorptive removal by PANI–Nickel ferrite magnetic nanocomposite is an efficient method for removing a MG dye from aqueous solution than work done before. The optimum conditions for the removal of the dye are initial concentration 30 mg l-1, adsorbent dose 5gm l-1 and pH 7. The adsorption capacity is found 4.09 mg g-1 at optimum condition 30 mg l^{-1}.

The adsorption followed pseudo-second-order kinetics. The experimental isotherm is found to fit with Langmuir equation. The prepared adsorbent is characterised by techniques SEM, EDS, XRD and VSM.

Baskaran et al [92] Reported the adsorption of Malachite Green Dye by Acid Activated Carbon. The ability of zea mays dust carbon to remove malachite green from aqueous solutions has been studied for different adsorbate concentrations by varying the amount of adsorbent, temperature, pH and shaking time. Thermodynamic parameters such as ΔH°, ΔS° and ΔG°, were calculated from the slope and intercept of the linear plots. Analysis of adsorption results obtained at 303, 313, 323 and 333 K showed that the adsorption pattern on zea mays dust carbon seems to follow the Langmuir and Freundlich. The numerical values of sorption free energy indicate physical adsorption. The kinetic data indicated an intra-particle diffusion process with sorption being first order. The concentration of malachite green oxalate was measured before and after adsorption by using UV-visible spectrophotometer.

Khattria et al [93] Studied the Removal of malachite green from dye wastewater using neem sawdust by adsorption. Neem sawdust (Azadirachta

indica) was used as an adsorbent for the removal of malachite green dye from an aqueous solution. The studies were carried out under various experimental conditions such as agitation time, dye concentration, adsorption dose, pH and temperature to assess the potentiality of neem sawdust for the removal of malachite green dye from wastewater. A greater percentage of dye removal was observed with decrease in the initial concentration of dye and increase in amount of adsorbent. The adsorption of dye on neem sawdust was found to follow a gradual process. Equilibrium isotherms were analyzed by the Langmuir models of adsorption and were applicable with maximum monolayer adsorption capacity of 4.354mgg^{-1}. The dimensionless factor, RL of the malachite green, neem sawdust isotherm revealed that the adsorption process is favourable in nature.

Karadag et al [94] Investigated the removal of some cationic dyes from aqueous solutions by acrylamide/itaconic acid hydrogels. Acrylamide/itaconic acid (AAm/IA) hydrogels prepared by irradiating with radiating were used in experiments on the uptake of some cationic dyes such as basic red 5 (BR-5), basic violet 3 (BV-3) and brilliant cresyl blue (BCB). The removal of the cationic dyes to AAm/IA hyrogels is studied by batch adsorption technique. In the experiments of the adsorption, L3 type (Langmiur) adsorption in Giles classification system was found. Adsorption studies indicated that monolayer coverages of AAm/IA hydrogel by these dyes were increased with following order; BCB > BR-5 >BV-3.

Kumar et al [95] Reported the removal of Malachite Green and Crystal Violet Dyes from Aqueous Solution with Bio-Materials. Malachite Green and Crystal violet are among millions of dyes which are being used in every aspect of day to day life of a human being. Approximately 12% of synthetic dyes are lost during manufacturing and processing operations and 20% of the resultant color enters the environment through effluents from industrial wastewater. They are toxic and having extremely harmful consequences;

hence many governmental and environmental agencies have put in place very strict regulation and restriction on discharge of industrial waste water/effluent containing dyes into the natural water bodies. There are various techniques available for removal of dyes from waste water but adsorption is the process of choice. Activated carbon is the best known adsorbent. But its use in treating the industrial waste water especially in developing countries is restricted due to very high cost. This high cost of activated carbon has forced the researchers to find out low cost and effective adsorbent which may be used as an efficient alternative of activated carbon. In this paper an attempt has been made to compile the work of various researchers on removal of crystal violet and malachite green dyes from aqueous solution by using biomaterials and agricultural waste during the last five years.

1.12. The aim of this study:

The aim of the present study is to remove the dyes from aqueous solution by using available and cheap adsorbent such as Sawdust and modified by using polyaniline. Therefore, the scope of the present work will involve the following steps:

1. Using natural, available, cheap and environment-friendly adsorbent (Sawdust) to remove BTB and MGox dyes from aqueous solutions.
2. Modifing the SD by polyaniline to promote the adsorption capacity of the adsorbent in the removal of BTB (anionic) and MGox (cationic) dyes.
3. The morphology of the surfaces of each of sawdust and modified sawdust were described by using scanning electron microscopy (SEM), atomic force microscopy (AFM), infrared spectroscopy (FTIR) and Nitrogen sorption.

4. Determining the effect of contact time, adsorbents dose, temperature and changing the function of the acidic solution on the adsorption of BTB and MGox on the surface of SD and SD/PANI by using batch adsorption methods.
5. Studying various isotherms (Langmuir, Freundlich and Dubinin-Radushkevich isotherm) to illustrate the nature of the adsorption of BTB and MGox dyes on the surface of SD and SD/PANI.
6. Determining the Thermodynamic parameters (ΔH^O, ΔS^O and ΔG^O) for adsorption process of both dyes on the surface of SD and SD/PANI composite.
7. Studying the adsorption kinetic models (pseudo-first order, second order and Intraparticle diffusion model) to describe the adsorption process of BTB and MGox dyes on the surfaces of SD and SD/PANI depending on the adsorption capacity.

2.1. The Adsorbent:

The adsorbent that used is sawdust which can be obtained from any carpentry wood shop. The type of wood used is Tectona Saj. It is low cost and availability in nature and it is possible to use it without any modification. First we used the untreated sawdust and then the modified sawdust by polyaniline.

2.1.1. Preparation of sawdust:

Sawdust was cleaned and washed several times with normal tap water followed by distilled water to remove adhered dust particles. The cleaned material was kept in an oven for 24hr at 110°C. The dried mass was then crushed and sieved. The size of the particles is 75 μm and less [6]. The cleaned sawdust is ready to use.

2.1.2. Preparation of sawdust coated polyaniline:

To prepare the Sawdust coated polyaniline (SD/PANI), 5.0g of sawdust (size 75μ & less) immersed in 100 mL of 0.20 M freshly distilled aniline in 1M HCl solution for 12 hrs before polymerization. The excess of the monomer solution was removed by simple decantation and then about 50 mL of oxidant solution (5g ammonium persulphate $(NH_4)_2S_2O_8$) in 50ml distilled water) was gradually added into the mixture, and leave the reaction to continue for 5 hrs at 298K. Sawdust coated polyaniline (SD/PANI) was filtered, washed with distilled water, then dried at temperature about 60^{o}C (in an oven) and crush and sieved (Sieve size is 75 μm) before use it [84].

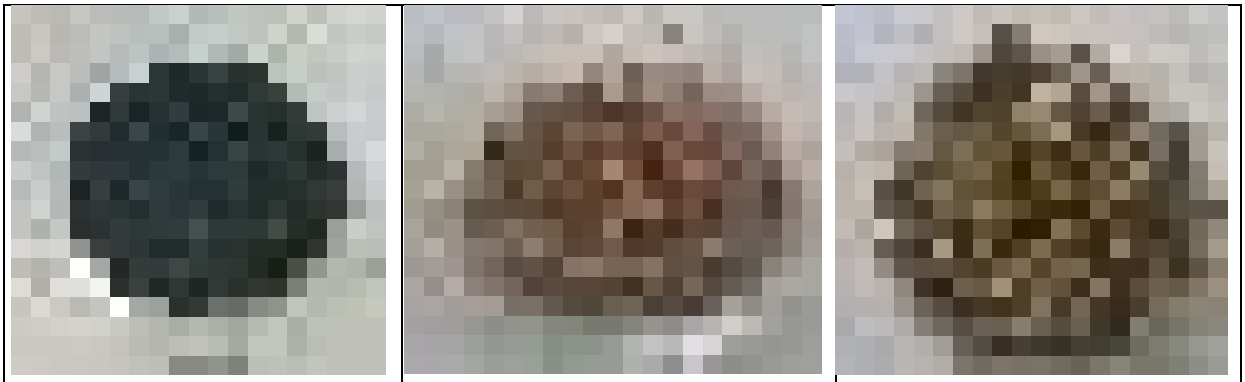

Sawdust coated polyaniline	Treated Sawdust	Raw Sawdust

Figure (2.1): Sawdust in different states.

2.2. The Adsorbates:

2.2.1. Bromothymol Blue BTB:

A triphenylmethane dye (3', 3"-Dibromothymolsulfonphthalein), Anionic dye from Polymethine type as shown in figure (2.2) and λmax=591nm.

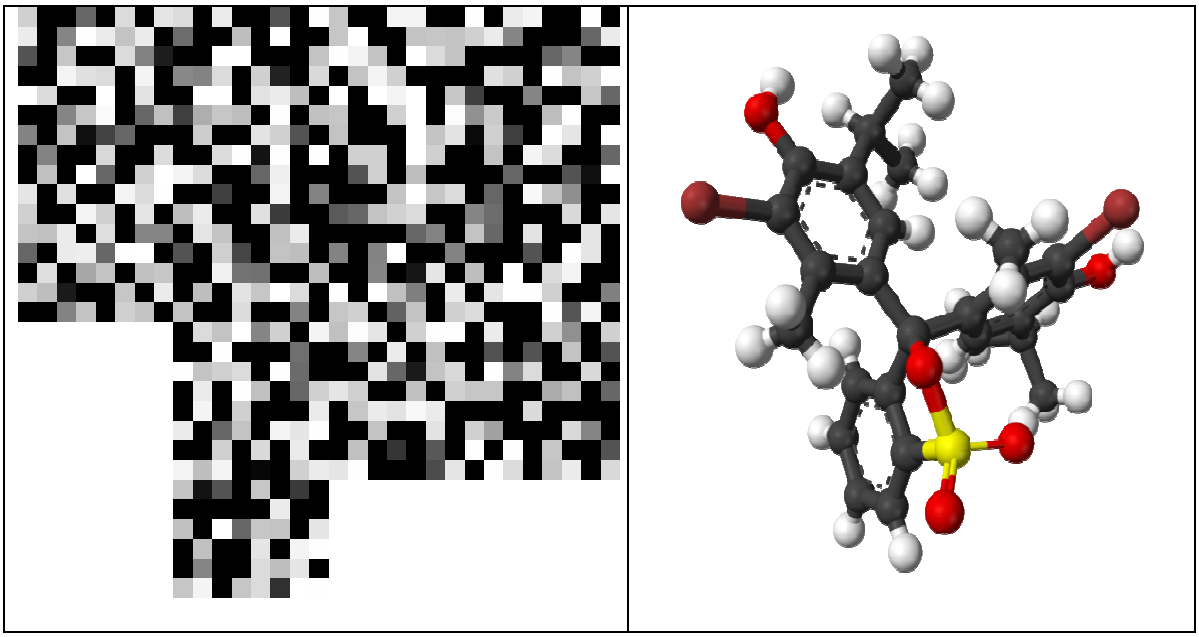

Figure (2.2): Chemical structure of BTB dye.

2.2.2. Malachite Green oxalate MGox:

([4-[[4-(dimethylamino) phenyl]-phenylmethylidene] cyclohexa-2, 5-dien-1-ylidene]-dimethylazanium oxalate, Cationic dye from Polymethine type as shown in figure (2.3) and λ_{max}=621nm.

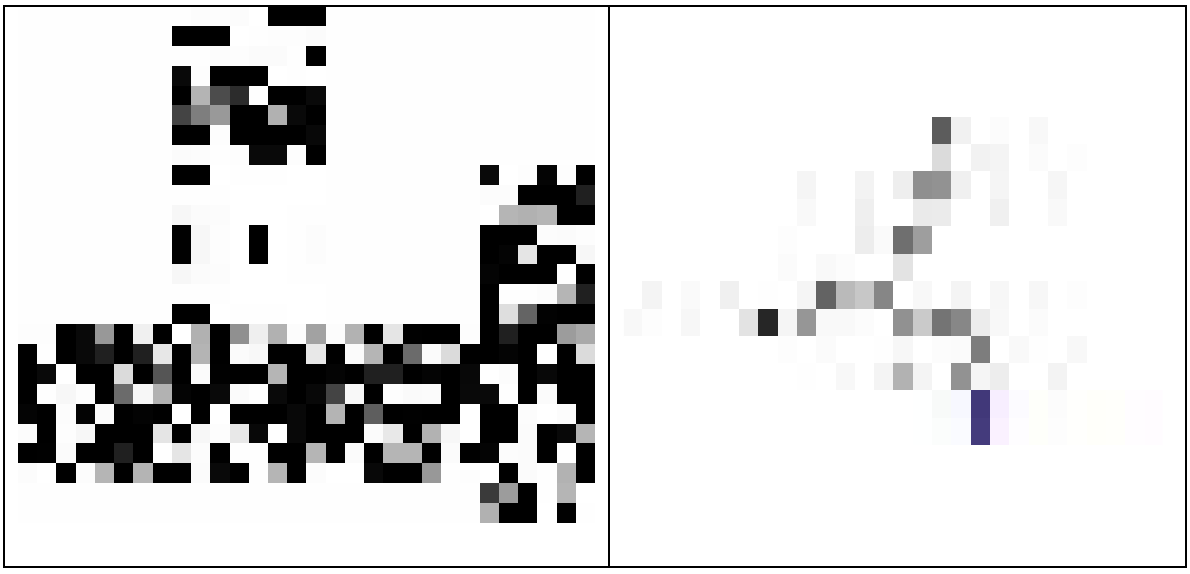

Figure (2.3): Chemical structure of MGox dye.

2.3. Chemicals:

The chemicals that used in this work were listed in table (2.1):

Table (2.1): The chemicals that used in the work.

No.	Material	Molar Mass ($g.mol^{-1}$)	% purity	Supplied
1	Hydrochloric acid (HCL)	36.46	37	HIMEDIA
2	Sodium hydroxide (NaOH)	40	99.9	Scharlau
3	Sodium chloride (NaCL)	58.44	99.5	Sentmenat Spain

4	Bromothymol Blue ($C_{27}H_{28}Br_2O_5S$)	624.38	99.5	RAL
5	Malachite Green oxalate ($C_{52}H_{54}N_4O_{12}$)	927.00476	99.5	SPI-chemicals
6	Aniline	93.13	99.9	Hi Media Leading Bio Sciences
7	Ammonium persulphate ($(NH_4)_2S_2O_8$)	228.18	98.5	Reach center
8	distilled water (H_2O)	18	High degree of purity	Lab.College of Science Al.Nahrain University

2.4. Instruments:

Table (2.2) illustrates the list of instruments used in this project work, their manufacturers, models, functions and the place of the instruments.

Table (2.2): List of instruments that used in this project.

No.	Instrument	Model	Function	Place Of Instrument
1	Vacum oven	Gallen Kamp	For drying the samples	Lab.College of Science Al.Nahrain University
2	Electronic balance	METTLER AE260Delta Range	Weight measurement	=
3	Hot plate with magnetic stirrer	IKAMAG®REO	To stir the solution of the sample	=
4	pH-meter	BP3001JiTrans instruments	Measurement of pH	=
5	Thermostat shaker	JEIOTECH (BS-11)	Shaking of conical	=

	water bath		flasks containing samples	
6	Centrifuge	HERMLE Z 200A	Separation of adsorbent from solution	=
7	UV-Visible	Shimadzu.PC 1650 Double Beam	absorbance measurements	=
8	Fourior transform Infrared Spectroscopy (FTIR)	SHIMADZU (IR PRESTIGE 21)	To determine the organic functional groups present in the samples	Laboratory of Ibn-Sina Scientific Company.
9	Scanning Electron Microscope (SEM)	Inspect S 50 FEI company	For studying the morphology of the samples	College of science, ALNahrain University
10	Atomic Force Microscope (AFM)	SPM-AA 3000,Advanced Angestrum Inc.	To determine the nano average particle size of the samples.	College of Science. Baghdad University
11	Gas Adsorption analysis	Micromeritics ASAP2020 V3.04G analyzer (micromeritics, Inc,USA	To determine the surface area, pore volume and Porosity (%).	Petroleum Research and Development Center in Iraq.

2.5. Determination of λmax:

A sample of 50 ppm solution of BTB or MGox dye was taken and a UV-VIS absorption spectrum was measured, they showed a λmax at 591 & 621 nm respectively as shown in figure (2.4).

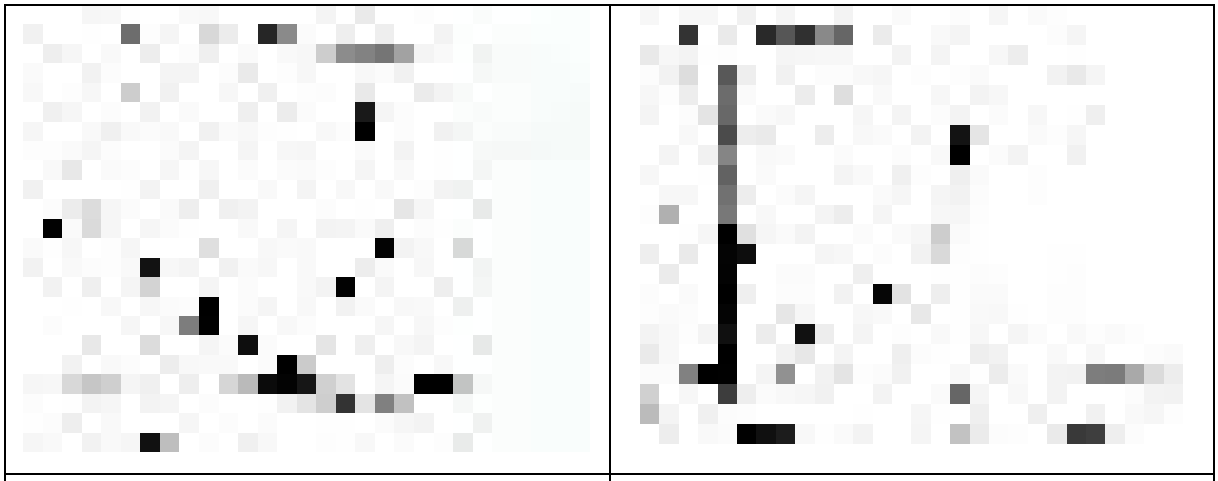

MGox	BTB

Figure (2.4): UV-Visible Absorption Spectrum for both dyes in 50 ppm solution.

2.6. Preparations of stock solution:

A solution of 50 ppm of both dyes solution as shown in figure (2.5) was prepared by dissolving 0.05g of dyes in distilled water in 1000ml volumetric flask and several concentrations were prepared from the stock solution by a subsequent dilution (for BTB: 2, 5, 10, 15, 20, 25, and 30, & for MGox: 2, 5, 10, 15, 20, 25, 30, 35, and 40) ppm.

Figure (2.5): The stock solution of both dyes (BTB & MGox) and some dilute solutions of MGox.

2.7. Calibration Curve:

The calibration curves were accomplished by measuring the absorbance of solutions that diluted from stock (and the all dilution solutions at different pH) of BTB and MGox dyes at 591 and 621 nm, respectively. Figure (2.6) represent the pH-meter devise that used in measurement the pH of solutions. Figures (2.7) & (2.8) show the plotting of absorbance vs. concentration for both dyes.

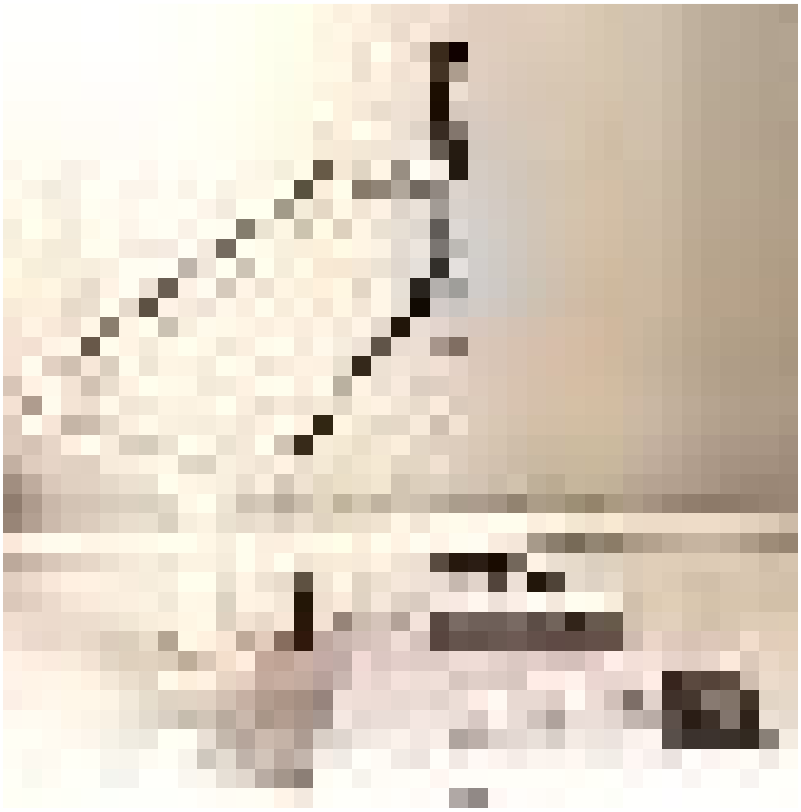

Figure (2.6): The pH meter device.

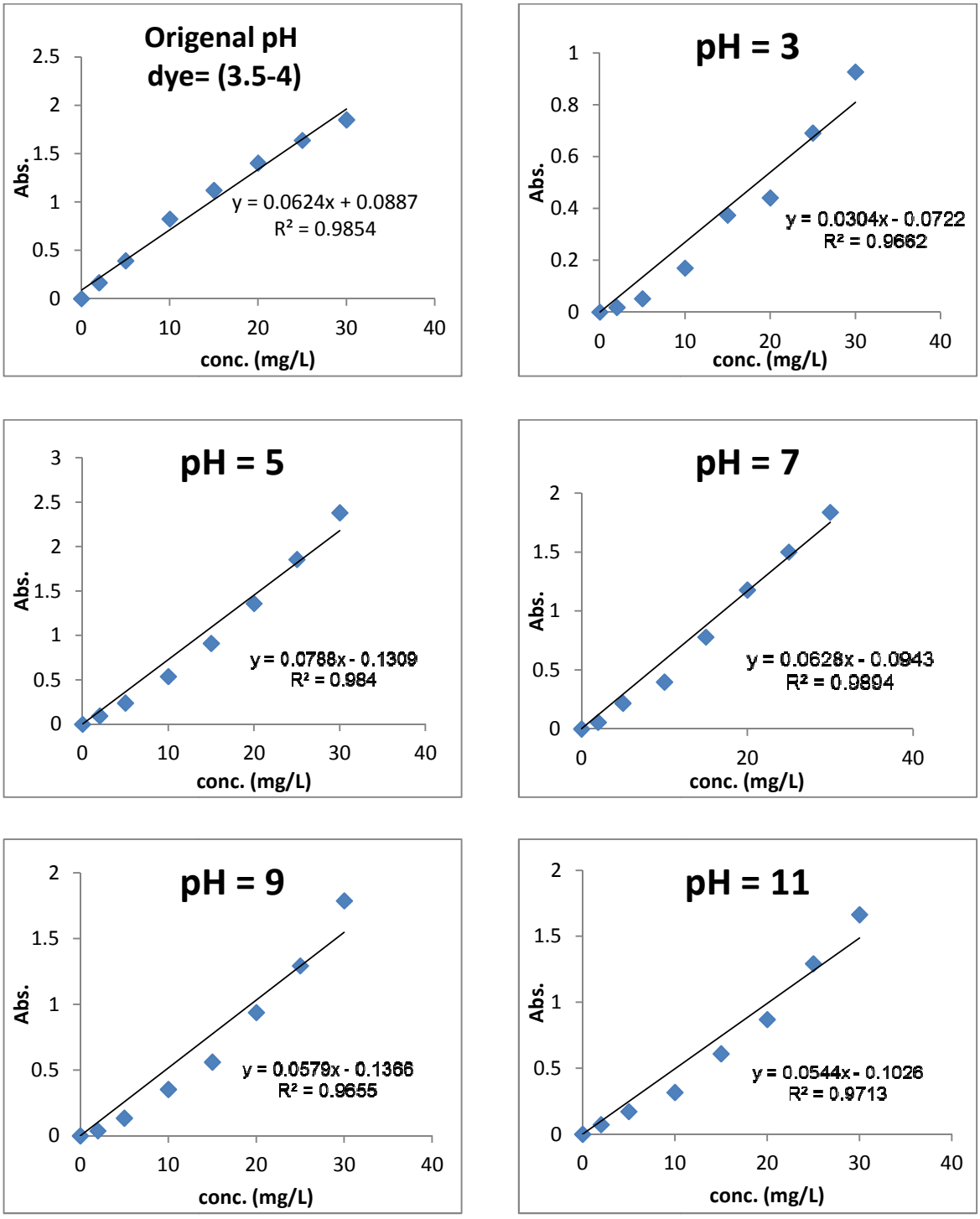

Figure (2.7): The calibration curves of BTB dye at different pH.

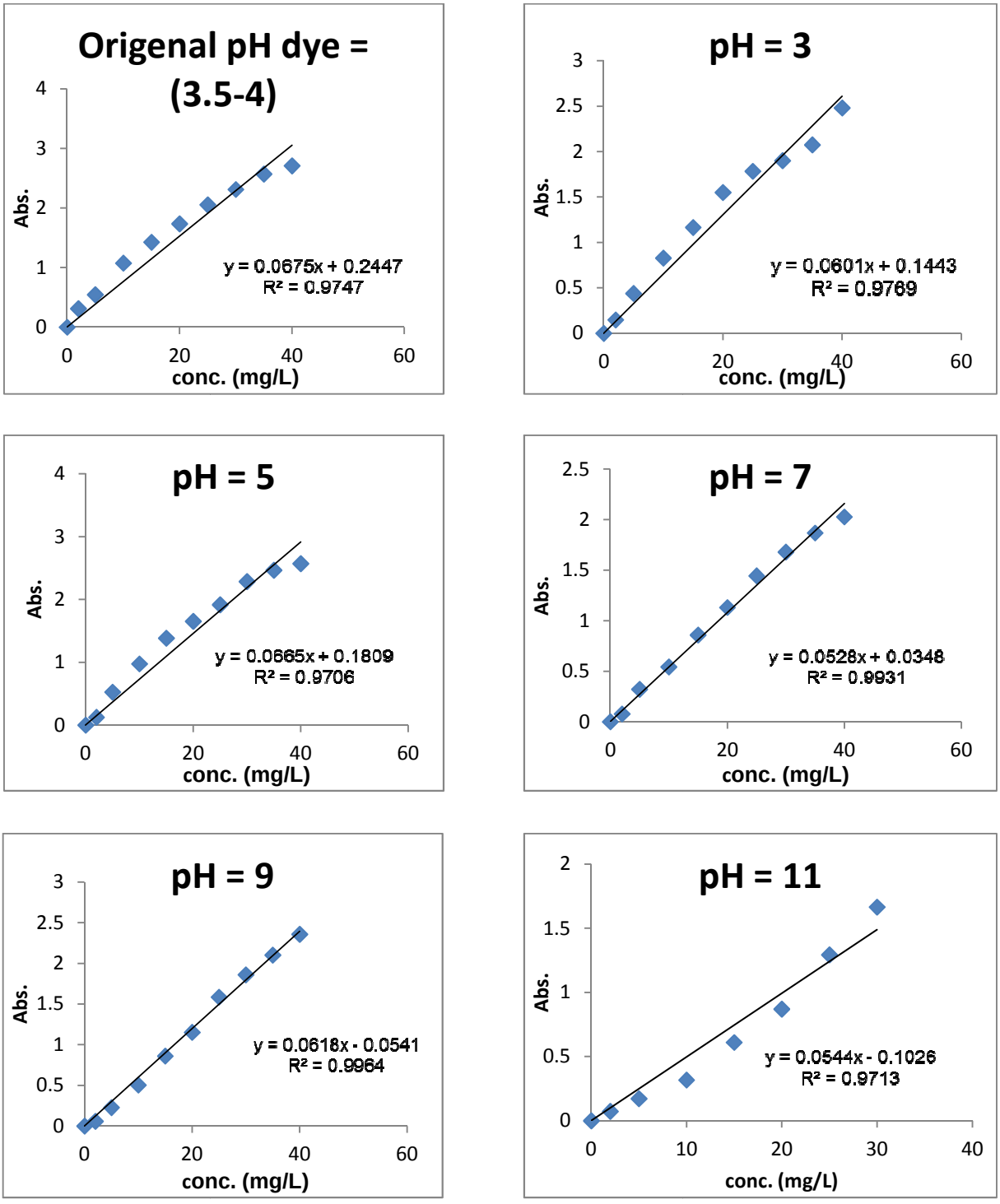

Figure (2.8): The calibration curves of MGox dye at different pH.

2.8. Determination several conditions on adsorption process:

2.8.1. Contact time:

To determine the equilibrium time for the adsorption process, a 0.03 g of SD was added into the conical flasks (containing 30 mL of 30 ppm of dye solution) at room temperature and original pH's dye (3.5-4) and for specific periods of time (5, 10, 15, 20, 25, 30, 35, and 40 minutes) by using thermostat shaker water bath and centrifuge devices as shown in figures (2.9) and (2.10), respectively. The time needed to reach the equilibrium was 15 and 20 minutes for BTB and MGox respectively.

Figure (2.9): Thermostat shaker water bath.

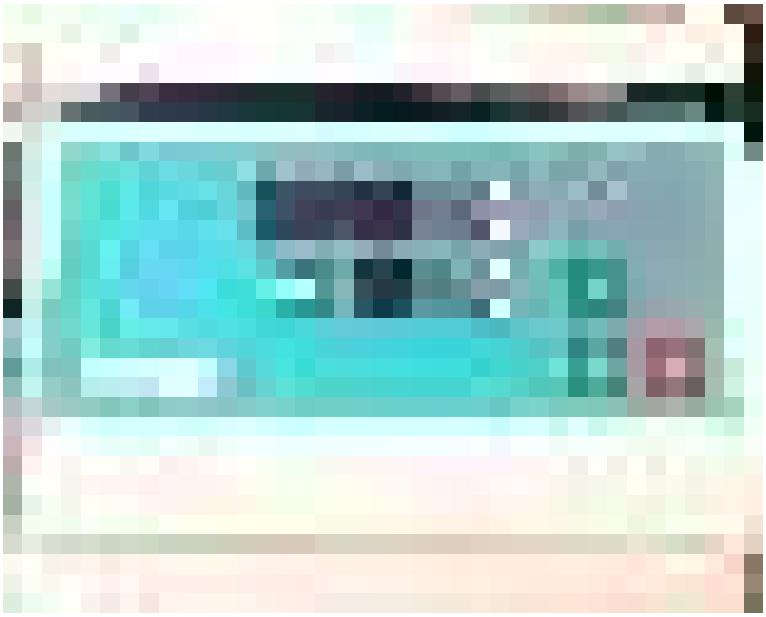

Figure (2.10): Centrifuge.

2.8.2. Adsorbent dose:

To determine the suitable amount of sawdust, the quantities (0.005, 0.007, 0.01, 0.015, 0.02, 0.025, 0.03 and 0.04g) for BTB and (0.007, 0.01, 0.015, 0.02, 0.025, 0.03 and 0.04g) for MGox were added into eight conical flasks containing 30 mL of 30 ppm dye solution for each and shaked for 15 and 20 minutes for BTB and MGox respectively.

2.8.3. Effect of temperature and pH:

A given dose (0.15 g for BTB & 0.025 g for MGox) of sawdust was added into conical flasks containing 30 mL of different concentrations of both dyes in different pH values (3, 5, 7, 9 and 11) that measured by using pH-meter and shakes for suitable time for both dyes (15min. for BTB & 20min. for MGox) and at different temperatures (298, 308 and 318)K. The absorbance of each solution was measured at 591 & 621 nm for BTB and MGox respectively by UV-VIS Spectrophotometer.

2.9. The devices that used in identification the adsorbent surfaces:

2.9.1. FT-IR analysis:

Fourier Transmission Infrared Spectroscopy technique has been widely used for the prediction of organic compounds present in the sample. Figure (2.11) represents FT-IR spectroscopy device. By studying the peak between a particular frequencies i.e. band, can identify the type of the functional group by scanning over a range of wavelengths (4000-400cm^{-1}). For the case of Sawdust, FTIR shows the change in properties of the surface of adsorbent on addition of both dyes BTB and MGox.

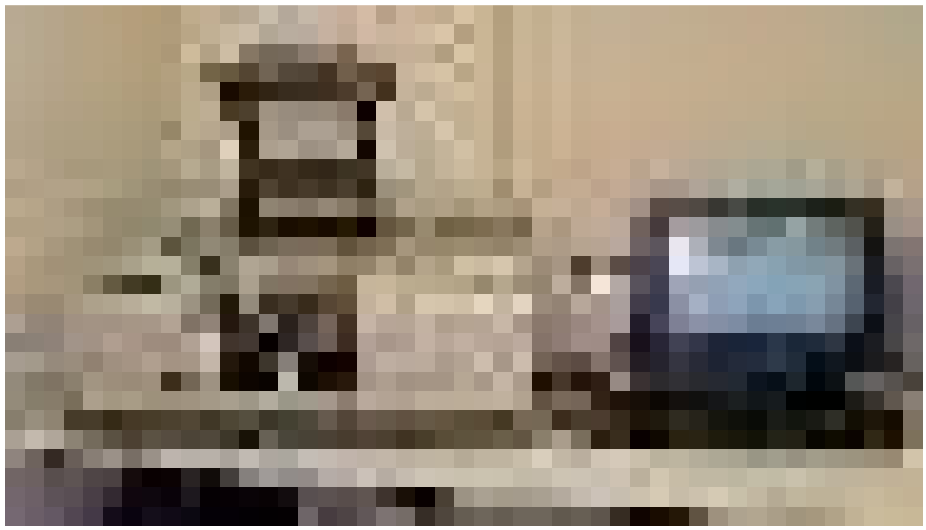

Figure (2.11): Fourier Transmission Infrared Spectroscopy (FT-IR) device.

2.9.2. SEM analysis:

Scanning Electron Microscope is an electron microscope that produces images of the solid surface by scanning it with electron beam which strike the atoms of the sample surface which generates various signals. These signals give information about the composition and surface structure of the sample. Electrical conductivity at the surface is the most important factor for

SEM characterization of samples. The preparation of the sample is done by coating it with gold to avoid ionization of the sample. The devise of SEM was presented in figure (2.12).

Figure (2.12): Scanning Electron Microscope (SEM) device.

2.9.3. AFM analysis:

The Atomic Force Microscope that given in figure (2.13) is an instrument which can analyze and characterize samples at the microscope level so we can look at surface characteristics with very accurate resolution ranging from 100 nm to less than 1nm.

Figure (2.13): Atomic Force Microscope (AFM) device.

2.9.4. Nitrogen Adsorption-Desorption analyzer:

Nitrogen adsorption/desorption measurements were done at -196°C with a Micrometitics ASAP 2020 static volumetric analyzer as shown in figure (2.14). All the adsorption data which including the BET surface area, pore volume and pore size distribution get from different models, are given by the workstation of ASAP200 analyzer.

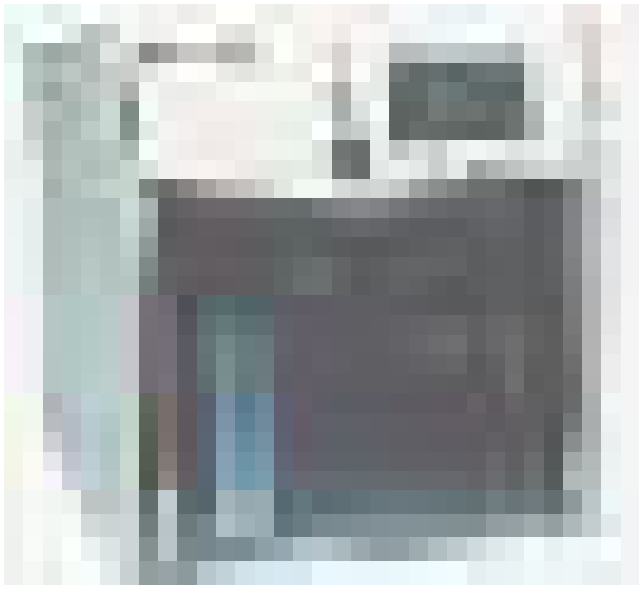

Figure (2.14): Nitrogen Adsorption - Desorption Analyzer.

2.10. Distillation of aniline:

The distillation of aniline done by packing a 250^{o}C thermometer with an air condenser, the thermometer adopted by screw-cap adaptor and the flask was heated over gauze using a Bunsen burner as shown in figure (2.15). Collect the fraction which distils between 180^{o}C and 185^{o}C and the yield was calculated. The boiling point of aniline is 184.4^{o}C.

Figure (2.15): Aniline distillation.

2.11. Calculation of adsorbate quantity:

The quantity of adsorbate was calculated by using the following formula:

$$q_{e.} = (c_{o.} - c_{e.})\ V(L) / mass \text{ --------- } (17)$$

Where,

q_e: Quantity of adsorbate (mg/g).

c_o: Initial concentration of adsorbate solution (mg/L).

c_e: Concentration of adsorbate solution at equilibrium (mg/L).

V: Total volume of adsorbate solution (L).

mass: Weight of adsorbent (g).

2.12. Calculation of sorption percentage:

The percentage of sorption was calculated by using the following formula:

$$\% R = (c_o - c_e / c_o) * 100 \text{ -------- } (18)$$

Where,

%R: sorption percentage

c_o: Initial concentration of adsorbate solution (mg/L).

c_e: Final concentration of adsorbate solution (mg/L).

3.1. Characterizations of Sorbent:

3.1.1. AFM analysis:

The topography and the roughness of the SD and SD/PANI composite were determined by using AFM at a scan size of 20μm. Figures (3.1) and (3.3) show the topographic structures in 2D and 3D view for the layers: SD and SD/PANI composite respectively. The SD in the form of nano-fibers and the fiber diameter does not exceed 160 nm and a length of 75 μm. From all the below images, it can be seen that one of the activation effects is to decrease the adsorbent diameter and to increase their multi-lobed character [96]. It was observed that the size of the particles of SD have average diameter of 75.65nm. On the other hand, after modification of SD by polyaniline polymer, the average particle diameter became 60.33nm indicating that the modification of SD by PANI led to decrease the size of surface particles and hence increase the efficiency of surface to adsorbed pollutant dyes. The 2D and 3D AFM topographic image of SD and SD/PANI surfaces are shown in figures (3.1) and (3.3), respectively and the Granularity Comutation Distribution chart of SD and SD/PANI surfaces are presented in figures (3.2) and (3.4), respectively.

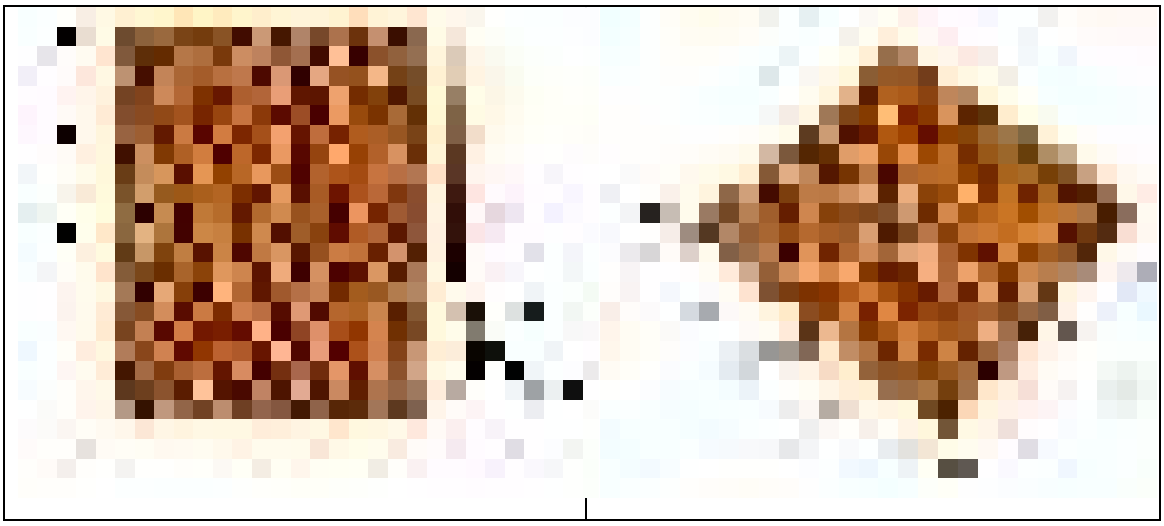

Figure (3.1): The 2D and 3D AFM topographic image of sawdust before the modification.

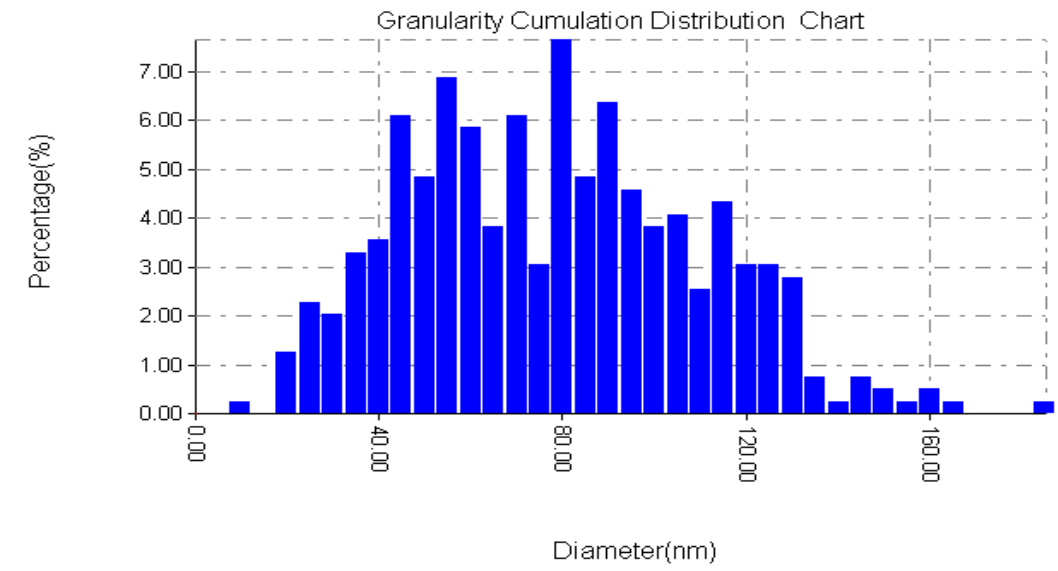

Figure (3.2): Granularity Cumulation Distribution chart of untreated Sawdust.

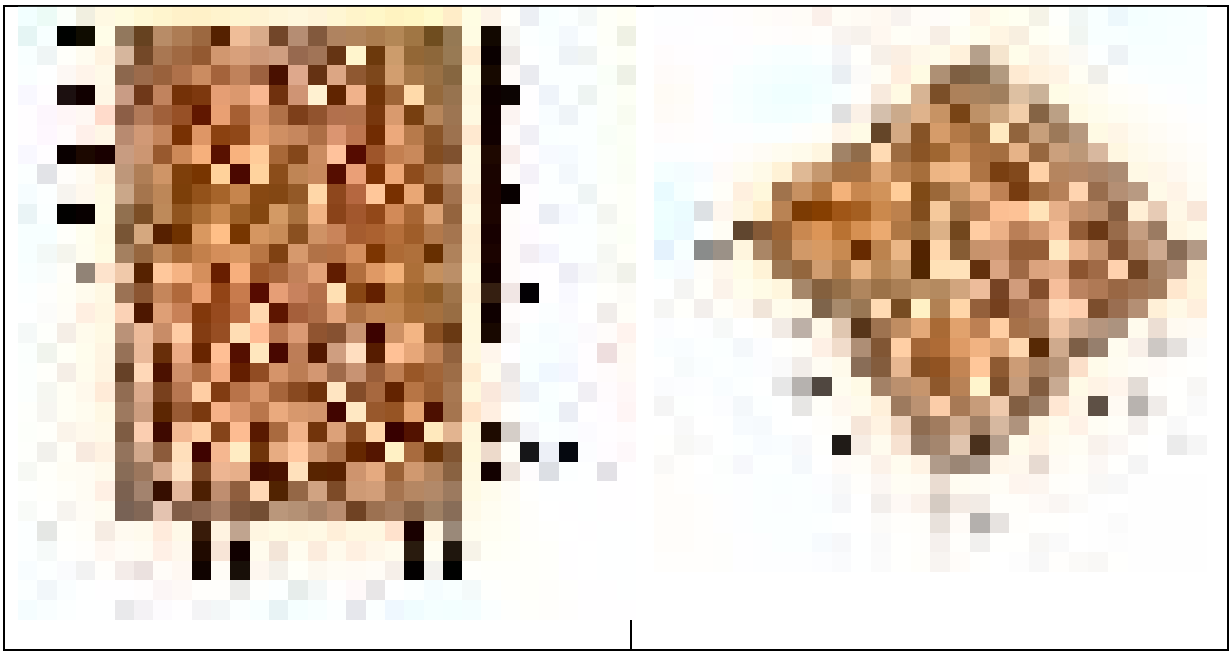

Figure (3.3): The 2D and 3D AFM topographic image of sawdust after modification by polyaniline.

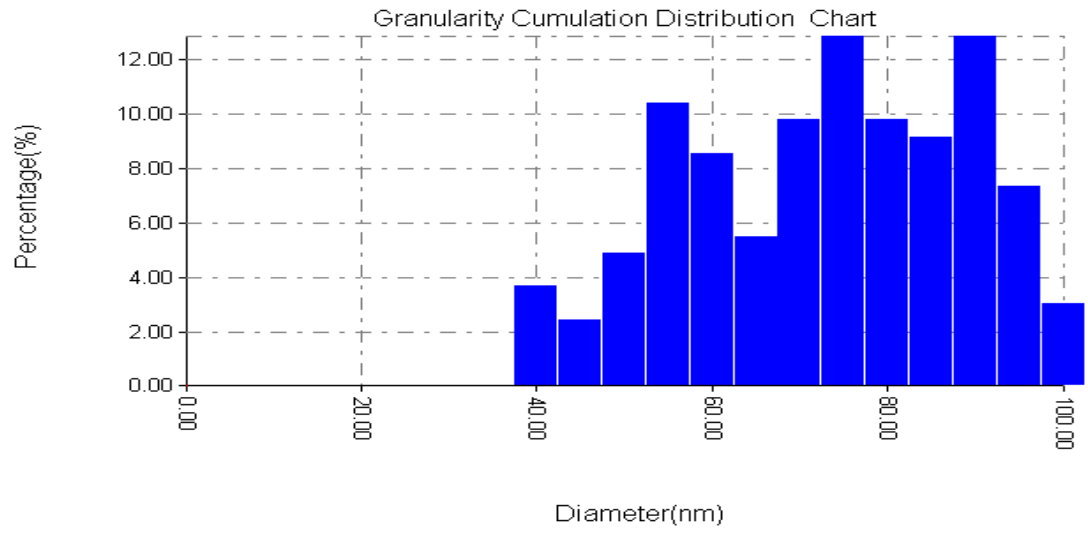

Figure (3.4): Granularity Cumulation Distribution chart of SD/PANI.

3.1.2. Gas Adsorption analysis:

From determining the specific surface area of SD and SD/PANI adsorbents surfaces that shown in table (3.1), the results present that the surface area of SD/PANI (2.7325 m^2/gm) greater than that on SD surface (0.8164 m^2/gm). The presence of the polyaniline layer on the surface of sawdust leads to morphological changes on it. The pores volume of SD/PANI (0.0377 gm/cm^3) greater than that on the SD surface (0.0282 gm/cm^3). The small pores do not allow for complete equilibrium due to slow diffusion rates and leads to decreasing in the adsorption rate.

Table (3.1): The measurements data of adsorbent before and after modification.

No.	Test	Results		Test Method
		Sample Code		
		SD	SD/PAN.	
1	Surface area (m^2/g)	0.8164	2.7325	ISO-9277-2010
2	Pore Volume (g/cm^3)	0.0282	0.0377	ISO-9277-2010

3	Porosity (%)	91.1535	83.81	*****

3.1.3. FT-IR analysis:

3.1.3.1. Sawdust:

The Transform Infrared Spectrum of SD before adsorption of dyes is shown in figure (3.5). The broad band at 3417.86 cm^{-1} is attributed to the O-H group stretching and the band on 1735.93 cm^{-1} was assigned to the C=O bonds. The absorption band at 2931.80 cm^{-1} is due to a contribution from C-H stretching and the band in 1654.92 cm^{-1} refers to C=C stretching. The strong band observed at 1060.95 cm^{-1} and 1037.70 cm^{-1} indicated the stretching of C-OH and C-O-C bonds. The medium band obtained in 1508.33 cm^{-1} evidenced to aromatic region. [97].

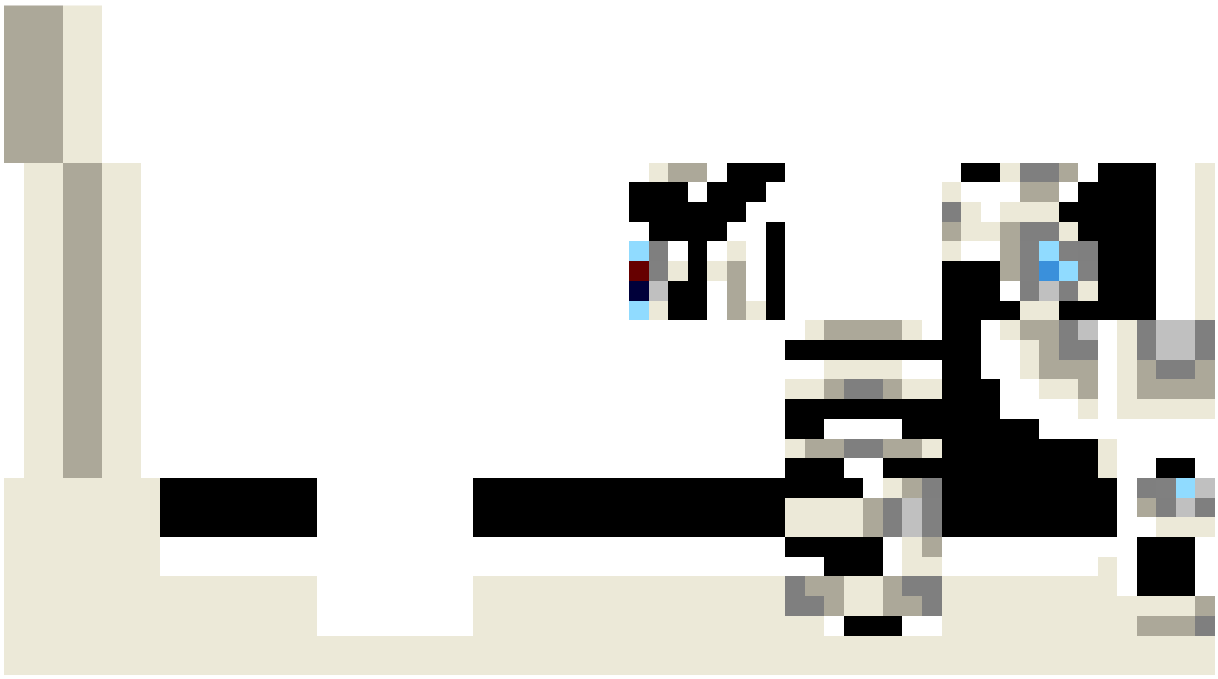

Figure (3.5): The FT-IR Spectrum for untreated sawdust before adsorption with dyes.

The FTIR spectrum of SD after adsorption of BTB dye is presented in figure (3.6). In a spectrum the band obtained at 3498.87 cm^{-1} to 3348.42 cm^{-1} after adsorption of BTB dye that refer to the O-H stretching band that indicates a high concentrations of phenol and alcohol. The band of C=O was shifting to 1732.08 cm^{-1}. The bands at 2935.66 cm^{-1} and 2908.65 cm^{-1} refers to the stretching C-H band. The strong bands from 651.94 cm^{-1} to 509.21 cm^{-1} refers to R-Br group. Figure (3.7) show that the spectrum of SD after adsorption of MGox dye is not much different from the spectrum of sawdust before adsorption but the bands are shifting such as the broad O-H bands at 3394.72 cm^{-1} and 3348.42 cm^{-1} and the stretching C-H bands are found at 2908.65 cm^{-1} and 2873.94 cm^{-1}, respectively [98].

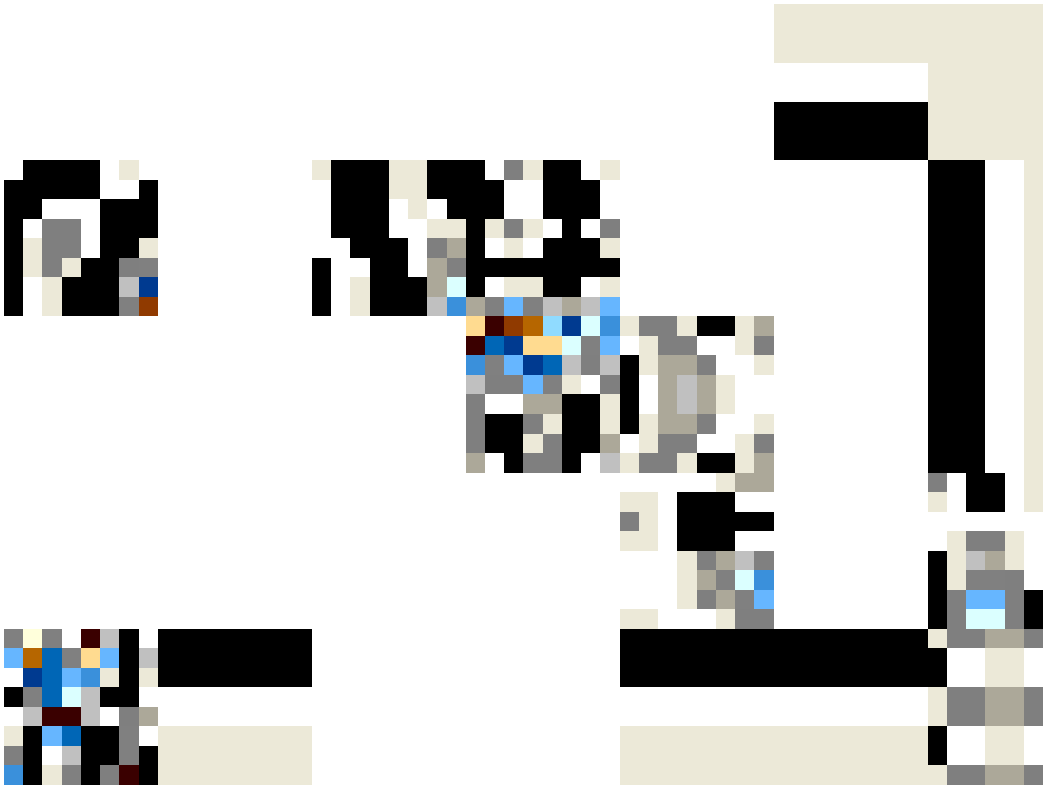

Figure (3.6): The FT-IR Spectrum for untreated sawdust after adsorption with BTB dye.

Figure (3.7): The FT-IR Spectrum for untreated sawdust after adsorption with MGox dye.

3.1.3.2. Sawdust coated polyaniline:

After modification of sawdust with polyaniline, some of the bands of SD have been disappeared and new bands are appeared when it coated with polyaniline polymer as shown in figure (3.8). This proves the formation of SD/PANI over SD. The band N-H stretching is found in 3448.72 cm^{-1} and 3387.00 cm^{-1}, the N-H bending at 1577.77 cm^{-1} and N-H out of plane in 794.67 cm^{-1}. The bands in 2935.66 cm^{-1} and 2877.79 cm^{-1} reveals the C-H stretching. Figure (3.9) show the spectrum of SD/PANI after adsorption with BTB dye. The adsorption bands appeared at 1303.88, 1246.02, 1122.57 and 802.39 cm-1 are attributed to the nitrogen-containing functional groups (such as C-N, C-N^+ and =N^+-H) bands. The nitrogen-containing functional groups can provide many adsorption sites and leads to increase the adsorption capacity for BTB dye by SD/PANI adsorbent [99]. As well as the spectrum of SD/PANI after adsorption with MGox dye as shown in figure (3.10) presented shifting in some of the bands and different in the intensity of the others.

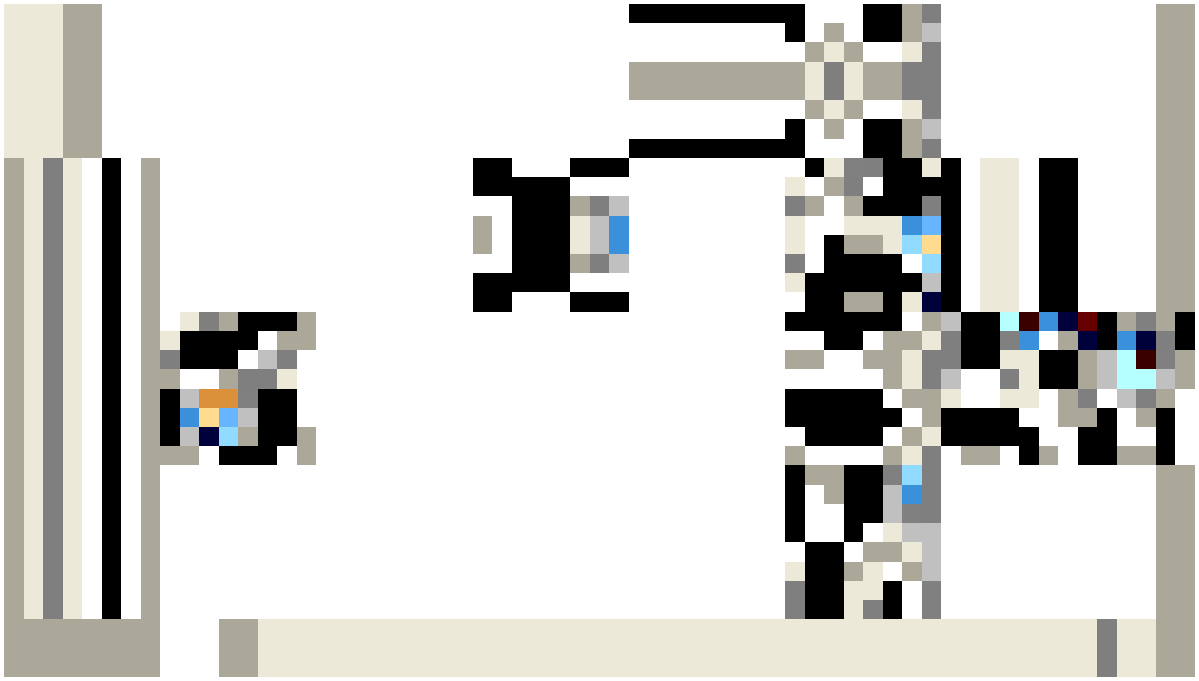

Figure (3.8): The FT-IR Spectrum for sawdust coated polyaniline before adsorption.

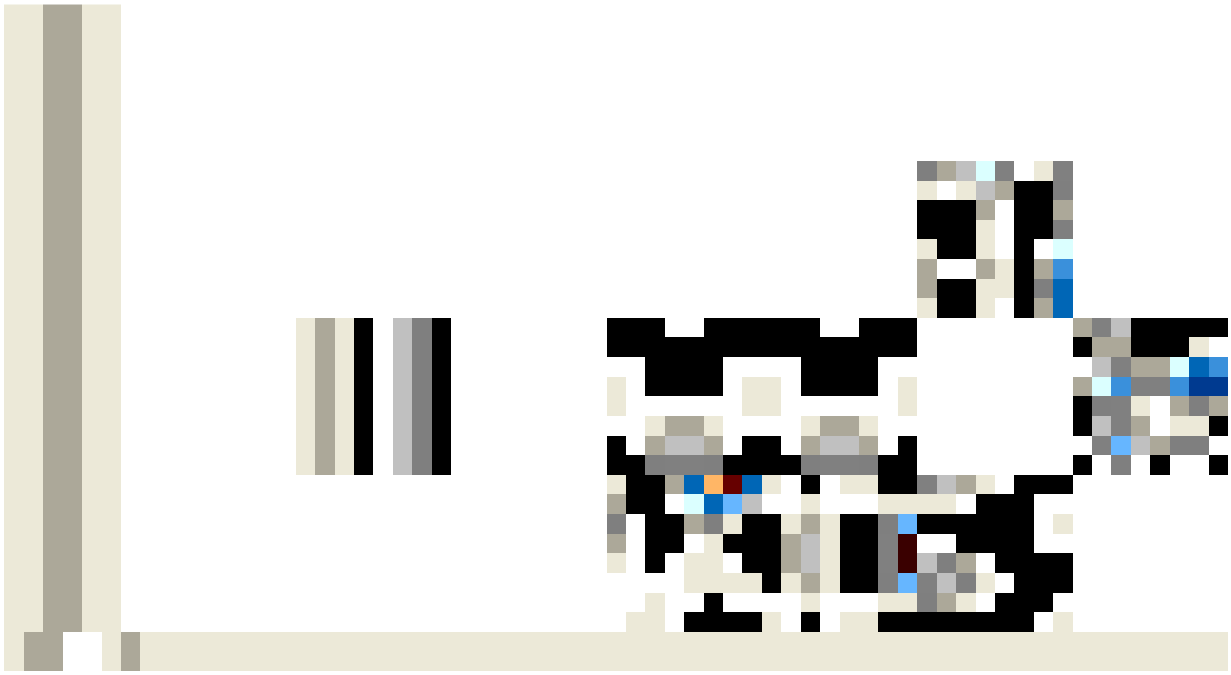

Figure (3.9): The FT-IR Spectrum for sawdust coated polyaniline after adsorption with BTB dye.

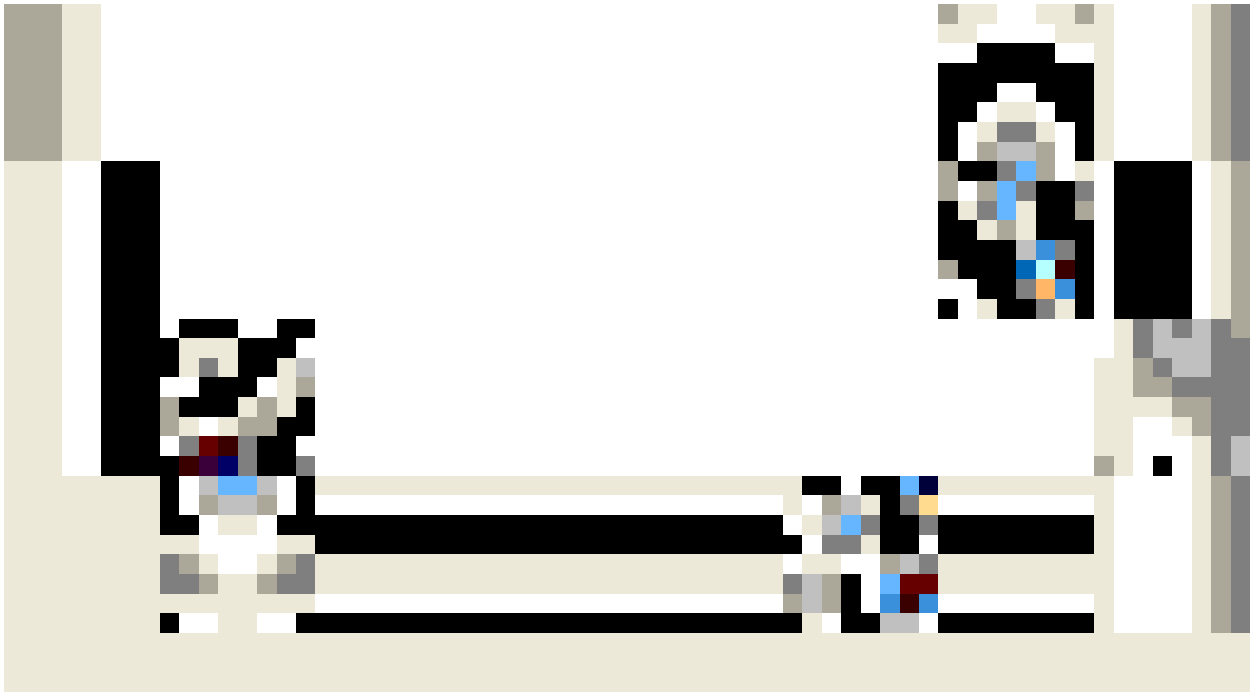

Figure (3.10): The FT-IR Spectrum for sawdust coated polyaniline after adsorption with MGox dye.

3.1.4. SEM analysis:

3.1.4.1. Untreated sawdust:

It is clear from the images of SEM as shown in figures (3.11) and (3.12) of SD before and after the adsorption of dyes, respectively that the surface of sawdust is rough with high porosity. Sawdust is a heterogeneous material consisting of particles of irregular shapes having considerable layers with pores of varying size so it is much possible to adsorb the dyes [78].

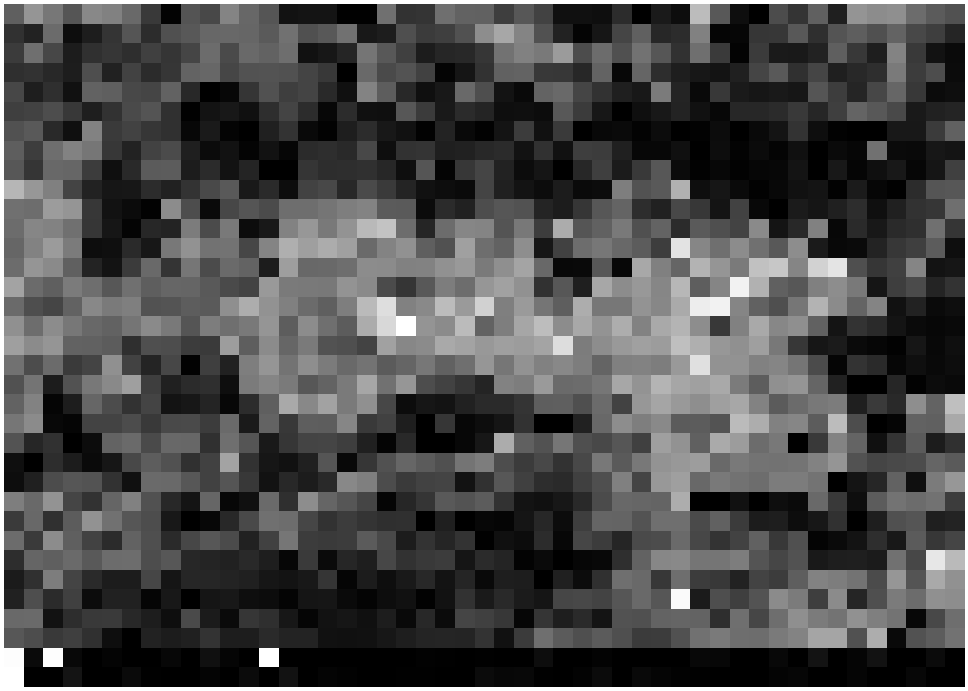

Figure (3.11): The Scanning Electron Microscope (SEM) for untreated sawdust.

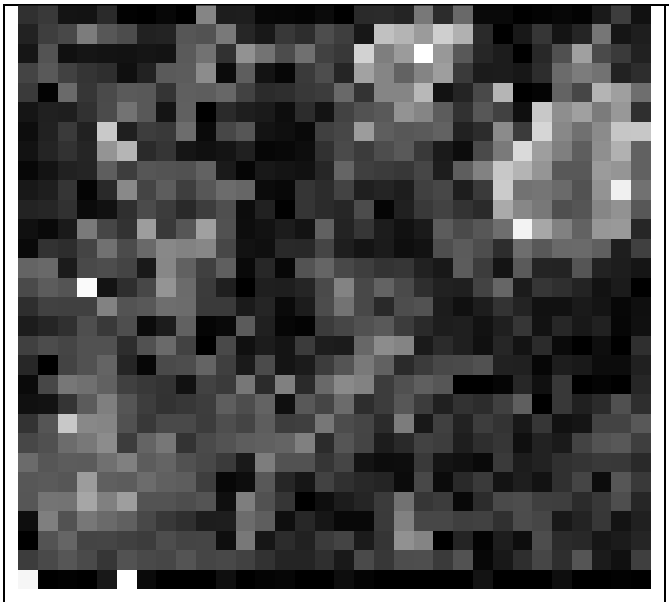

With BTB dye

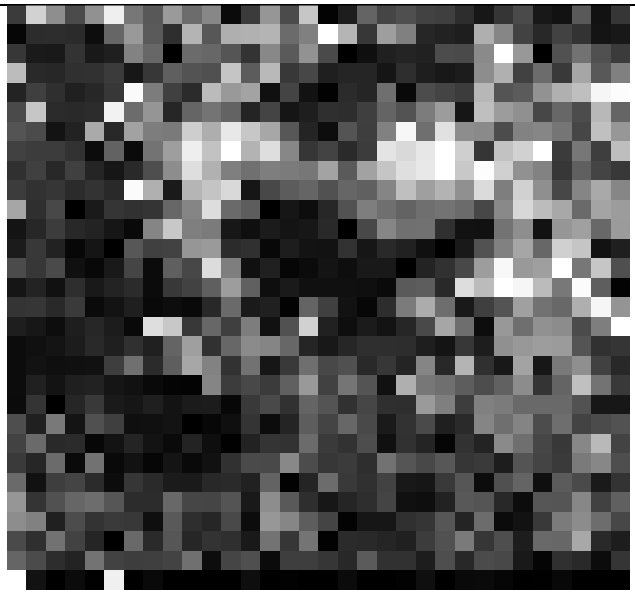

With MGox dye

Figure (3.12): The Scanning Electron Microscope (SEM) for sawdust after adsorption with both dyes.

3.1.4.2. Sawdust coated polyaniline:

The morphology of sawdust surface after coating with polyaniline is illustrated in figure (3.13). It is indicating the formation of the polyaniline on the sawdust surface because the coating with conducting polymer produced by surface polymerization is very clear [100,101]. Not only the small particles of sawdust were coated at the surface but also the big sizes of sawdust have been coated. This means that the reaction mixture diffuses into particles and all SD inside the particles are coated with polyaniline [101].

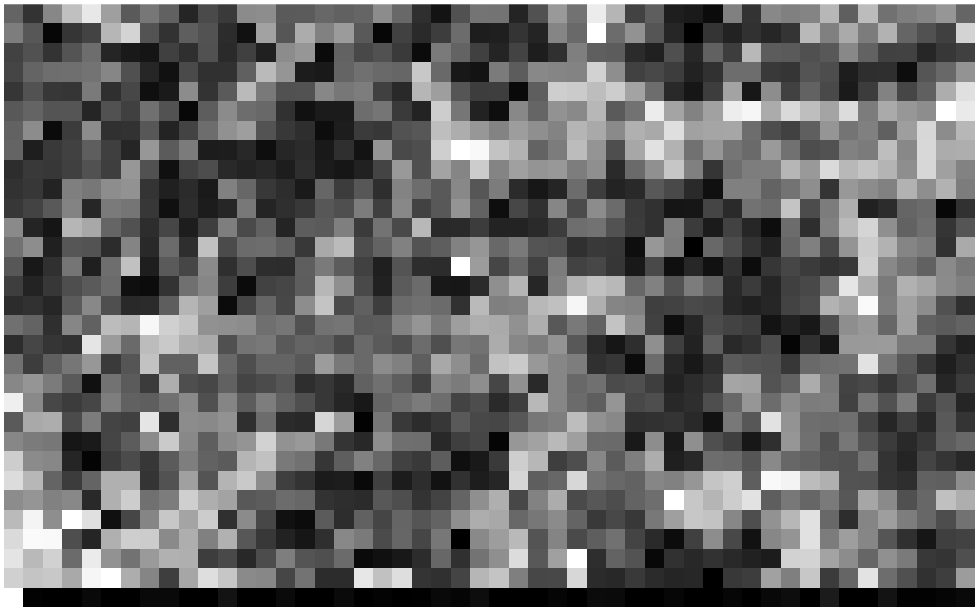

Figure (3.13): The Scanning Electron Microscope (SEM) for sawdust coated polyaniline.

The SEM image for the sawdust coated polyaniline after the adsorption with BTB and MGox dyes shown in figure (3.14), presents a different morphology with sized particles responsible for the especial adsorption properties [99].

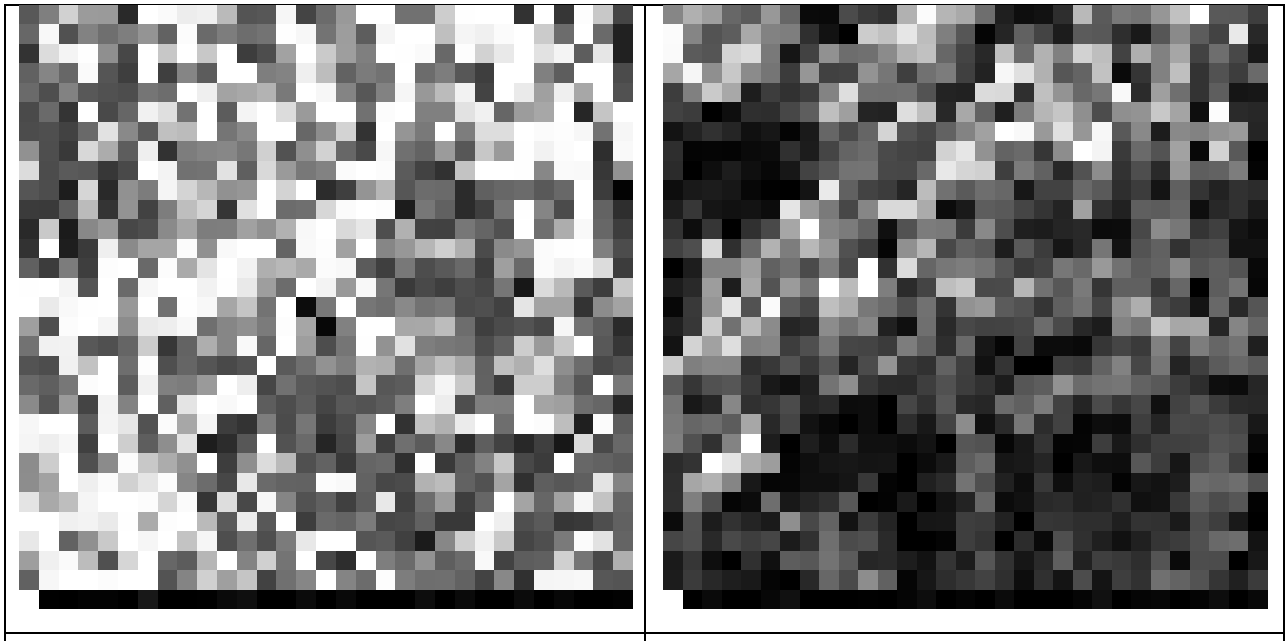

With BTB dye	With MGox dye

Figure (3.14): The Scanning Electron Microscope (SEM) for sawdust coated polyaniline after adsorption with both dye.

3.2. Batch adsorption method of BTB and MGox dyes by SD and SD/PANI composite:

The optimum conditions of dye adsorption on the surface of each of SD and SD/PANI were explained by investigating the effect of contact time, adsorption dose, pH value and temperature.

3.2.1. Effect of contact time:

Adsorption of both dyes (BTB, MGox) at different contact times (5, 10, 15, 20, 25, 30, 35 & 40) minutes were studied at 298 K using a fixed concentration of both dyes (30ppm), the weight of adsorbent (0.03g), 30 mL of dyes solutions and at the original pH of dyes.

3.2.1.1. Effect of contact time on the BTB adsorption:

The adsorption capacity of BTB on SD and SD/PANI surfaces were investigated as shown in figure (3.15). This figure shows that the maximum percentage removal of BTB on SD and SD/PANI composite are 49% and 99% respectively achieved at 15 minutes as shown in table (3.2). These results attributed to the presence of many active binding sites on SD/PANI surface and with the gradual saturation of these sites, the adsorption reaches to a fixed percentage removal [102].

Table (3.2): Adsorption percentage of BTB dye on the SD and SD/PANI surfaces at 298 K.

Time (min.)	Sawdust			Sawdust coated polyaniline		
	c_e (mg/L)	q_e (mg/g)	%R	c_e (mg/L)	q_e (mg/g)	%R
5	22.014	7.986	26.62	4.071	51.858	86.43
10	17.222	12.778	42.59	2.612	54.776	91.293
15	15.215	14.785	49.28	1.153	57.694	96.157
20	15.182	14.818	49.39	0.755	58.49	97.483
25	15.165	14.835	49.45	0.058	59.884	99.807
30	15.0829	14.9171	49.72	0.041	59.918	99.863
35	15.0995	14.9005	49.66	0.041	59.918	99.863
40	15.082	14.918	49.72	0.008	59.984	99.973

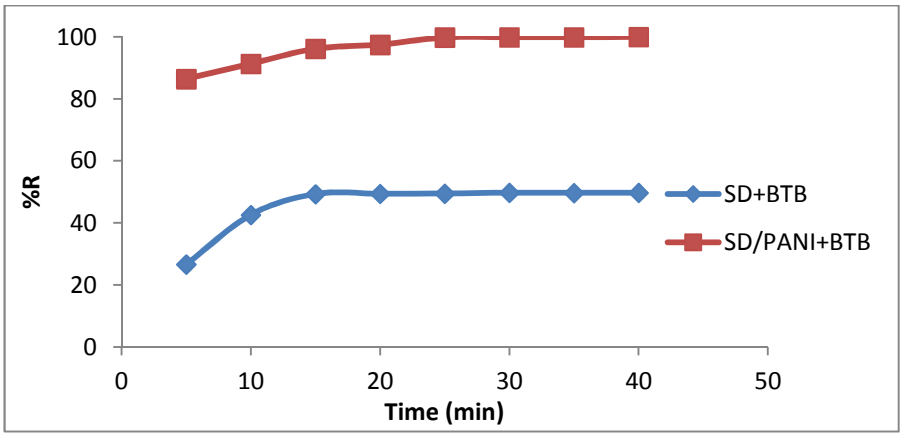

Figure (3.15): Effect of contact time on the adsorption of BTB dye on the SD and SD/PANI surfaces.

3.2.1.2. Effect of contact time on MGox adsorption:

From the analysis of adsorption MGox dye on both adsorbents under study as shown in figure (3.16), it was found that about 87% percentage removal of dye was occurred on SD surface at 20 min due to the presence of large amounts of unoccupied active sites and this percentage decreased to 20% on the SD/PANI surface. These findings are consistent with the results that have been obtained from FT-IR measurements which explained that the surface of SD is anionic charge because of the presence of O-H group so the adsorption of cationic MGox dye is better on SD surface as compared with the cationic SD/PANI surface which contained of N-H group [103].

Table (3.3): Percentage removal of MGox dye on the SD and SD/PANI surfaces at 298 K.

Time (min.)	Sawdust			Sawdust coated polyaniline		
	c_e (mg/L)	q_e (mg/g)	%R	c_e (mg/L)	q_e (mg/g)	%R
5	9.871	20.126	67.096	28.849	1.151	3.837
10	5.130	24.870	82.900	27.397	2.603	8.677
15	4.404	25.596	85.32	25.279	4.721	15.737
20	3.634	26.366	87.886	23.96	6.04	20.133
25	3.619	26.381	87.936	23.901	6.099	20.33
30	3.604	26.396	87.986	23.886	6.114	20.38
35	3.604	26.396	87.986	23.871	7.355	20.43
40	3.590	26.410	88.033	23.841	7.391	20.53

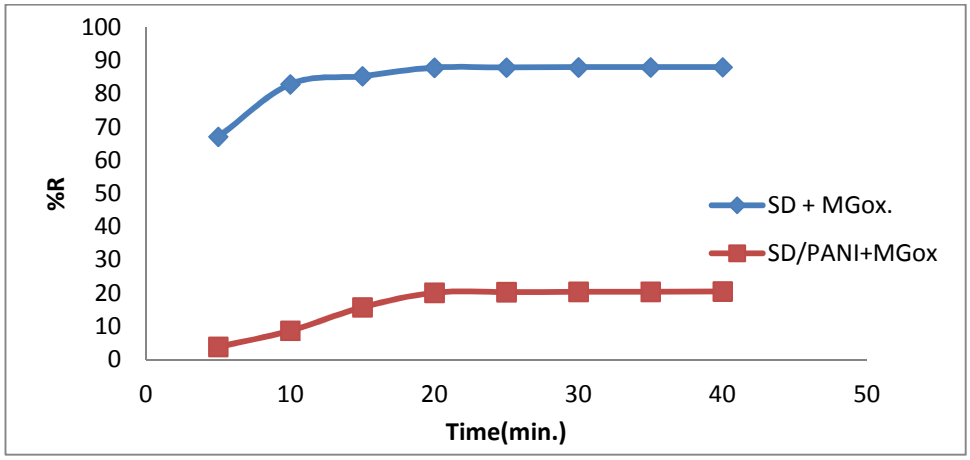

Figure (3.16): Effect of contact time on the adsorption of MGox dye on the SD and SD/PANI surfaces.

3.2.2. Effect of adsorbent dose:

Adsorbent dosage is representing an important parameter due to its strong effect on the adsorbent capacity at a given initial concentration of the adsorbate. The effect of adsorbent dose on the adsorption of BTB and MGox dye was studied by contacting different dose of SD and SD/PANI adsorbents, from 0.005 to 0.05 gm of adsorbent with 30 ml of 30 ppm of dyes solutions for the optimum time of each of dye at original pH of dyes and temperature 298 K.

3.2.2.1. Effect of adsorbent dose on the BTB adsorption:

Table (3.4) shows the values of BTB dye adsorption from aqueous solution by SD and SD/PANI adsorbents at fixed concentration of dye and the data were represented graphically as shown in figure (3.17). The optimum weight of SD and SD/PANI adsorbents to remove the BTB dye is 0.015gm and the percentage removal is 69% and 97% for SD and SD/PANI, respectively. This figure shows that an increase in adsorbent dosage from 0.005gm to 0.05gm resulted in an increase in the percentage removal of BTB dye until it reaches the optimum amount. The decrease in concentration of

BTB in the experimental data after the modification of SD by polyaniline reaches to high removal percentage due to the large amount of unoccupied site in the SD/PANI compared with the sites in SD surface [104].

Table (3.4): BTB dye adsorption values from solution at 298 K on different weight of each of SD and SD/PANI surfaces.

Dose (g)	Sawdust			Sawdust coated Polyaniline		
	c_e (mg/L)	q_e (mg/g)	%R	c_e (mg/L)	q_e (mg/g)	%R
0.005	19.046	65.724	36.513	10.390	117.66	65.367
0.007	15.746	61.088	47.513	6.277	101.67	79.077
0.01	11.484	55.548	61.72	2.678	81.966	91.073
0.015	9.245	41.51	69.183	0.771	58.458	97.43
0.02	9.212	31.182	69.293	0.721	43.919	97.597
0.025	9.179	24.985	69.403	0.705	35.154	97.65
0.03	9.079	20.921	69.736	0.688	29.312	97.707
0.04	9.063	15.702	69.79	0.672	21.996	97.76
0.05	9.046	12.572	69.847	0.655	17.607	97.817

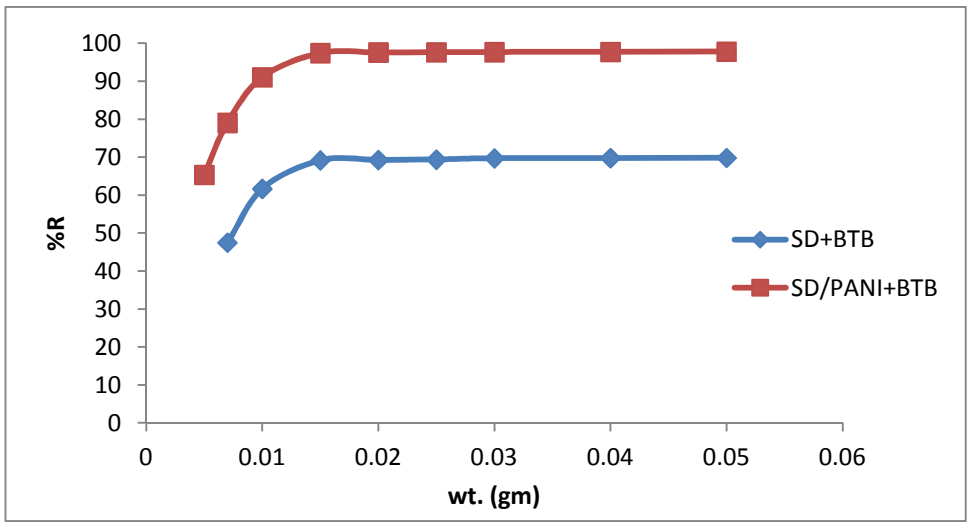

Figure (3.17): Effect of adsorbent dose on BTB dye on each of SD and SD/PANI surfaces at 298 K.

3.2.2.2. Effect of adsorbent dose on the MGox adsorption:

MGox removal efficiencies increase when increasing the adsorbent doses. The worst removal efficiency of MGox (18%) was observed for the SD/PANI surface at the optimum weight (0.025gm) as compared with the percentage for SD surface before the modification (84%) as shown in table (3.5) and figure (3.18). This result is attributed to a conjugate effect of an excess of H^+ ions in the cationic surface of SD/PANI, which could be competed with the positively charged ions of MGox, and also to the relatively low availability of adsorption sites. For SD surface, the removal efficiencies exceeded 84% due to the presence of abundant active sites that could react with MGox ions which facilitates the dye adsorption onto the negative charged surface area of SD [105].

Table (3.5): MGox dye adsorption values from solution at 298 K on different weight of each of SD and SD/PANI surfaces.

Dose (g)	Sawdust		Sawdust coated polyaniline	
	c_e (mg/L)	%R	c_e (mg/L)	%R
0.005	29.441	1.863	29.649	1.170
0.01	24.463	18.456	28.419	5.270
0.015	16.345	45.516	27.086	9.713
0.02	11.071	63.096	25.960	13.467
0.025	4.745	84.183	24.523	18.257
0.03	4.730	84.233	24.493	18.357
0.04	4.685	84.383	24.464	18.453
0.05	4.671	84.43	24.449	18.503
0.06	4.656	84.48	24.434	18.553

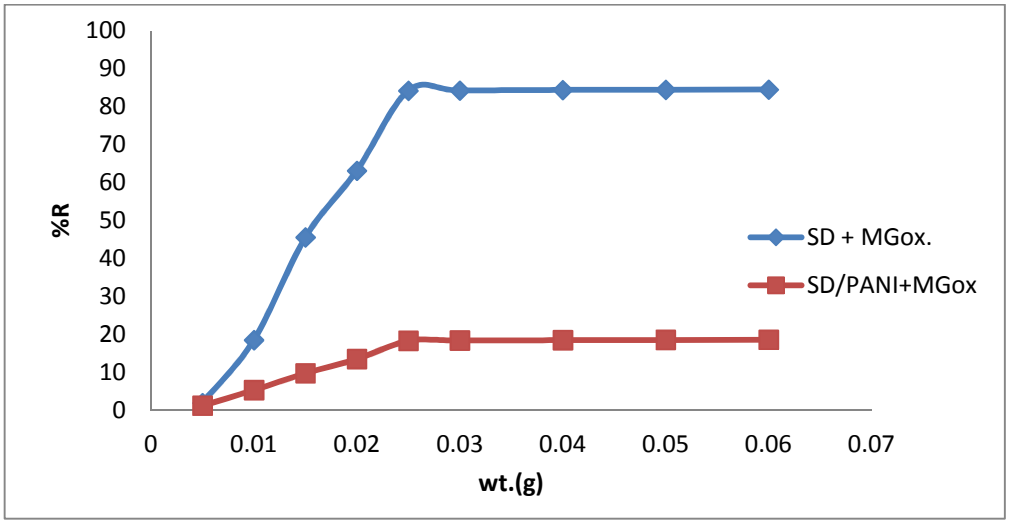

Figure (3.18): Effect of adsorbent dose on MGox dye on each of SD and SD/PANI surfaces at 298 K.

3.2.3. Adsorption Isotherm:

Adsorption isotherms are used to describe the equilibrium actions of dyes on the SD adsorbent before and after modification with polyaniline at different pH (dye's pH, 3, 5, 7, 9 & 11) that involved different concentrations of dyes solutions and at various temperatures (298, 308, & 318)K. The pH solution is very important in the adsorption process because the variation of pH might promote changes in the charges of adsorbents and the adsorbates [106].

3.2.3.1. Adsorption isotherm of BTB on SD and SD/PANI surfaces:

In order to study the effect of pH value and temperature on the adsorption capacity of BTB dye solution at SD and SD/PANI composite, several experiments were carried out. The results of these studies are shown in tables (3.6) & (3.7) and figures (3.19) & (3.20) for SD and SD/PANI surfaces, respectively using different concentrations of BTB dye solution (10, 15, 20, 25 and 30) ppm at different temperatures (298, 308 and 318)K and

solution pH of values (dye pH (3.5-4), 3, 5, 7, 9 and 11). The pH's of the solutions are maintained by means of solutions composed with HCL and NaOH. The data presents in table (3.6) explained that the optimum pH which gives the high percentage removal of BTB dye on SD surface (reaches to 81%, concentration 30ppm, at 318K) is pH=3. On the other hand, the optimum pH of BTB dye adsorption on the SD/PANI surface is the original dye's pH (3.5-4) with percentage removal reaches to 98%, concentration at 30ppm, at 318K as shown in table (3.7). Figure (3.21) shows the effect of pH solution on the removal of BTB dye on SD and SD/PANI surfaces at concentration 30 ppm.

In the adsorption of BTB on the SD surface before modification, high adsorption capacity of BTB dye was appeared in the acidic medium due to the increase the concentration of hydrogen ions (H^+). This happened by adding a proton to the SD surface that lead to increase the forces of attraction between the BTB dye and SD surface and thus gives a higher percentage of adsorption. On the other hand, the increase in pH value lead to decrease the percentage removal of BTB dye on SD surface from 81% to 36% because the surfaces of SD gain more negative charges so electrostatic repulsion result between the BTB dye molecules and SD surface [6, 75].

Table (3.6): Percentage removal of BTB Dye on SD surface at different pH and Temperatures.

pH	298 K				308 K			318 K		
	c_o (mg /L)	c_e (mg/L)	q_e (mg/g)	%R	c_e (mg/L)	q_e (mg/g)	%R	c_e (mg/L)	q_e (mg/g)	%R.
pH dye (3.5-4)	10	4.453	11.094	55.47	4.270	11.46	57.3	4.055	11.89	59.45
	15	6.410	17.18	57.267	6.227	17.546	58.487	5.929	18.142	60.473
	20	8.483	23.034	57.585	8.284	23.432	58.58	7.769	24.462	61.155
	25	9.859	30.282	60.564	9.577	30.846	61.692	9.245	31.51	63.02

	30	11.086	37.828	63.047	10.871	38.258	63.763	10.489	39.022	65.037
3	10	4.043	11.914	59.57	4.012	11.976	59.88	3.794	12.412	62.06
	15	4.479	21.042	70.14	4.448	21.104	70.34	4.261	21.478	71.59
	20	4.071	29.858	74.64	4.009	29.982	74.95	4.635	30.73	76.82
	25	5.538	38.924	77.84	5.476	39.048	78.09	5.040	39.92	79.84
	30	6.224	47.552	79.25	6.161	47.678	79.46	5.538	48.924	81.54
5	10	7.108	5.784	28.92	6.913	6.174	30.87	6.840	6.32	31.6
	15	10.173	9.654	32.18	9.941	10.118	33.72	9.880	10.24	34.13
	20	13.360	13.28	33.2	12.688	14.624	36.56	12.664	14.672	36.68
	25	14.849	20.302	40.60	14.788	20.424	40.84	14.703	20.594	41.18
	30	16.717	26.566	44.27	16.473	27.054	45.09	16.437	27.126	45.21
7	10	8.095	3.81	19.05	8.003	3.994	19.97	7.910	4.18	20.9
	15	11.705	6.59	21.966	11.658	6.684	22.28	11.628	6.744	22.48
	20	14.807	10.386	25.965	14.792	10.416	26.04	14.746	10.508	26.27
	25	17.603	14.794	29.588	17.572	14.856	29.712	17.526	14.948	29.896
	30	20.614	18.772	31.286	20.506	18.988	31.646	20.322	19.356	32.26
9	10	9.080	1.84	9.2	9.014	1.972	9.86	8.982	2.036	10.18
	15	12.544	4.912	16.373	12.495	5.01	16.7	12.200	5.6	18.66
	20	16.122	7.756	19.39	16.073	7.854	19.635	16.024	7.952	19.88
	25	19.553	10.894	21.788	19.374	11.252	22.504	19.341	11.318	22.636
	30	19.668	20.664	34.44	19.586	20.828	34.713	19.553	20.894	34.823
11	10	6.911	6.178	30.89	6.876	6.248	31.24	6.788	6.424	32.12
	15	10.204	9.592	31.973	10.169	9.662	32.206	10.116	9.768	32.56
	20	13.25	13.500	33.75	13.144	13.712	34.28	13.091	13.818	34.545
	25	16.454	17.092	34.184	16.419	17.162	34.748	15.996	18.008	36.016
	30	19.235	21.530	35.88	19.200	21.6	36.0	19.077	21.846	36.41

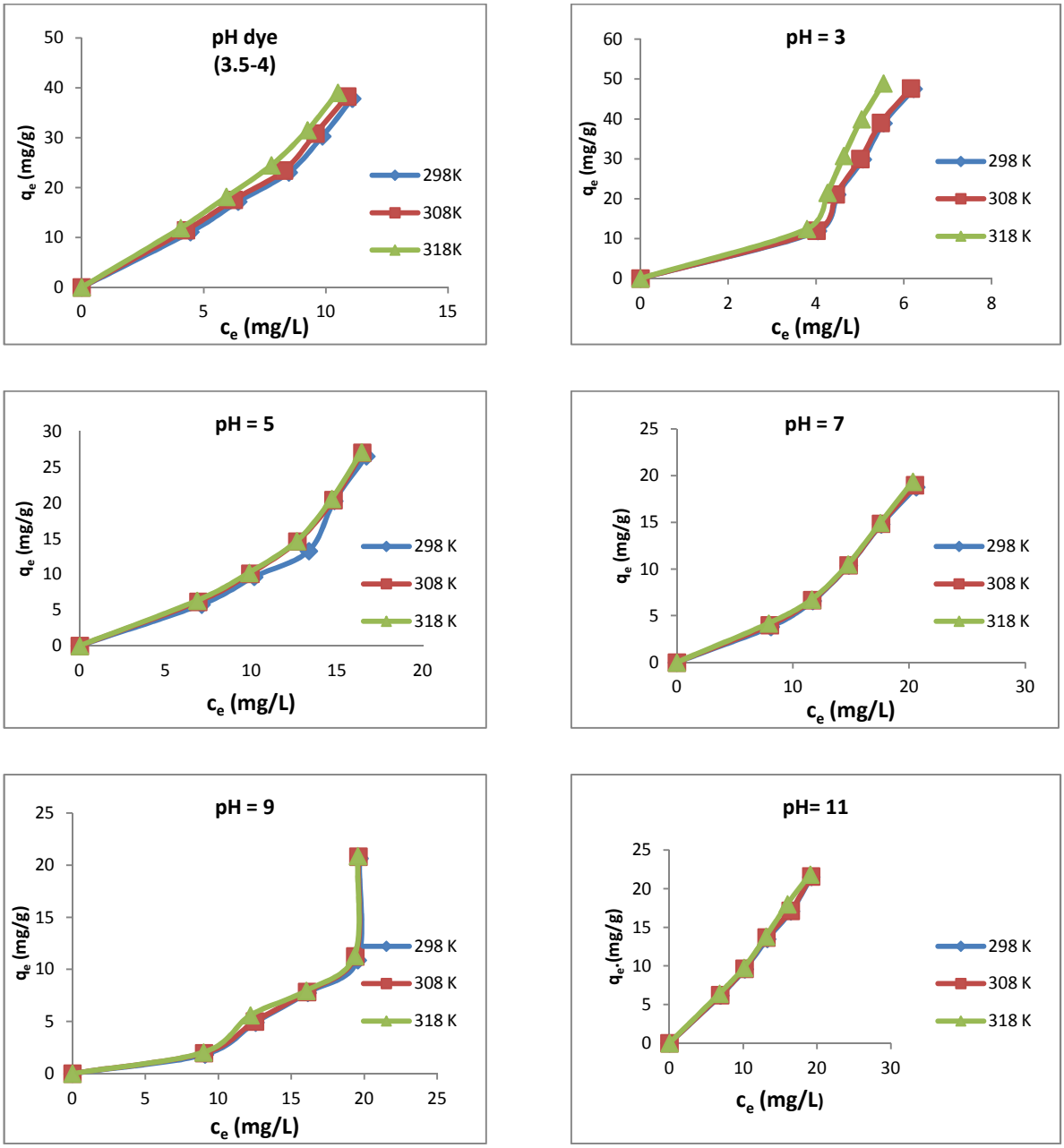

Figure (3.19): Adsorption isotherm of BTB on the SD surface at different pH and temperatures.

For SD/PANI composite surface, the adsorption capacity of BTB dye getting its high value at original dye's pH (3.5-4) which give 99% percentage removal because of the presence of polyaniline that lead to increase the surface area of the SD and increase the adsorption capacity of BTB dye. The presence of (H^+) ions influence the adsorption capacity to a very large extent

so when the pH is low (pH=3), the percentage removal of BTB dye decrease due to the electrostatic repulsion between the H^+ ions in the acidic solution and the functional groups in SD/PANI surface. At the original pH of BTB dye, the percentage removal of dye increase because there is a high degree of protonation occurs in the groups like N-H and N-H_2 present on the surface of SD/PANI that in turn increases the electrostatic attraction. This subsequently leads to hydrogen bond formation between the positive charge on the surface of SD/PANI and the functional groups on BTB dye. When the pH increase to 9, the percentage removal of BTB dye was decreased to 74% due to hydroxyl ions occupy the active sites of the SD/PANI surface which reduces the uptake capacity [66, 74].

Table (3.7): The percentage removal of BTB dye on SD/PANI surface at different pH and temperatures.

pH		298K			308K			318K		
	c_o (mg/L)	c_e (mg/L)	q_e (mg/g)	%R	c_e (mg/L)	$q_{e.}$ (mg/g)	%R	c_e (mg/L)	q_e (mg/g)	%R
pH dye (3.5-4)	10	0.556	18.888	94.44	0.423	19.154	95.77	0.340	19.32	96.6
	15	0.605	28.79	95.967	0.456	29.088	96.96	0.390	29.22	97.4
	20	0.638	38.724	96.81	0.522	38.956	97.39	0.456	39.088	97.72
	25	0.688	48.624	97.248	0.572	48.856	97.712	0.489	49.022	98.044
	30	0.804	58.392	97.32	0.655	58.69	97.817	0.556	58.888	98.147
3	10	3.981	12.038	60.19	3.919	12.162	60.81	3.794	12.412	62.06
	15	4.106	21.788	72.627	4.044	21.912	73.04	3.981	22.038	73.46
	20	4.262	31.476	78.69	4.168	31.664	79.16	4.075	31.85	79.625
	25	4.636	40.728	81.456	4.573	40.854	81.708	4.386	41.228	82.456
	30	4.885	50.23	83.717	4.822	50.356	83.927	4.667	50.666	84.448
5	10	2.786	14.428	72.14	2.737	14.526	72.63	2.554	14.892	74.46
	15	2.847	24.306	81.02	2.750	24.5	81.667	2.579	24.842	82.807
	20	3.360	33.28	83.2	3.006	33.988	84.97	2.945	34.11	85.275
	25	3.934	42.132	84.264	3.531	42.938	85.876	3.409	43.182	86.364
	30	4.496	51.008	85.013	4.142	51.716	86.193	3.971	52.058	86.763
7	10	2.934	14.132	70.66	2.873	14.254	71.27	2.780	14.44	72.2
	15	3.026	23.948	79.827	2.888	24.224	80.747	2.811	24.378	81.26
	20	3.610	32.78	81.95	3.318	33.364	83.41	3.026	33.948	84.87
	25	4.240	41.52	83.04	4.101	41.798	83.596	3.763	42.474	84.948
	30	4.869	50.262	83.77	4.608	50.784	84.64	4.316	51.368	85.613
	10	4.211	11.578	57.89	3.998	12.004	60.02	3.802	12.396	61.98

9	15	5.109	19.782	65.94	4.848	20.304	67.68	4.521	20.958	69.86
	20	6.564	26.872	67.18	6.319	27.362	68.405	5.534	28.932	72.33
	25	7.887	34.226	68.452	7.528	34.944	69.888	6.580	36.84	73.68
	30	8.949	42.102	70.17	8.263	43.474	72.457	7.789	44.422	74.037

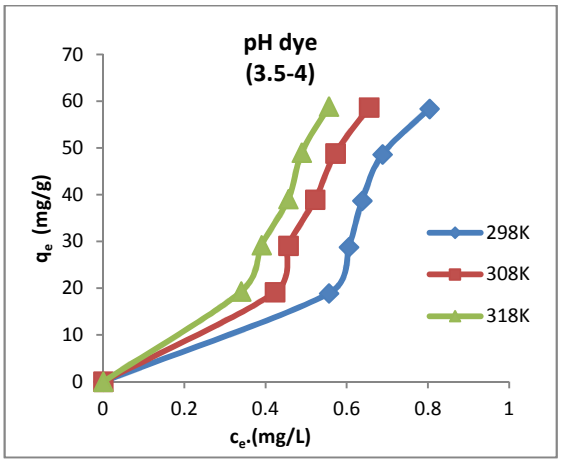

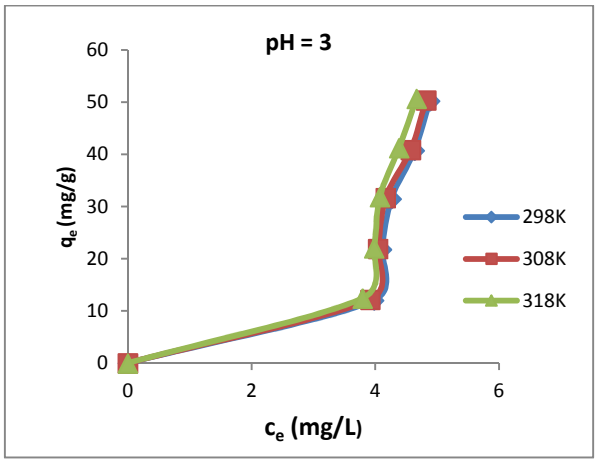

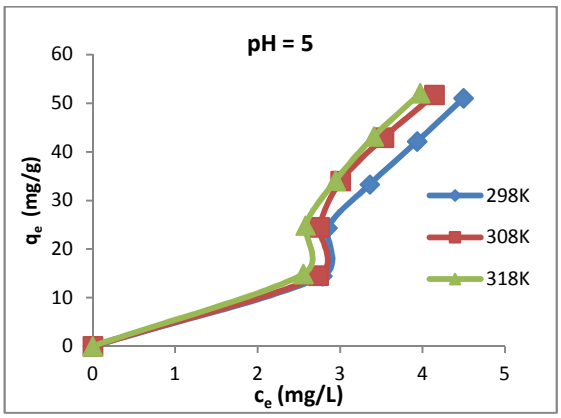

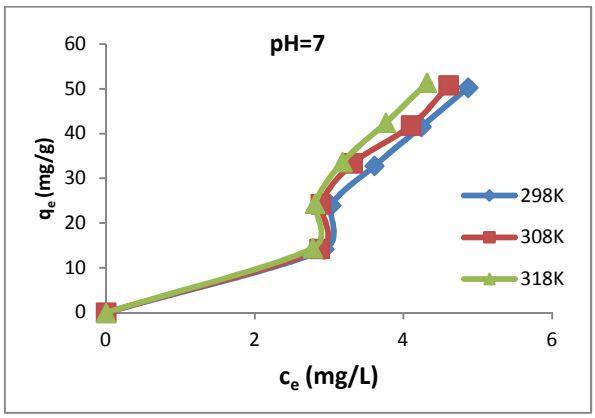

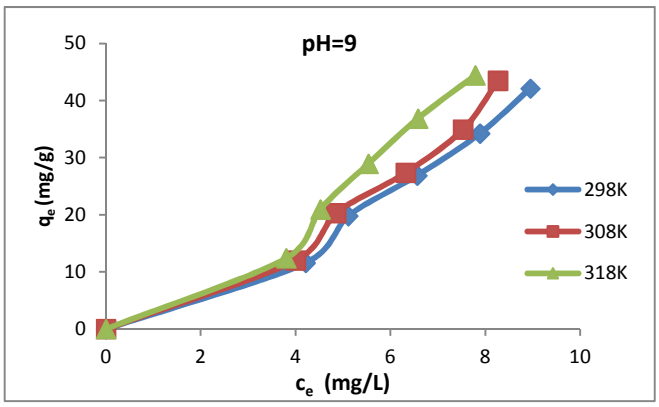

Figure (3.20): Adsorption isotherm of BTB on the SD/PANI surface at different pH and temperatures.

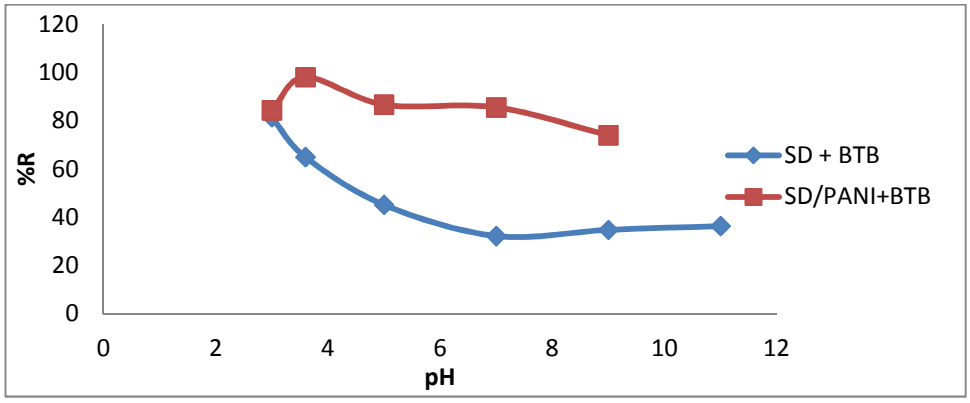

Figure (3.21): The effect of pH values of the adsorption of BTB on SD and SD/PANI at 30ppm and 318K.

3.2.3.2. Adsorption isotherm of MGox on SD and SD/PANI surfaces:

This effect of pH values on the adsorption of MGox dye on the SD and SD/PANI composite surfaces were investigated at different initial dye concentrations (15, 20, 25, 30, 35 and 40) ppm at various temperatures as shown in table (3.8) and figure (3.22). The mechanism and extent of dye adsorption are affected by the pH of the solution because of the presence of different functional groups and atoms on dye and adsorbent surface. The effect of pH of the MGox dye solution was studied by varying pH values. The optimum pH value that gives maximum percentage removal (99%) of MGox dye on SD surface is 5 for 25 ppm initial MGox concentration at 318K as shown in figure (3.24). The percentage removal of MGox decreased with increase the concentration of it. At lower MGox concentration, adsorbent surface area to reactive vacant site ratio is much higher which causes higher extent of dye removal. Gradual increase in MGox concentrations leads to increase in the ratio of free MGox molecules to unoccupied sites that significantly reduce the mass transport and removal efficiency. At lower pH (< 5) all reactive sites (SD surface and MGox molecules) got positively charged because of increase the protons (H^+) in aqueous media so the

repulsive forces between all groups is likely to be raised when the pH decreased leads to decreasing the percentage removal of dye. The gradual rise to pH 5 leads to deprotonation of groups causing electrostatic interaction, hydrogen bonding. This increases the magnitude of dye migration and diffusion to the SD surface. On the other hand, the percentage removal significantly decreased at pH up to 5 due to the negative charges of both adsorbent and dye molecules are causing repulsion [89,107].

Table (3.8): The percentage removal of MGox dye on SD surface at different pH and temperatures.

pH	298K				308K			318K		
	c_o (mg/L)	c_e (mg/L)	q_e (mg/g)	%R	c_e (mg/L)	q_e (mg/g)	%R	c_e (mg/L)	q_e (mg/g)	%R
3	15	8.347	7.983	44.353	7.632	8.841	49.12	6.284	10.459	58.106
	20	12.723	8.732	36.385	12.008	9.590	39.96	10.993	10.808	45.035
	25	17.698	8.762	29.208	16.917	9.700	32.332	15.202	11.757	39.192
	30	21.292	10.449	29.026	20.510	11.388	31.633	19.612	12.465	34.626
	35	25.236	11.716	27.897	24.920	12.096	28.817	24.004	13.195	31.417
	40	29.429	12.685	26.427	28.946	13.264	27.635	28.181	14.182	29.547
pH dye (3.5-4)	15	2.197	15.364	85.358	1.841	15.791	87.727	1.308	16.430	91.28
	20	3.116	20.261	84.42	2.804	20.635	85.98	2.479	21.025	87.605
	25	4.390	24.732	82.44	4.034	25.159	83.864	3.649	25.621	85.404
	30	5.338	29.594	82.207	5.027	29.968	83.243	4.641	30.431	84.53
	35	6.671	33.995	80.94	6.316	34.421	81.954	6.153	34.616	82.42
	40	8.538	37.754	78.655	8.227	38.128	79.433	7.767	38.680	80.583
5	15	----	----	----	----	----	----	----	----	----
	20	----	----	----	----	----	----	----	----	----
	25	1.099	28.681	95.604	0.618	29.258	97.52	0.076	29.908	99.699
	30	2.693	32.768	91.023	0.918	34.898	96.94	0.663	35.204	97.79
	35	5.234	35.719	85.045	2.557	38.931	92.69	1.911	39.706	94.54
	40	6.783	39.860	83.042	5.565	41.322	86.08	2.903	44.516	92.74
7	15	1.291	16.451	91.393	0.571	17.314	96.193	0.306	17.632	97.96
	20	2.162	21.405	89.19	1.481	22.222	92.595	0.534	23.359	97.33
	25	3.091	26.291	87.636	2.825	26.61	88.7	1.859	27.769	92.564
	30	4.928	30.086	83.573	4.075	31.11	86.416	2.371	33.154	92.096
	35	7.541	32.951	78.454	5.628	35.246	83.92	3.431	37.882	90.197
	40	9.056	37.132	77.36	8.242	38.109	79.395	5.079	41.905	87.302
9	15	2.234	15.319	85.106	1.797	15.843	88.02	1.344	16.387	91.04
	20	3.464	19.843	82.68	2.509	20.989	87.45	2.137	21.435	89.315
	25	4.629	24.445	81.484	3.707	25.551	85.172	2.898	26.522	88.408

	30	6.037	28.755	79.87	4.629	30.445	84.57	3.966	31.240	86.78
	35	7.364	33.163	78.96	6.991	33.610	80.02	6.118	34.658	82.52
	40	8.836	37.396	77.91	8.059	38.329	79.85	7.331	39.202	81.67
11	15	7.467	9.040	50.22	6.133	10.640	59.113	5.467	11.440	63.553
	20	10.8	11.04	46.00	8.8	13.44	56.00	7.467	15.040	62.665
	25	13.625	13.65	45.5	11.125	16.65	55.5	9.875	18.15	60.5
	30	16.75	15.9	44.16	13.625	19.65	54.58	12.375	21.15	58.75
	35	19.875	18.15	43.21	16.125	22.65	53.92	14.875	24.15	57.5
	40	23.625	19.65	40.93	20.5	23.4	48.75	18.133	26.240	54.668

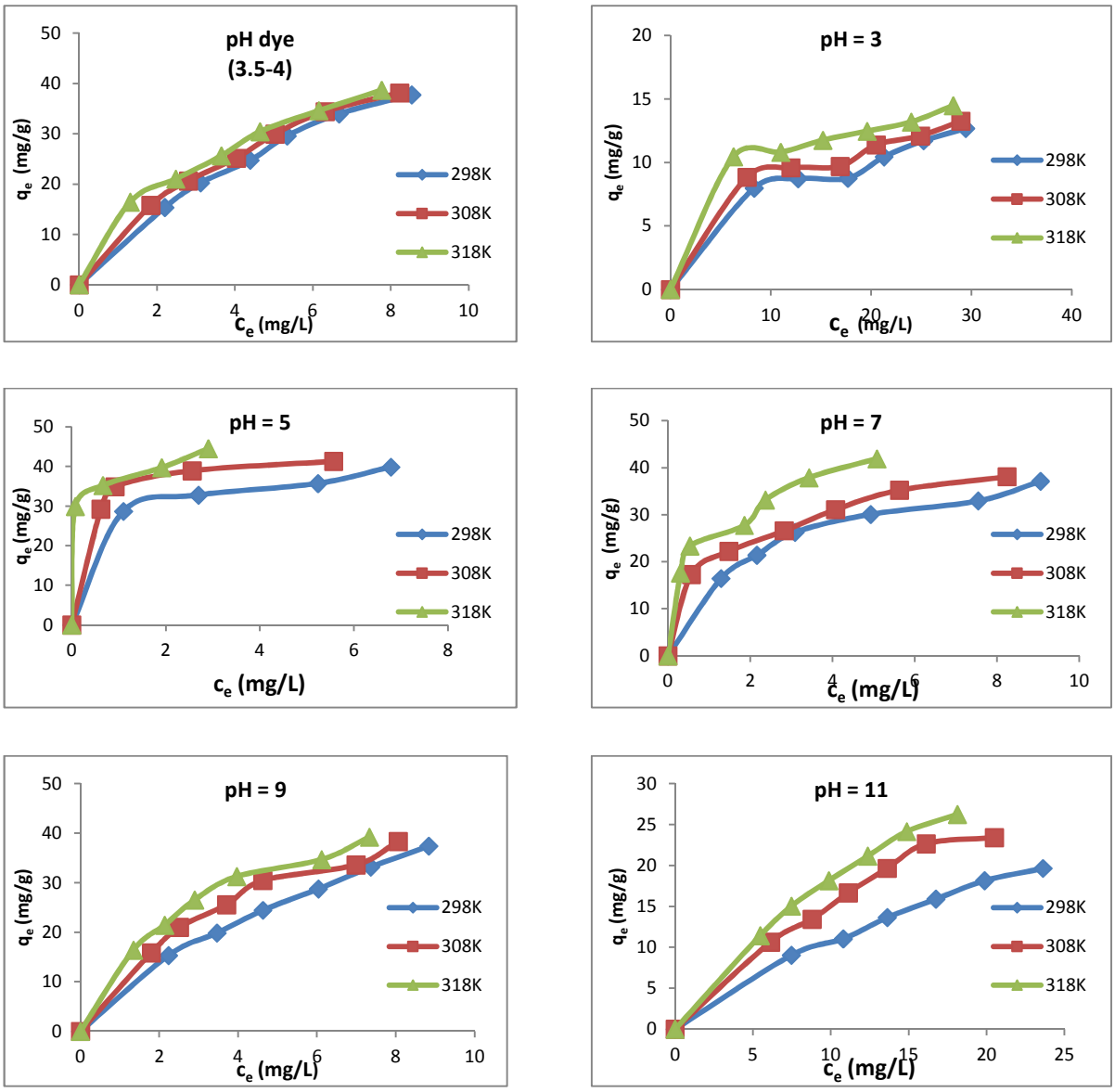

Figure (3.22): Adsorption isotherm of MGox on the SD surface at different pH and temperatures.

The adsorption capacities of MGox dye on the SD/PANI surface are given in table (3.9) and figure (3.23). The data shows that the percentage removal of dye on the SD/PANI surface is lower than those on the SD surface. The optimum pH for MGox adsorption by SD/PANI was found at the original pH of the dye but the percentage removal remains little (reaches to 30%) as compared to the results that found on the unmodified SD surface. Lower percentage removal at highly acidic pH might be due to the competition between the positively charges of MGox and hydrogen ions. Also at low pH (pH < 4), the SD/PANI surface became more positively charged thus reducing attraction between the adsorbent and dye. Further increase in pH (beyond pH 4) may be attributed to the precipitation of MGox as complexes leads to reduces the concentration of MGox in the solution and thus decreases the removal efficiency of SD/PANI adsorbent [108,109]. Figure (3.24) explained the results of MGox removal on the surface each of SD and SD/PANI at initial concentration (25ppm) that give high percentage removal compared with the other concentrations and at 318K which are show that the percentage removal of dye on the SD higher than the removal on the SD/PANI surface.

Table (3.9): The percentage removal of MGox dye on SD/PANI surface at different pH and temperatures.

pH	c_o. (mg/L)	298K			308K			318K		
		c_e. (mg/L)	q_e. (mg/g)	%R	c_e. (mg/L)	q_e. (mg/g)	%R	c_e. (mg/L)	q_e. (mg/g)	%R
pH dye (3.5-4)	15	10.893	4.928	27.38	10.790	5.052	28.067	10.464	5.443	30.240
	20	15.086	5.897	24.57	14.804	6.235	25.98	14.538	6.554	27.310
	25	20.064	5.923	19.744	19.441	6.671	22.236	19.056	7.133	23.776
	30	24.390	6.732	18.700	24.227	6.928	19.243	23.782	7.462	20.727
	35	28.716	7.541	17.983	28.641	7.631	18.169	28.464	7.843	18.674
	40	33.693	7.568	15.768	33.427	7.888	16.433	33.175	8.19	17.063
	15	12.227	3.328	18.487	11.535	4.153	23.1	10.814	5.023	27.907
	20	16.904	3.715	15.48	15.836	4.997	20.82	15.325	5.61	23.375

5	25	21.701	3.959	13.196	20.468	5.438	19.932	19.4	6.72	22.400
	30	26.618	4.058	11.273	25.355	5.574	15.483	23.701	7.559	20.097
	35	31.295	4.446	10.586	30.062	5.926	14.109	28.558	7.730	18.406
	40	36.152	4.618	9.62	34.528	6.566	13.68	33.265	8.082	16.838
9	15	12.769	2.677	14.873	12.380	3.144	17.467	11.830	3.804	21.133
	20	17.251	3.299	13.745	16.733	3.920	16.334	16.005	4.794	19.975
	25	22.057	3.532	11.772	21.604	4.075	13.584	20.827	5.008	16.692
	30	26.846	3.785	10.513	26.215	4.542	12.617	25.503	5.396	14.990
	35	31.749	3.901	9.289	31.183	4.580	10.906	30.341	5.591	13.311
	40	36.523	4.172	8.693	36.134	4.639	9.665	35.244	5.707	11.890

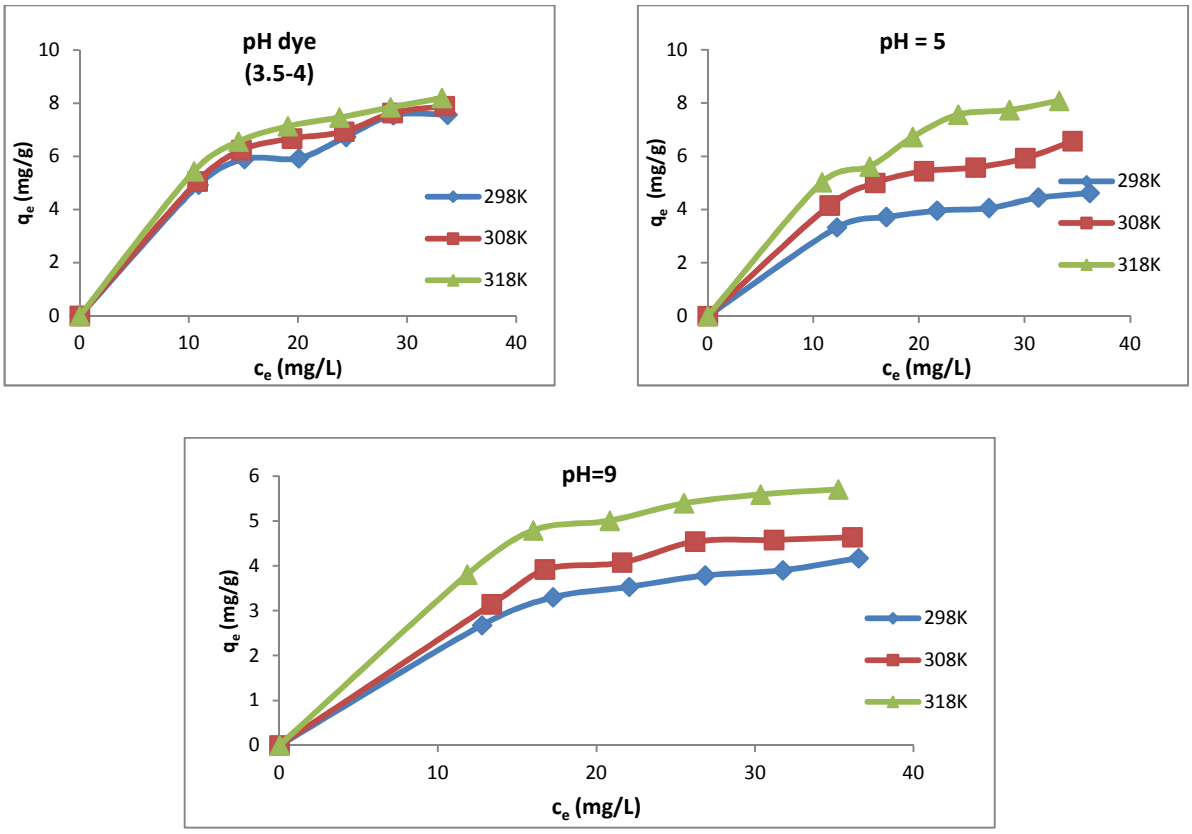

Figure (3.23): Adsorption isotherm of MGox on the SD/PANI surface at different pH and temperatures.

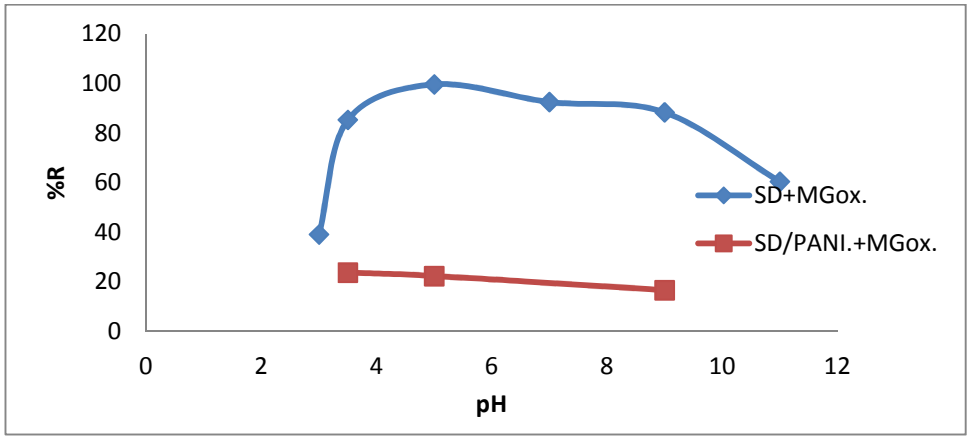

Figure (3.24): The effect of pH of the adsorption of MGox on SD and SD/PANI at 30ppm and 318K.

3.3. Equilibrium isotherm modeling of dye adsorption:

Adsorption properties and equilibrium parameters, usually known as adsorption isotherms which describe the interactions between the adsorbent and adsorbate and understanding the nature of these interactions at different temperatures and pH values. The most common models were employed for describing the adsorption data, which were Langmuir, Freundlich and Dubinin-Radushkevich isotherms. These isotherms were carried out for each of BTB and MGox dyes on the SD and SD/PANI surfaces.

3.3.1. Equilibrium isotherm modeling of BTB dye on the SD and SD/PANI surfaces:

3.3.1.1. Langmuir isotherm model:

The Langmuir adsorption isotherm data that previously shown in equation (1.1) for BTB adsorption onto each of SD and SD/PANI surface were indicated in tables (3.10) and (3.11), respectively. The graphical plots of c_e/q_e versus c_e of a linearized Langmuir equation for each adsorbent surface were also represented in figures (3.25) and (3.26), respectively. From the slope and intercept of the plot between c_e/q_e versus c_e, the Langmuir constants

which are k_L and q_{max} that related to the energy of adsorption were calculated. Also the R_L (separation factor) was determined from equation (1.2).

Table (3.10): Adsorption values of BTB on SD surface with Langmuir isotherm model calculations at different temperatures and pH.

pH	c_o (mg/L)	298 K		308 K		318 K	
		c_e (mg/L)	c_e/q_e (g/L)	c_e (mg/L)	c_e/q_e (g/L)	c_e (mg/L)	c_e/q_e (g/L)
3	10	4.043	0.339	4.012	0.335	3.794	0.305
	15	4.479	0.212	4.448	0.210	4.261	0.198
	20	5.071	0.169	4.009	0.167	4.635	0.150
	25	5.538	0.174	5.476	0.140	5.040	0.126
	30	6.224	0.130	6.161	0.129	5.538	0.113
pH dye (3.5-4)	10	4.453	0.401	4.270	0.373	4.055	0.341
	15	6.410	0.373	6.227	0.355	5.929	0.327
	20	8.483	0.368	8.284	0.354	7.769	0.318
	25	9.859	0.326	9.577	0.310	9.245	0.293
	30	11.086	0.293	10.871	0.284	10.489	0.269
5	10	7.108	1.228	6.913	1.119	6.840	1.082
	15	10.173	1.053	9.941	0.982	9.880	0.964
	20	13.360	1.006	12.688	0.867	12.664	0.863
	25	14.849	0.731	14.788	0.724	14.703	0.713
	30	16.717	0.629	16.473	0.608	16.437	0.605
7	10	8.095	2.124	8.003	2.003	7.910	1.892
	15	11.705	1.776	11.658	1.744	11.628	1.724
	20	14.807	1.425	14.792	1.420	14.746	1.403
	25	17.603	1.189	17.572	1.182	17.526	1.172
	30	20.614	1.098	20.506	1.079	20.322	1.049
9	10	9.080	4.934	9.014	4.570	8.982	4.411
	15	12.544	2.553	12.495	2.494	12.200	2.178
	20	16.122	2.078	16.073	2.046	16.024	2.015
	25	19.553	1.794	19.374	1.721	19.341	1.708
	30	19.668	0.951	19.586	0.940	19.553	0.935
11	10	6.911	1.118	6.876	1.100	6.788	1.056
	15	10.204	1.063	10.169	1.052	10.116	1.035
	20	13.25	0.981	13.144	0.958	13.091	0.947
	25	16.454	0.962	16.419	0.956	15.996	0.888
	30	19.235	0.893	19.200	0.888	19.077	0.873

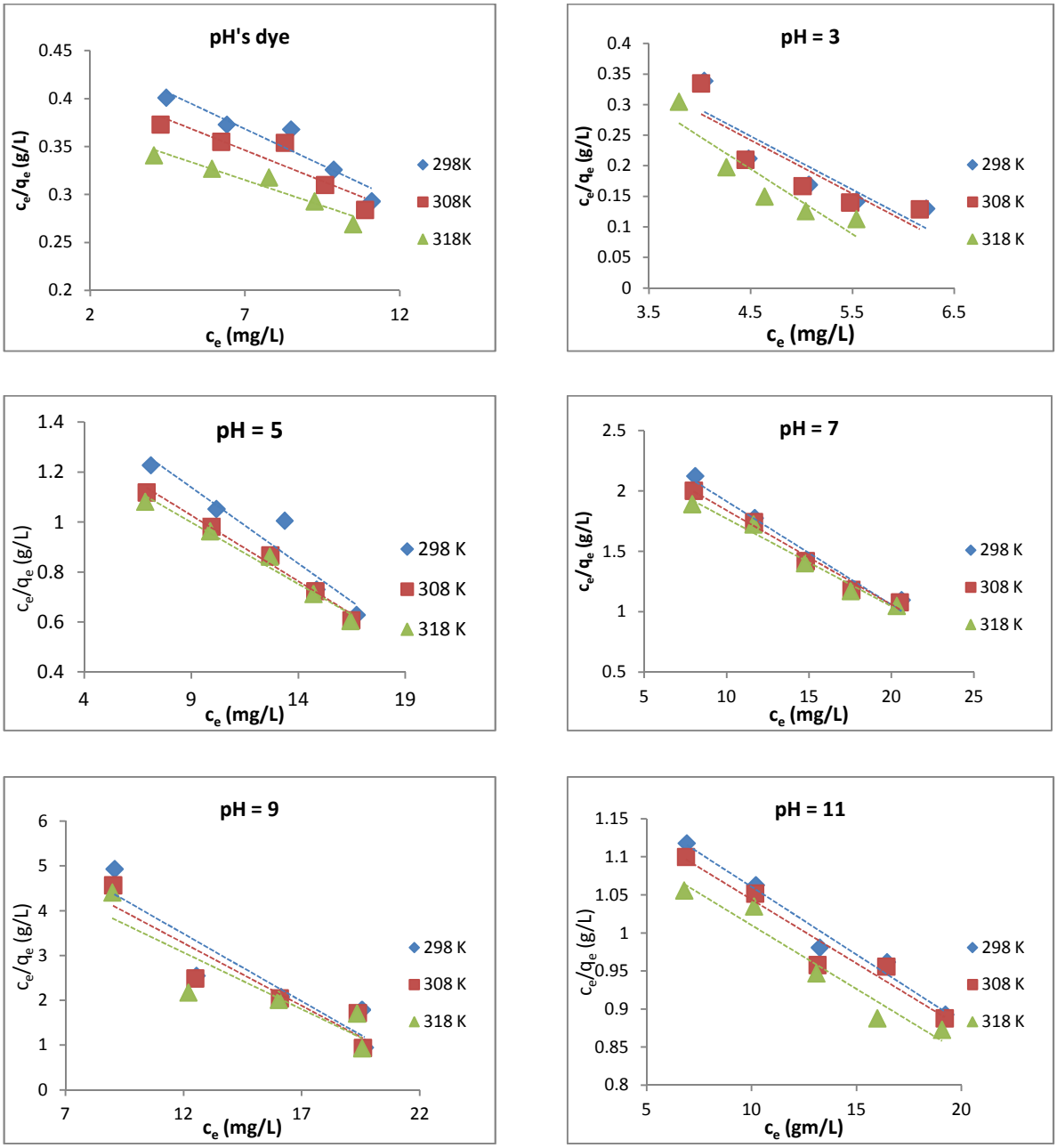

Figure (3.25): Langmuir adsorption isotherm for the adsorption of BTB dye on SD surface at different temperatures and pH.

Table (3.11): Adsorption values of BTB on SD/PANI surface with Langmuir isotherm model calculations at different temperatures and pH.

pH	c_o mg/L	298K		308K		318K	
		c_e mg/L	c_e/q_e g/L	c_e mg/L	c_e/q_e g/L	c_e mg/L	c_e/q_e g/L
pH dye (3.5-4)	10	0.556	0.029	0.423	0.022	0.340	0.018
	15	0.605	0.021	0.456	0.016	0.390	0.013
	20	0.638	0.016	0.522	0.013	0.456	0.012
	25	0.688	0.014	0.572	0.012	0.489	0.010
	30	0.804	0.014	0.655	0.011	0.556	0.009
3	10	3.981	0.331	3.919	0.322	3.794	0.306
	15	4.106	0.188	4.044	0.185	3.981	0.181
	20	4.262	0.135	4.168	0.132	4.075	0.128
	25	4.636	0.114	4.573	0.112	4.386	0.106
	30	4.885	0.097	4.822	0.096	4.667	0.092
5	10	2.786	0.193	2.737	0.188	2.554	0.172
	15	2.847	0.117	2.750	0.112	2.579	0.104
	20	3.360	0.101	3.006	0.088	2.945	0.086
	25	3.934	0.093	3.531	0.082	3.409	0.079
	30	4.496	0.088	4.142	0.080	3.971	0.076
7	10	2.934	0.208	2.873	0.202	2.780	0.193
	15	3.026	0.126	2.888	0.119	2.811	0.115
	20	3.610	0.110	3.318	0.099	3.180	0.095
	25	4.240	0.102	4.101	0.098	3.763	0.089
	30	4.869	0.097	4.608	0.091	4.316	0.084
9	10	4.211	0.364	3.998	0.333	3.802	0.307
	15	5.109	0.258	4.848	0.239	4.521	0.216
	20	6.564	0.244	6.319	0.231	5.534	0.191
	25	7.887	0.230	7.528	0.215	6.580	0.179
	30	8.949	0.213	8.263	0.190	7.789	0.175

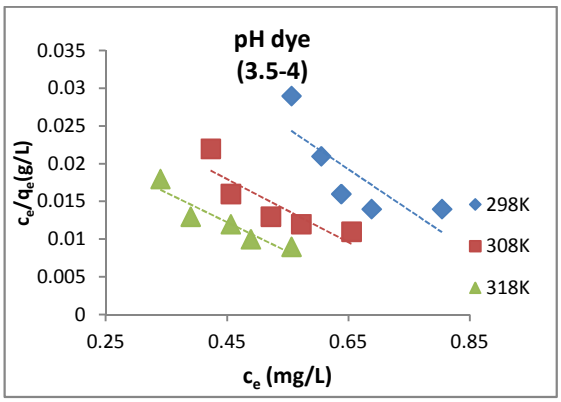

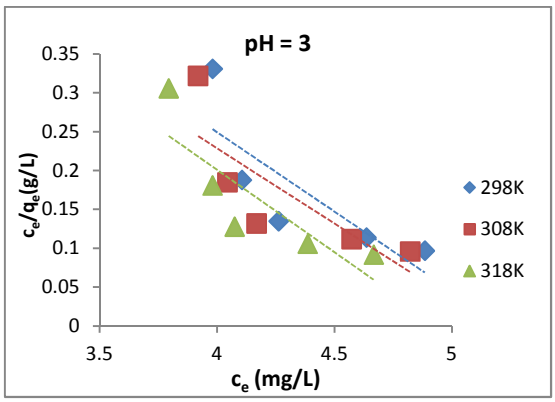

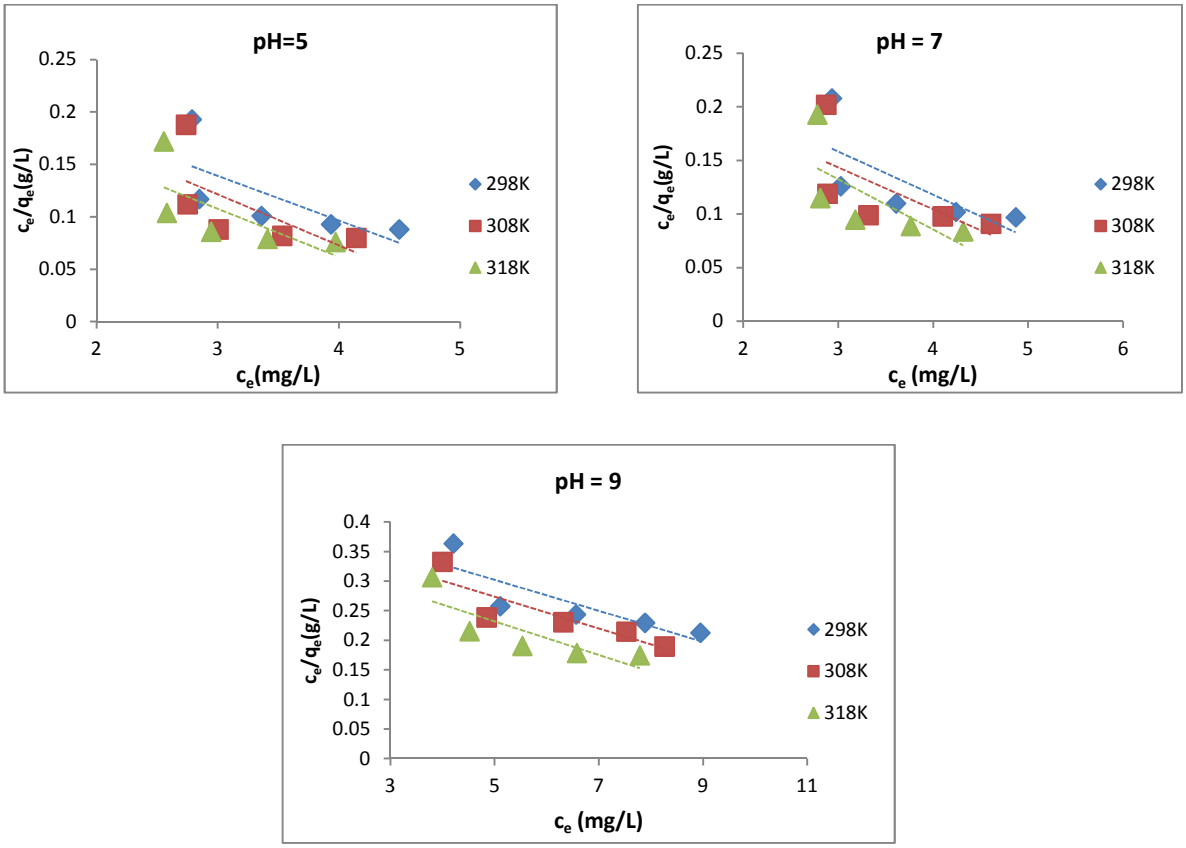

Figure (3.26): Langmuir adsorption isotherm for the adsorption of BTB dye on SD/PANI surface at different temperatures and pH.

3.3.1.2. Freundlich isotherm model:

The Freundlich isotherm model is earliest relationship that used to describing the adsorption and the applicability of heterogeneous surface in the adsorption process. From the equation (1.4) the Freundlich data was determine by the plot between Log q_e versus Log c_e and from the slope and intercept, the freundlich isotherm constants k_F and n which are the adsorption capacity of the adsorbent and the adsorption intensity, respectively were obtained. The Freundlich isotherm data of BTB adsorption on each of SD and SD/PANI surface are shown in tables (3.12) and (3.13), respectively. Also the adsorption isotherm data for BTB dye on both adsorbents are presented in figures (3.27) and (3.28).

Table (3.12): Adsorption values of BTB on SD surface with Freundlich isotherm model calculations at different temperatures and pH.

pH	c_o mg/L	298 K		308 K		318 K	
		Log c_e	Log q_e	Log c_e	Log q_e	Log c_e	Log q_e
3	10	0.606	1.076	0.603	1.078	0.579	1.093
	15	0.651	1.323	0.648	1.324	0.629	1.331
	20	0.705	1.475	0.699	1.476	0.666	1.487
	25	0.743	1.590	0.738	1.591	0.702	1.601
	30	0.794	1.677	0.789	1.678	0.743	1.689
pH dye (3.5-4)	10	0.649	1.045	0.630	1.059	0.608	1.075
	15	0.807	1.235	0.794	1.244	0.773	1.259
	20	0.929	1.362	0.918	1.370	0.890	1.388
	25	0.994	1.481	0.981	1.489	0.966	1.498
	40	1.045	1.578	1.036	1.583	1.021	1.591
5	10	0.851	0.762	0.839	0.790	0.835	0.800
	15	1.007	0.984	0.997	1.005	0.994	1.010
	20	1.125	1.123	1.103	1.165	1.102	1.166
	25	1.171	1.307	1.169	1.310	1.167	1.313
	30	1.223	1.424	1.216	1.432	1.215	1.433
7	10	0.908	0.581	0.903	0.601	0.898	0.621
	15	1.068	0.818	1.066	0.825	1.065	0.828
	20	1.170	1.016	1.170	1.017	1.168	1.021
	25	1.245	1.170	1.244	1.171	1.243	1.174
	30	1.314	1.273	1.311	1.278	1.307	1.286
9	10	0.958	0.264	0.954	0.294	0.953	0.308
	15	1.098	0.691	1.096	0.699	1.086	0.748
	20	1.207	0.889	1.206	0.895	1.204	0.900
	25	1.291	1.037	1.287	1.051	1.286	1.053
	30	1.293	1.315	1.291	1.318	1.291	1.320
11	10	0.839	0.790	0.837	0.795	0.831	0.807
	15	1.008	0.981	1.007	0.985	1.005	0.989
	20	1.122	1.130	1.118	1.137	1.116	1.140
	25	1.216	1.232	1.215	1.234	1.204	1.255
	30	1.284	1.333	1.283	1.334	1.280	1.339

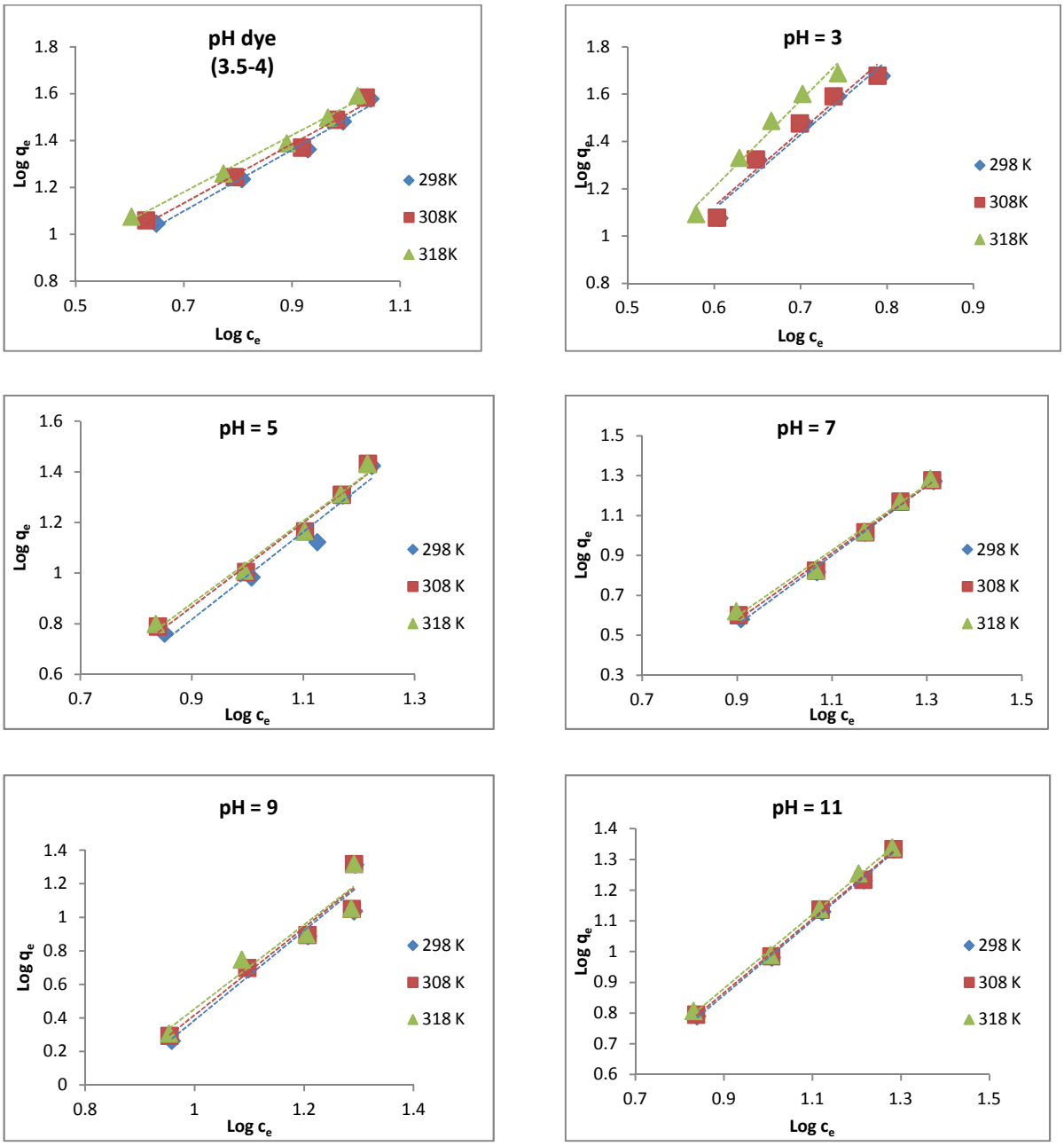

Figure (3.27): Freundlich adsorption isotherm for the adsorption of BTB dye on SD surface at different temperatures and pH.

Table (3.13): Adsorption values of BTB on SD/PANI surface with Freundlich isotherm model calculations at different temperatures and pH.

pH	c_o (mg/L)	298K		308K		318K	
		Log c_e	Log q_e	Log c_e	Log q_e	Log c_e	Log q_e
pH dye (3.5-4)	10	-0.255	1.276	-0.374	1.282	-0.469	1.286
	15	-0.218	1.459	-0.341	1.464	-0.409	1.466
	20	-0.195	1.588	-0.282	1.591	-0.341	1.592
	25	-0.162	1.687	-0.243	1.689	-0.311	1.690
	30	-0.095	1.766	-0.184	1.769	-0.255	1.770
3	10	0.600	1.081	0.593	1.085	0.579	1.094
	15	0.613	1.338	0.607	1.341	0.600	1.343
	20	0.630	1.498	0.620	1.501	0.610	1.503
	25	0.666	1.610	0.660	1.611	0.642	1.615
	30	0.689	1.701	0.683	1.702	0.669	1.705
5	10	0.445	1.159	0.437	1.162	0.407	1.173
	15	0.454	1.386	0.439	1.389	0.412	1.395
	20	0.526	1.522	0.478	1.531	0.469	1.533
	25	0.595	1.625	0.548	1.633	0.533	1.635
	30	0.653	1.708	0.617	1.714	0.599	1.716
7	10	0.467	1.150	0.458	1.154	0.444	1.160
	15	0.481	1.379	0.461	1.384	0.449	1.387
	20	0.558	1.516	0.521	1.523	0.502	1.527
	25	0.627	1.618	0.613	1.621	0.576	1.628
	30	0.687	1.701	0.664	1.706	0.635	1.711
9	10	0.624	1.064	0.602	1.079	0.580	1.093
	15	0.708	1.296	0.686	1.308	0.655	1.321
	20	0.817	1.429	0.801	1.437	0.743	1.461
	25	0.897	1.534	0.877	1.543	0.818	1.566
	30	0.952	1.624	0.917	1.638	0.891	1.648

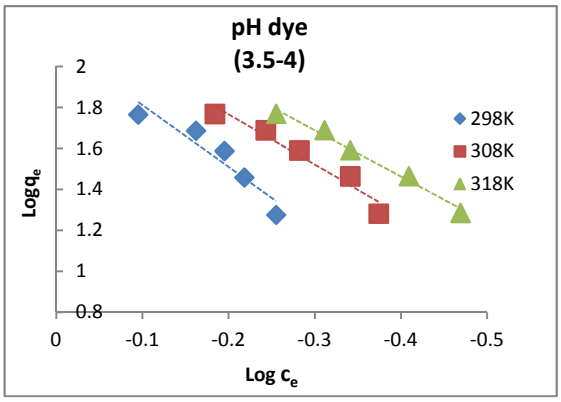

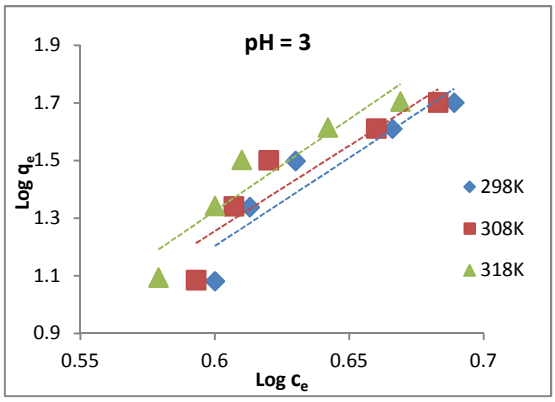

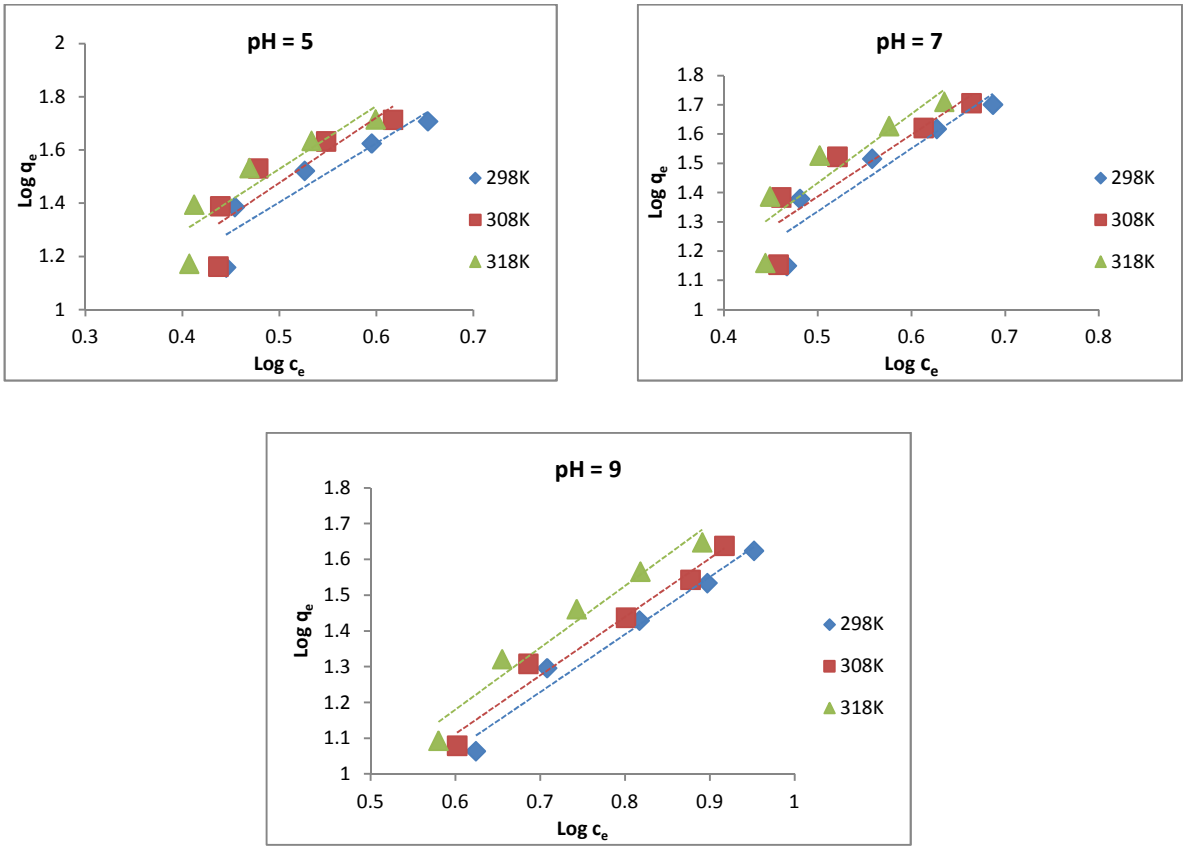

Figure (3.28): Freundlich adsorption isotherm for the adsorption of BTB dye on SD/PANI surface at different temperatures and pH.

3.3.1.3. Dubinin – Radushkevich (D-R) isotherm model:

The D-R isotherm linear equation (equation 1.5) was used for studying the adsorption isotherm for BTB on each of SD and SD/PANI surface at different temperatures and the data obtained are given in tables (3.14) and (3.15). The D-R isotherm constants β (D-R isotherm constant) and q_{max} (maximum amount of adsorbate that can be adsorbed on adsorbent), were obtained from the slop and intercept of the plot of ε^2 versus ln q_e. E values (the mean free energy of the adsorption per molecule of adsorbate) were calculated by using equation (1.7). The results of D-R isotherm data for the adsorption of BTB dye on SD and SD/PANI surfaces are presented in figures (3.29) and (3.30), respectively.

Table (3.14): Adsorption values of BTB on SD surface with D-R isotherm model calculations at different temperatures and pH.

pH	c_o	298K		308 K		318 K	
		ε^2 J/mol	Ln q_e	ε^2 J/mol	Ln q_e	ε^2 J/mol	Ln q_e
3	10	299824	2.478	324713	2.483	882460	2.519
	15	249218	3.047	269691	3.049	310529	3.067
	20	198714	3.396	217226	3.401	266730	3.425
	25	169063	3.662	184490	3.665	229021	3.687
	30	136195	3.862	148363	3.864	192518	3.890
pH dye (3.5-4)	10	251990	2.406	289244	2.439	338395	2.476
	15	129090	2.844	145612	2.865	170148	2.898
	20	75649	3.137	85238	3.154	102365	3.197
	25	57770	3.411	64283	3.429	73753	3.450
	30	45410	3.633	50792	3.644	57898	3.664
5	10	106260	1.755	119632	1.820	130012	1.844
	15	53874	2.267	60150	2.314	65522	2.326
	20	31948	2.586	37734	2.683	40322	2.686
	25	26046	3.011	28064	3.017	30260	3.025
	30	20712	3.280	22776	3.298	24357	3.300
7	10	83258	1.338	90852	1.385	98463	1.430
	15	41233	1.886	44344	1.900	47482	1.909
	20	26196	2.340	28064	2.343	28225	2.352
	25	18739	2.694	20087	2.698	21485	2.705
	30	13772	2.932	14830	2.944	16128	2.963
9	10	66985	0.610	72546	0.679	77466	0.711
	15	36104	1.592	38848	1.611	43325	1.723
	20	22217	2.048	23882	2.061	25617	2.073
	25	15250	2.388	16603	2.421	17299	2.426
	30	15076	3.028	16228	3.036	17365	3.039
11	10	111122	1.821	120252	1.832	131608	1.860
	15	53665	2.261	57327	2.268	62066	2.279
	20	32113	2.603	35192	2.618	37801	2.626
	25	21321	2.839	22922	2.843	25697	2.891
	30	15719	3.069	16855	3.073	18238	3.084

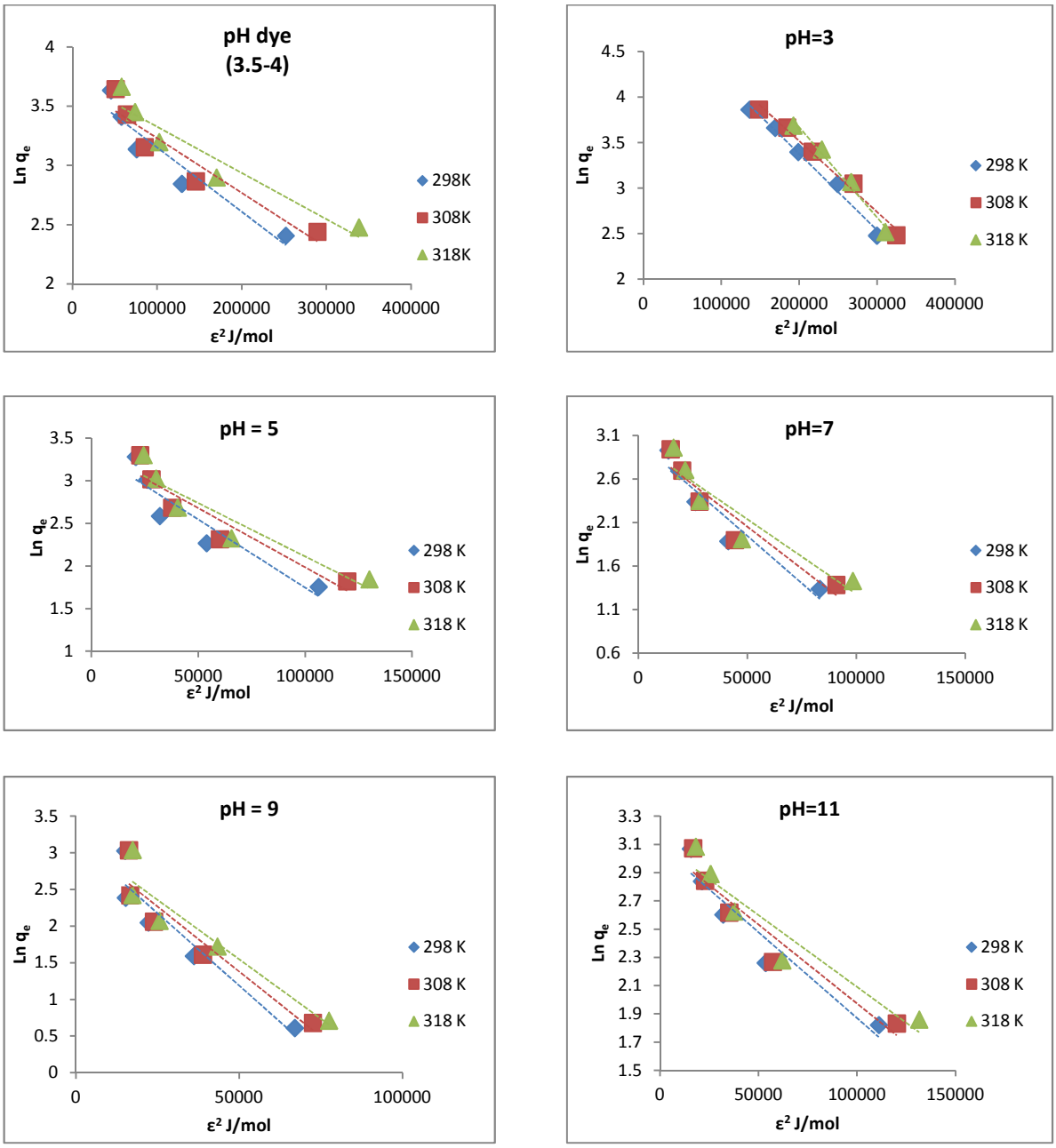

Figure (3.29): The D-R adsorption isotherm for the adsorption of BTB dye on SD surface at different temperatures and pH.

Table (3.15): Adsorption values of BTB on SD/PANI surface with D-R isotherm model calculations at different temperatures and pH.

pH	c_o.	298K		308K		318K	
		ε^2 J/mol	Ln q_e	ε^2 J/mol	Ln q_e	ε^2 J/mol	Ln q_e
pH dye (3.5-4)	10	6502446	2.939	9652843	2.953	13150954	2.961
	15	5844477	3.360	8840776	3.370	11293015	3.375
	20	5458607	3.656	7510782	3.662	9424172	3.666
	25	4945799	3.884	6703447	3.889	8668766	3.892
	30	4010092	4.067	5635227	4.072	7404547	4.076
3	10	308341	2.488	338770	2.499	382652	2.519
	15	291701	3.081	320339	3.087	350812	3.093
	20	272763	3.449	303182	3.455	336723	3.461
	25	234241	3.707	256520	3.710	294929	3.719
	30	212957	3.917	232939	3.919	263526	3.925
5	10	578674	2.669	636093	2.676	763296	2.701
	15	556378	3.191	630933	3.199	750729	3.213
	20	416750	3.505	540933	3.526	597524	3.530
	25	313598	3.741	407835	3.760	462614	3.765
	30	247642	3.932	306008	3.946	352704	3.952
7	10	528143	2.648	582450	2.657	660127	2.670
	15	500571	3.176	579836	3.187	647633	3.194
	20	367101	3.490	453667	3.507	522723	3.516
	25	275320	3.726	312290	3.733	388289	3.749
	30	214235	3.917	251964	3.928	303628	3.939
9	10	278558	2.449	326877	2.485	381217	2.517
	15	196198	2.985	230666	3.011	279178	3.043
	20	123455	3.291	141561	3.309	192913	3.365
	25	87493	3.533	101990	3.554	139946	3.607
	30	68896	3.740	85598	3.772	102007	3.794

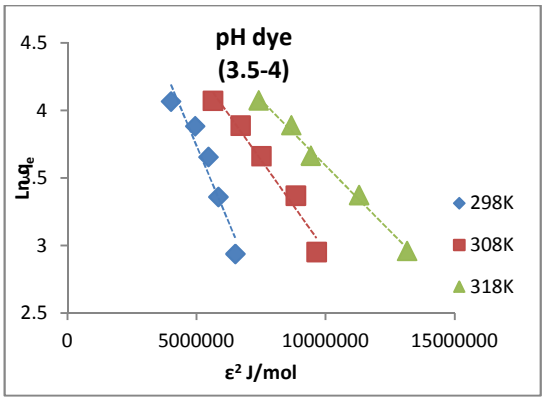

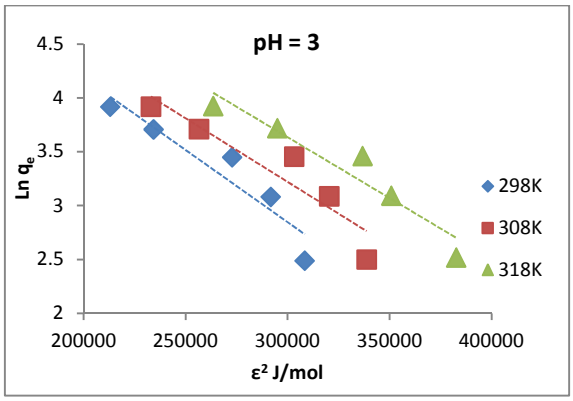

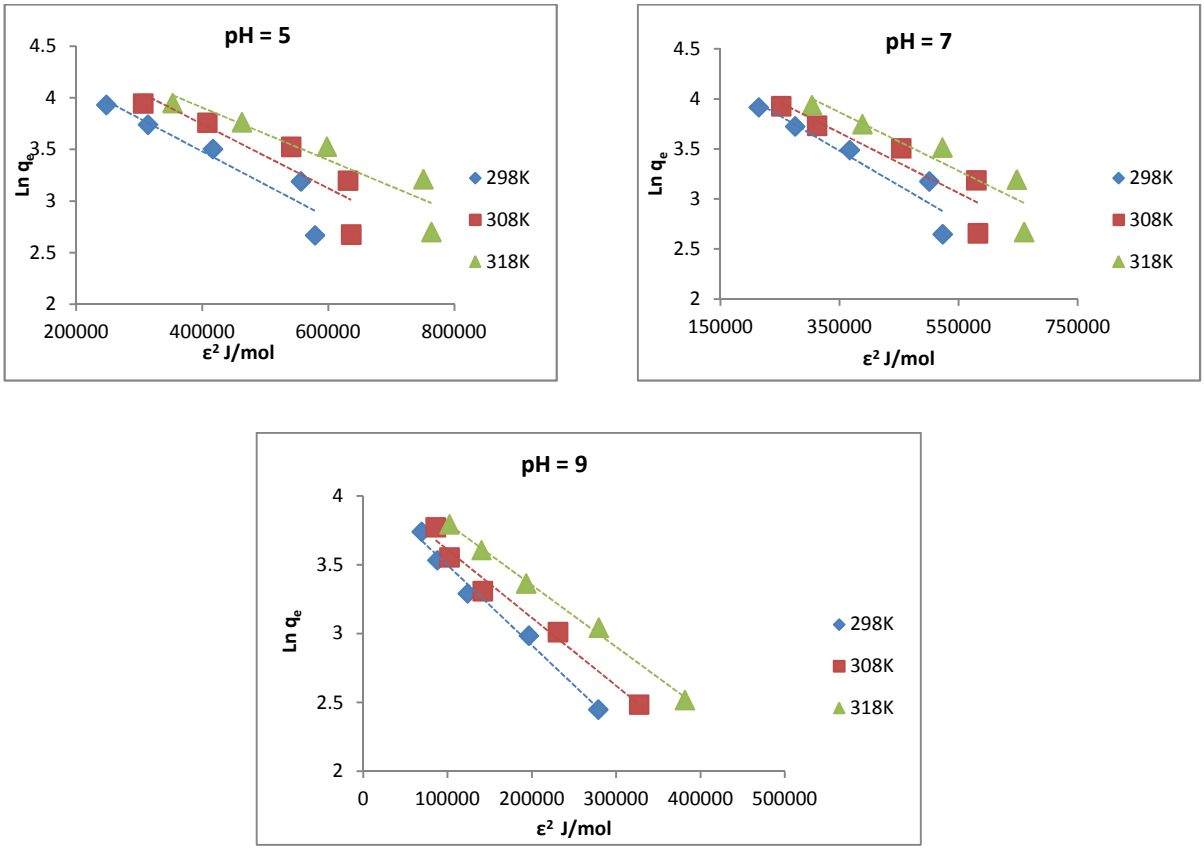

Figure (3.30): The D-R adsorption isotherm for the adsorption of BTB dye on SD/PANI surface at different temperatures and pH.

All the data of the equilibrium isotherm modeling of BTB dye on each of SD and SD/PANI surface were included in tables (3.16) and (3.17), respectively. Because of the negative values of R_L (which is Langmuir constant), it makes Langmuir model unfavorable in the BTB adsorption on each of SD and SD/PANI surface. For D-R isotherm, If the values of energy E in D-R model between 8 and 16 kJ/mol then the adsorption process refers to chemical ion-exchange, if E less than 8 kJ/mol then the process is physisorption and if the energy values more than 16 kJ/mol it refers to chemisorption process [110]. The results obtained show that the Freundlich model yields a better fit for the experimental adsorption data than the Langmuir model and D-R model because of the higher correlation factor (R^2) values. From the constants, unfavorable adsorption occurs when (n < 1) which

characterized by predominantly physical interactions, while the favorable adsorption happens by stronger bonds when the (n > 1) [111]. The results show that the type of BTB adsorption on each of SD and SD/PANI surface is physical adsorption.

Table (3.16): Adsorption isotherm constants of BTB dye on the SD surface at different pH and temperatures.

pH	T (K)	Langmuir constants				Freundlich constants			Dubinin and Radushkevich constants			
		q max	K_L	R_L	R^2	n	K_F	R^2	β	q max	E	R^2
3	298	-11.467	-0.136	-0.324	0.784	0.765	1.528	0.988	$8*10^{-3}$	156.35	7.937	0.958
	308	-11.428	-0.136	-0.324	0.781	0.794	1.781	0.988	$8*10^{-3}$	159.86	7.937	0.956
	318	-9.398	-0.158	-0.267	0.851	0.825	2.145	0.992	$2*10^{-3}$	52.404	15.823	0.810
pH dye (3.5-4)	298	-65.789	-0.032	25.000	0.900	0.318	0.171	0.987	$-5*10^{-3}$	40.217	10.000	0.908
	308	-77.519	-0.030	10.000	0.848	0.315	0.167	0.986	$-5*10^{-3}$	40.129	10.000	0.903
	318	-93.458	-0.025	4.000	0.928	0.272	0.101	0.976	$-4*10^{-3}$	41.112	11.236	0.914
5	298	-16.420	-0.061	-12.048	0.905	0.579	0.183	0.960	$2*10^{-2}$	28.323	5.000	0.863
	308	-18.975	-0.035	-18.867	0.986	0.601	0.233	0.983	$1*10^{-2}$	29.122	7.092	0.890
	318	-20.284	-0.034	-43.478	0.976	0.614	0.259	0.981	$1*10^{-2}$	28.898	7.092	0.887
7	298	-11.668	-0.031	13.698	0.969	0.574	0.096	0.995	$2*10^{-2}$	20.855	5.000	0.917
	308	-12.804	-0.029	9.433	0.981	0.592	0.113	0.993	$2*10^{-2}$	20.493	5.000	0.903
	318	-13.755	-0.029	7.874	0.980	0.605	0.129	0.988	$2*10^{-2}$	20.099	5.000	0.880
9	298	-3.312	-0.042	-3.676	0.851	0.374	0.005	0.932	$4*10^{-2}$	23.605	3.534	0.900
	308	-3.575	-0.042	-3.802	0.873	0.383	0.006	0.936	$4*10^{-2}$	23.486	3.534	0.895
	318	-3.949	-0.041	-4.132	0.802	0.398	0.008	0.922	$3*10^{-2}$	23.769	4.082	0.901
11	298	-56.176	-0.014	1.751	0.974	0.825	0.585	0.998	$1*10^{-2}$	21.924	7.092	0.921
	308	-59.523	-0.013	1.706	0.943	0.831	0.608	0.998	$1*10^{-2}$	22.014	7.092	0.920
	318	-59.523	-0.014	1.742	0.942	0.829	0.624	0.997	$1*10^{-2}$	22.385	7.092	0.911

Table (3.17): Adsorption isotherm constants of BTB dye on the SD/PANI surface at different pH and temperatures.

pH	T (K)	Langmuir constants				Freundlich constants			Dubinin and Radushkevich constants			
		q max	K_L	R_L	R^2	n	K_F	R^2	β	q max	E	R^2
pH dye (3.5-4)	298	-18.416	-0.996	-0.035	0.649	0.332	129.778	0.926	$5*10^{-4}$	411.702	31.250	0.892
	308	-23.866	-1.139	-0.030	0.765	0.406	182.222	0.966	$3*10^{-4}$	285.659	41.667	0.946
	318	-25.641	-1.259	-0.027	0.879	0.441	234.207	0.993	$2*10^{-4}$	252.775	50.000	0.986
3	298	-4.895	-0.192	-0.210	0.661	0.163	0.003	0.888	$1*10^{-2}$	956.518	7.092	0.864
	308	-5.171	-0.193	-0.209	0.640	0.168	0.005	0.869	$1*10^{-2}$	861.866	7.092	0.845
	318	-4.726	-0.202	-0.198	0.709	0.157	0.003	0.913	$1*10^{-2}$	1128.788	7.092	0.885
5	298	-23.419	-0.160	-0.263	0.524	0.450	1.957	0.889	$3*10^{-3}$	117.684	12.987	0.854
	308	-20.576	-0.182	-0.224	0.414	0.408	1.781	0.802	$3*10^{-3}$	146.907	12.987	0.762
	318	-21.786	-0.187	-0.217	0.480	0.423	2.223	0.856	$3*10^{-3}$	137.455	12.987	0.820
7	298	-24.876	-0.144	-0.301	0.523	0.466	1.829	0.892	$3*10^{-3}$	109.870	12.987	0.868
	308	-25.575	-0.150	-0.286	0.429	0.473	2.130	0.832	$3*10^{-3}$	111.676	12.987	0.807
	318	-21.368	-0.171	-0.242	0.472	0.424	1.787	0.849	$3*10^{-3}$	133.220	12.987	0.813
9	298	-38.314	-0.060	-1.25	0.724	0.629	1.268	0.988	$6*10^{-3}$	58.962	9.091	0.973
	308	-37.313	-0.066	-1.020	0.772	0.611	1.349	0.979	$5*10^{-3}$	60.364	10.000	0.974
	318	-35.336	-0.076	-0.781	0.683	0.578	1.390	0.997	$4*10^{-3}$	69.791	11.236	0.962

3.3.2. Equilibrium isotherm modeling of MGox dye on the SD and SD/PANI surfaces:

3.3.2.1. Langmuir isotherm model:

The Langmuir adsorption isotherm data for MGox adsorption onto both SD and SD/PANI surfaces were presented in tables (3.18) and (3.19), respectively. Also, the plot of c_e/q_e versus c_e for SD and SD/PANI surface were explained in figures (3.31) and (3.32), respectively.

Table (3.18): Adsorption values of MGox on SD surface with Langmuir isotherm model calculations at different temperatures and pH.

pH	c_o (mg/L)	298 K		308 K		318 K	
		c_e (mg/L)	c_e/q_e (g/L)	c_e (mg/L)	c_e/q_e (g/L)	c_e (mg/L)	c_e/q_e (g/L)
3	15	8.347	1.046	7.632	0.863	6.284	0.601
	20	12.723	1.457	12.008	1.252	10.993	1.017
	25	17.698	2.020	16.917	1.744	15.202	1.293
	30	21.292	2.038	20.510	1.801	19.612	1.573
	35	25.236	2.154	24.920	2.060	24.004	1.819
	40	29.429	2.320	28.946	2.182	28.181	1.987
pH dye (3.5-4)	15	2.197	0.143	1.841	0.117	1.308	0.080
	20	3.116	0.154	2.804	0.136	2.479	0.118
	25	4.390	0.178	4.034	0.160	3.649	0.142
	30	5.338	0.180	5.027	0.168	4.641	0.153
	35	6.671	0.196	6.316	0.183	6.153	0.178
	40	8.538	0.226	8.227	0.216	7.767	0.201
5	15	----	----	----	----	----	----
	20	----	----	----	----	----	----
	25	1.099	0.038	0.618	0.021	0.076	0.002
	30	2.693	0.082	0.918	0.026	0.663	0.019
	35	5.234	0.147	2.557	0.066	1.911	0.048
	40	6.783	0.170	5.565	0.135	2.903	0.065
7	15	1.291	0.078	0.571	0.033	0.306	0.017
	20	2.162	0.101	1.481	0.067	0.534	0.023
	25	3.091	0.118	2.825	0.106	1.859	0.067
	30	4.928	0.164	4.075	0.131	2.371	0.072
	35	7.541	0.229	5.628	0.160	3.431	0.091
	40	9.056	0.244	8.242	0.216	5.079	0.121
9	15	2.234	0.146	1.797	0.113	1.344	0.082
	20	3.464	0.175	2.509	0.120	2.137	0.100
	25	4.629	0.189	3.707	0.145	2.898	0.109
	30	6.037	0.210	4.629	0.152	3.966	0.127
	35	7.364	0.222	6.991	0.208	6.118	0.177
	40	8.836	0.236	8.059	0.210	7.331	0.187
11	15	7.467	0.826	6.133	0.576	5.467	0.479
	20	10.8	0.978	8.8	0.655	7.467	0.496
	25	13.625	0.998	11.125	0.668	9.875	0.544
	30	16.75	1.053	13.625	0.693	12.375	0.585
	35	19.875	1.095	16.125	0.712	14.875	0.616
	40	23.625	1.202	20.5	0.871	18	0.682

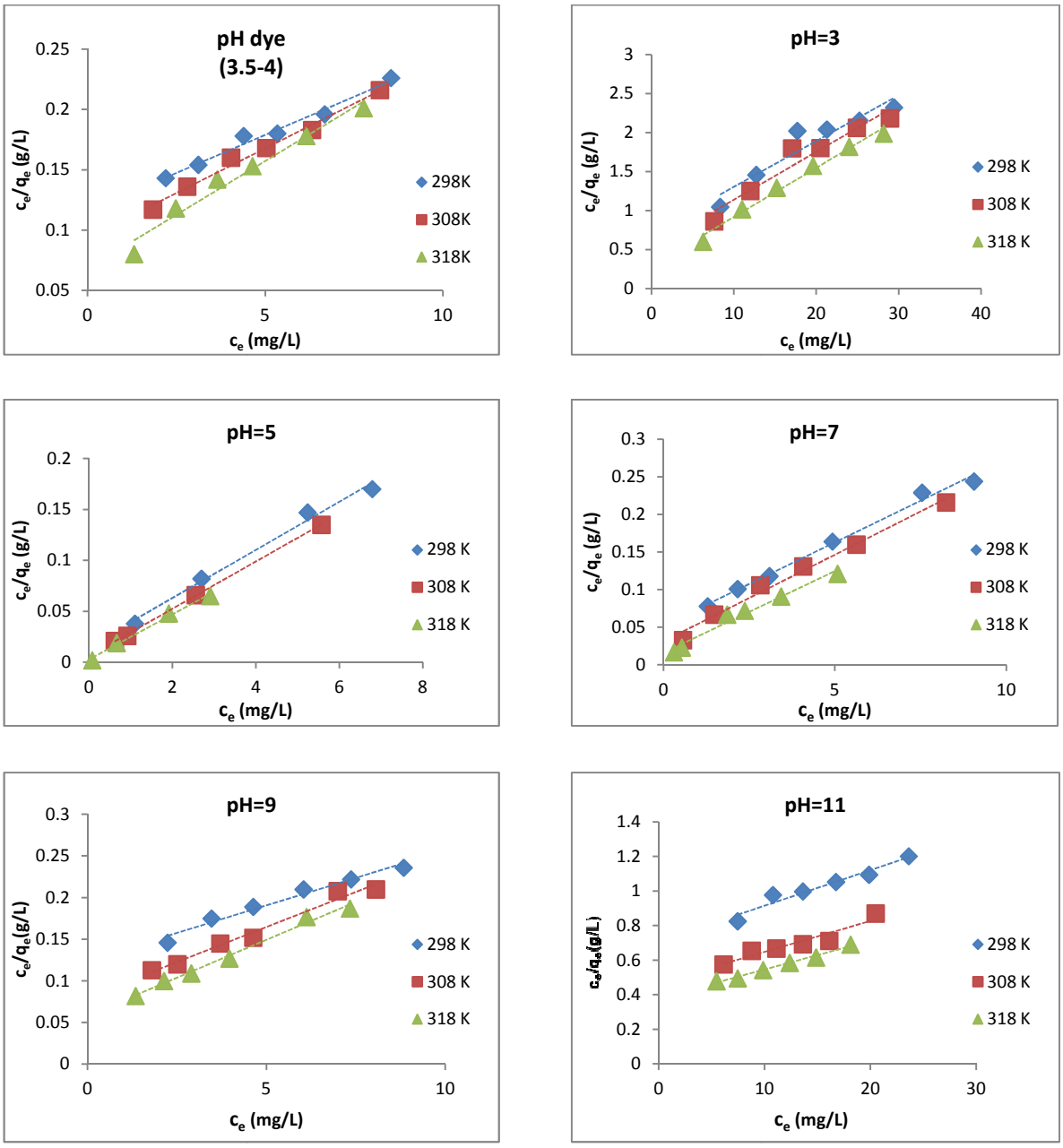

Figure (3.31): Langmuir adsorption isotherm for the adsorption of MGox dye on SD surface at different temperatures and pH.

Table (3.19): Adsorption values of MGox on SD/PANI surface with Langmuir isotherm model calculations at different temperatures and pH.

pH	c_o	298K		308K		318K	
		c_e (mg/L)	c_e/q_e (g/L)	c_e (mg/L)	c_e/q_e (g/L)	c_e (mg/L)	c_e/q_e (g/L)
pH dye (3.5-4)	15	10.893	2.210	10.790	2.136	10.464	1.922
	20	15.086	2.558	14.804	2.374	14.538	2.218
	25	20.064	3.387	19.441	2.914	19.056	2.672
	30	24.390	3.623	24.227	3.497	23.782	3.187
	35	28.716	3.808	28.641	3.753	28.464	3.629
	40	33.693	4.452	33.427	4.238	33.175	4.051
5	15	12.227	3.674	11.535	2.778	10.814	2.153
	20	16.904	4.550	15.836	3.169	15.325	2.732
	25	21.701	5.481	20.468	3.764	19.4	2.887
	30	26.618	6.559	25.355	4.549	23.701	3.135
	35	31.295	7.039	30.062	5.073	28.558	3.694
	40	36.152	7.828	34.528	5.259	33.265	4.116
9	15	12.769	4.770	12.380	3.938	11.830	3.110
	20	17.251	5.229	16.733	4.269	16.005	3.339
	25	22.057	6.245	21.604	5.302	20.827	4.159
	30	26.846	7.093	26.215	5.772	25.503	4.726
	35	31.749	8.139	31.183	6.809	30.341	5.427
	40	36.523	8.754	36.134	7.789	35.244	6.176

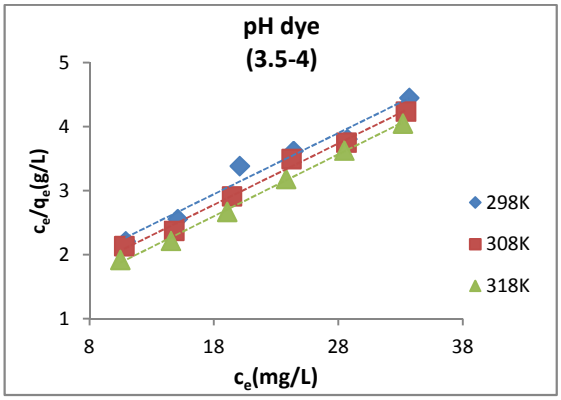

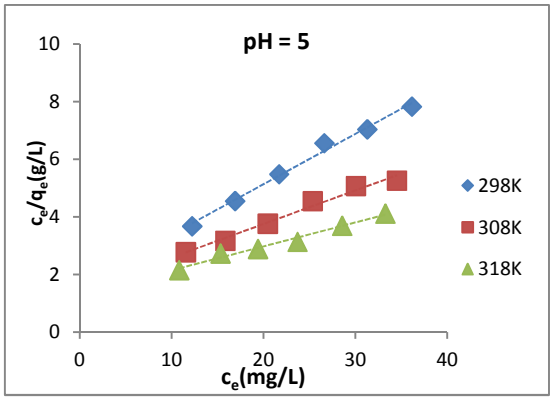

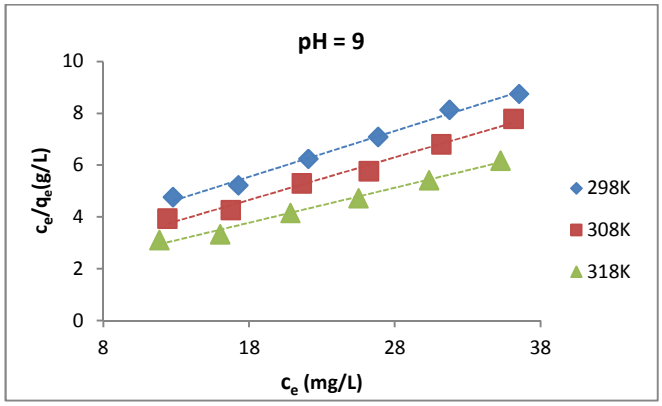

Figure (3.32): Langmuir adsorption isotherm for the adsorption of MGox dye on SD/PANI surface at different temperatures and pH.

3.3.2.2. Freundlich isotherm model:

Freundlich isotherm data for MGox dye on SD and SD/PANI surfaces were presented and plotted in tables (3.20 and 3.21) and figures (3.33 and 3.34), respectively.

Table (3.20): Adsorption values of MGox on SD surface with Freundlich isotherm model calculations at different temperatures and pH.

pH	c_o mg/L	298K		308K		318K	
		Log c_e	Log q_e	Log c_e	Log q_e	Log c_e	Log q_e
3	15	0.922	0.902	0.883	0.947	0.798	1.019
	20	1.105	0.941	1.079	0.982	1.041	1.034
	25	1.248	0.943	1.228	0.987	1.182	1.070
	30	1.328	1.019	1.312	1.056	1.293	1.096
	35	1.402	1.069	1.397	1.083	1.380	1.120
	40	1.469	1.103	1.462	1.123	1.450	1.152
pH dye (3.5-4)	15	0.342	1.187	0.265	1.198	0.117	1.126
	20	0.494	1.307	0.448	1.315	0.394	1.328
	25	0.642	1.393	0.606	1.401	0.562	1.409
	30	0.727	1.471	0.701	1.477	0.667	1.483
	35	0.824	1.531	0.800	1.537	0.789	1.539
	40	0.931	1.577	0.915	1.581	0.890	1.587
5	15	----	----	----	----	----	----
	20	----	----	----	----	----	----
	25	0.041	1.458	-0.209	1.466	-1.119	1.476
	30	0.430	1.515	-0.037	1.543	-0.178	1.546
	35	0.719	1.553	0.408	1.590	0.281	1.599
	40	0.831	1.601	0.745	1.616	0.463	1.649

7	15	0.111	1.216	-0.243	1.238	-0.514	1.246
	20	0.335	1.331	0.171	1.347	-0.272	1.368
	25	0.490	1.420	0.451	1.425	0.269	1.444
	30	0.693	1.478	0.610	1.493	0.375	1.521
	35	0.877	1.518	0.750	1.547	0.535	1.578
	40	0.957	1.570	0.916	1.581	0.706	1.622
9	15	0.349	1.185	0.255	1.200	0.128	1.214
	20	0.540	1.298	0.400	1.322	0.330	1.331
	25	0.665	1.388	0.569	1.407	0.462	1.424
	30	0.781	1.459	0.665	1.484	0.598	1.495
	35	0.867	1.521	0.845	1.526	0.787	1.540
	40	0.946	1.573	0.906	1.584	0.865	1.593
11	15	0.873	0.956	0.788	1.027	0.738	1.058
	20	1.033	1.043	0.944	1.128	0.873	1.177
	25	1.134	1.135	1.046	1.221	0.995	1.259
	30	1.224	1.201	1.134	1.293	1.093	1.325
	35	1.298	1.259	1.207	1.355	1.172	1.383
	40	1.373	1.293	1.312	1.369	1.258	1.419

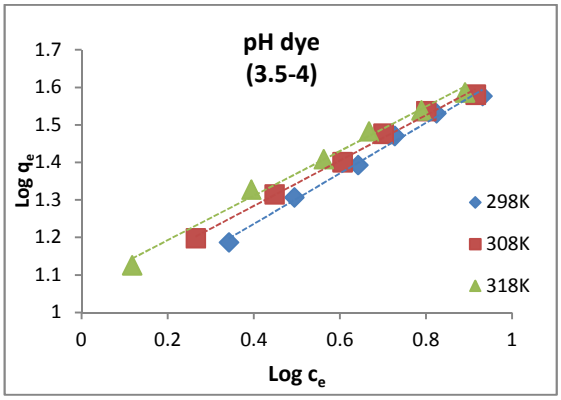

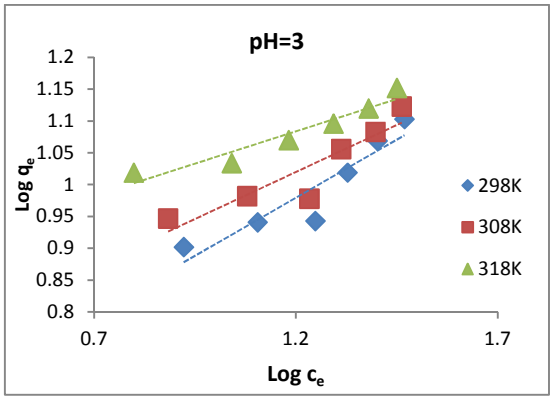

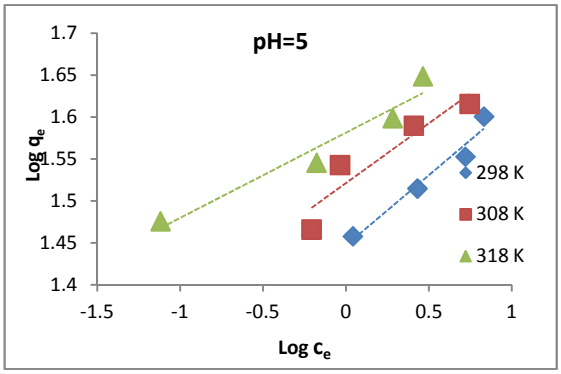

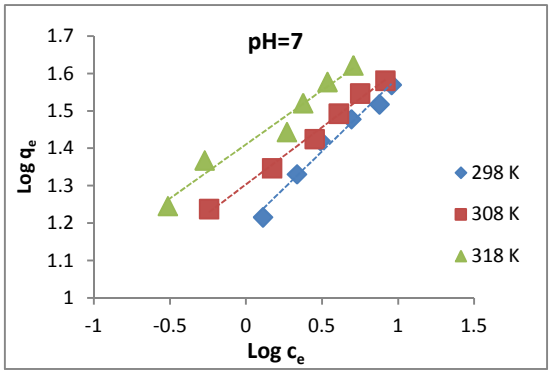

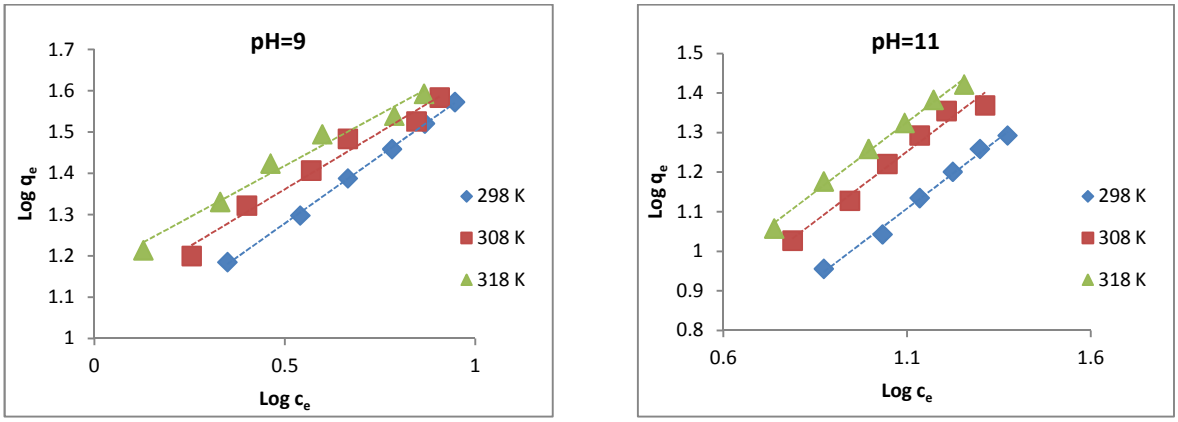

Figure (3.33): Freundlich adsorption isotherm for the adsorption of MGox dye on SD surface at different temperatures and pH.

Table (3.21): Adsorption values of MGox on SD/PANI surface with Freundlich isotherm model calculations at different temperatures and pH.

pH	c_o (mg/L)	298K		308K		318K	
		Log c_e	Log q_e	Log c_e	Log q_e	Log c_e	Log q_e
pH dye (3.5-4)	15	1.037	0.693	1.033	0.703	1.020	0.736
	20	1.179	0.771	1.170	0.795	1.163	0.817
	25	1.302	0.773	1.289	0.824	1.280	0.853
	30	1.387	0.828	1.384	0.841	1.376	0.873
	35	1.458	0.877	1.457	0.883	1.454	0.894
	40	1.528	0.879	1.524	0.897	1.521	0.913
5	15	1.087	0.522	1.062	0.618	1.034	0.701
	20	1.228	0.570	1.200	0.699	1.185	0.749
	25	1.336	0.598	1.311	0.735	1.288	0.827
	30	1.425	0.608	1.404	0.746	1.375	0.878
	35	1.495	0.648	1.478	0.773	1.456	0.888
	40	1.558	0.664	1.538	0.817	1.522	0.908
9	15	1.106	0.428	1.093	0.497	1.073	0.580
	20	1.237	0.518	1.224	0.593	1.204	0.681
	25	1.344	0.548	1.335	0.610	1.319	0.700
	30	1.429	0.578	1.419	0.657	1.407	0.732
	35	1.502	0.591	1.494	0.661	1.482	0.747
	40	1.563	0.620	1.558	0.666	1.547	0.756

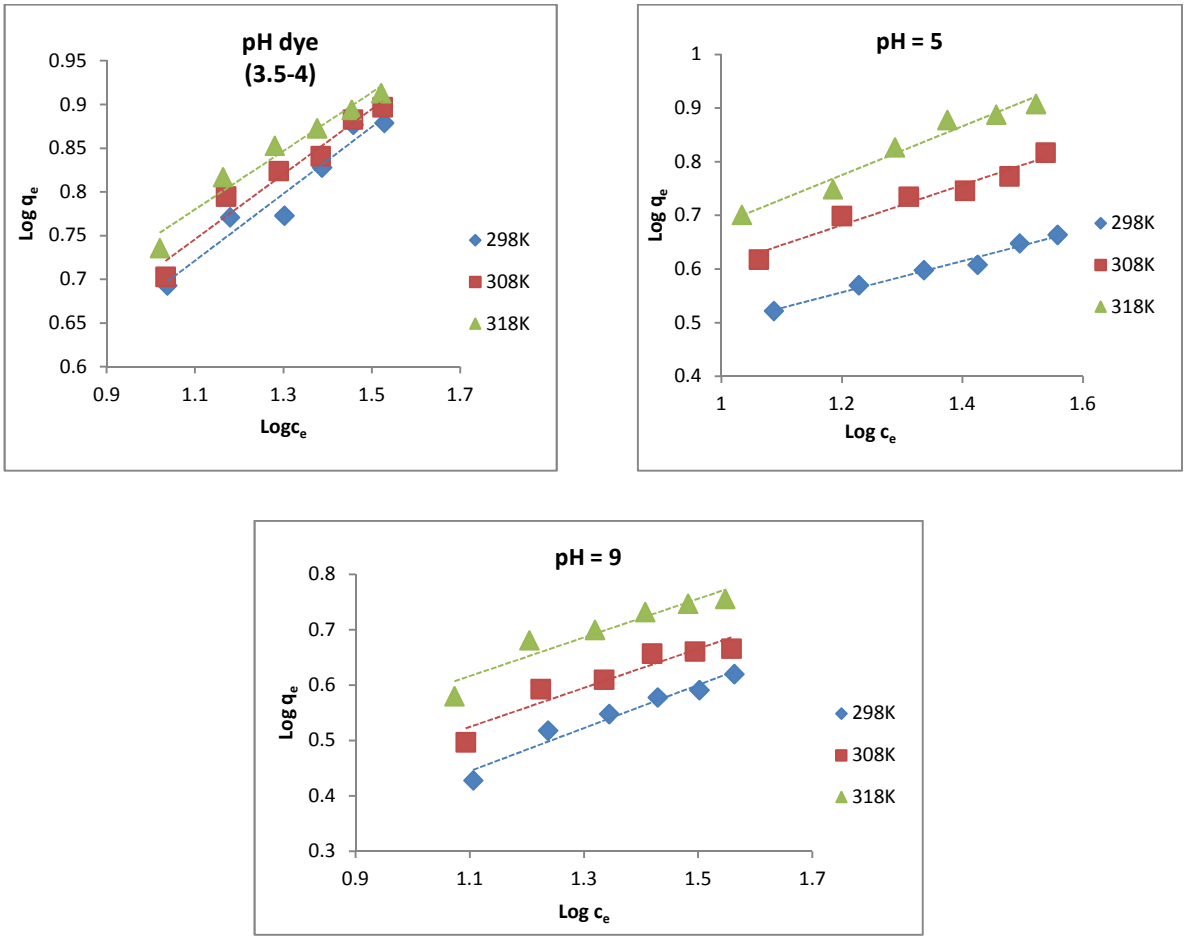

Figure (3.34): Freundlich adsorption isotherm for the adsorption of MGox dye on SD/PANI surface at different temperatures and pH.

3.3.2.3. Dubinin – Radushkevich (D-R) isotherm model:

The adsorption isotherm for MGox on each of SD and SD/PANI surface at different temperatures are presented in tables (3.22) and (3.23). The plots of D-R isotherm on SD and SD/PANI surfaces are shown in figures (3.35) and (3.36), respectively.

Table (3.22): Adsorption values of MGox on SD surface with D-R isotherm model calculations at different temperatures and pH.

pH	c_o	298 K		308 K		318 K	
		ε^2 J/mol	Ln q_e	ε^2 J/mol	Ln q_e	ε^2 J/mol	Ln q_e
3	15	78399	2.077	99228	2.179	153145	2.347
	20	35464	2.167	41976	2.261	52920	2.380
	25	18573	2.170	21310	2.272	28638	2.464
	30	12433	2.347	15112	2.433	17479	2.523
	35	9339	2.461	9976	2.493	11753	2.580
	40	6686	2.540	7582	2.585	8565	2.652
pH dye (3.5-4)	15	863968	2.732	1235394	2.759	2255669	2.799
	20	474511	3.009	610135	3.027	803486	3.046
	25	258571	3.208	320339	3.225	409458	3.243
	30	181034	3.388	214874	3.400	265857	3.415
	35	119787	3.526	141730	3.539	159416	3.544
	40	75318	3.631	86740	3.641	102365	3.655
5	15	----	----	----	----	----	----
	20	----	----	----	----	----	----
	25	2570672	3.356	6075600	3.376	49108851	3.398
	30	612259	3.489	3561011	3.552	6061123	3.561
	35	187694	3.576	714614	3.662	1238439	3.682
	40	116119	3.685	179117	3.721	612582	3.796
7	15	2022930	2.800	6717180	2.852	9804083	2.870
	20	886593	3.064	1746326	3.101	7781865	3.151
	25	481364	3.269	602159	3.281	1292753	3.324
	30	210136	3.404	314568	3.438	865788	3.501
	35	95935	3.495	176406	3.562	457393	3.634
	40	67692	3.614	86011	3.640	226529	3.735
9	15	840208	2.729	1283845	2.763	2162988	2.796
	20	394937	2.988	738029	3.044	1030959	3.065
	25	234885	3.196	374107	3.241	612579	3.278
	30	144244	3.359	251964	3.416	353500	3.442
	35	99550	3.501	117230	3.515	159416	3.546
	40	70576	3.622	89737	3.646	114551	3.669
11	15	97476	2.202	149548	2.365	197290	2.437
	20	48634	2.402	75980	2.598	110441	2.711
	25	30951	2.614	48593	2.812	65054	2.899
	30	20654	2.766	32901	2.978	42220	3.052
	35	14796	2.899	23745	3.120	29597	3.184
	40	10321	2.978	14878	3.153	20148	3.267

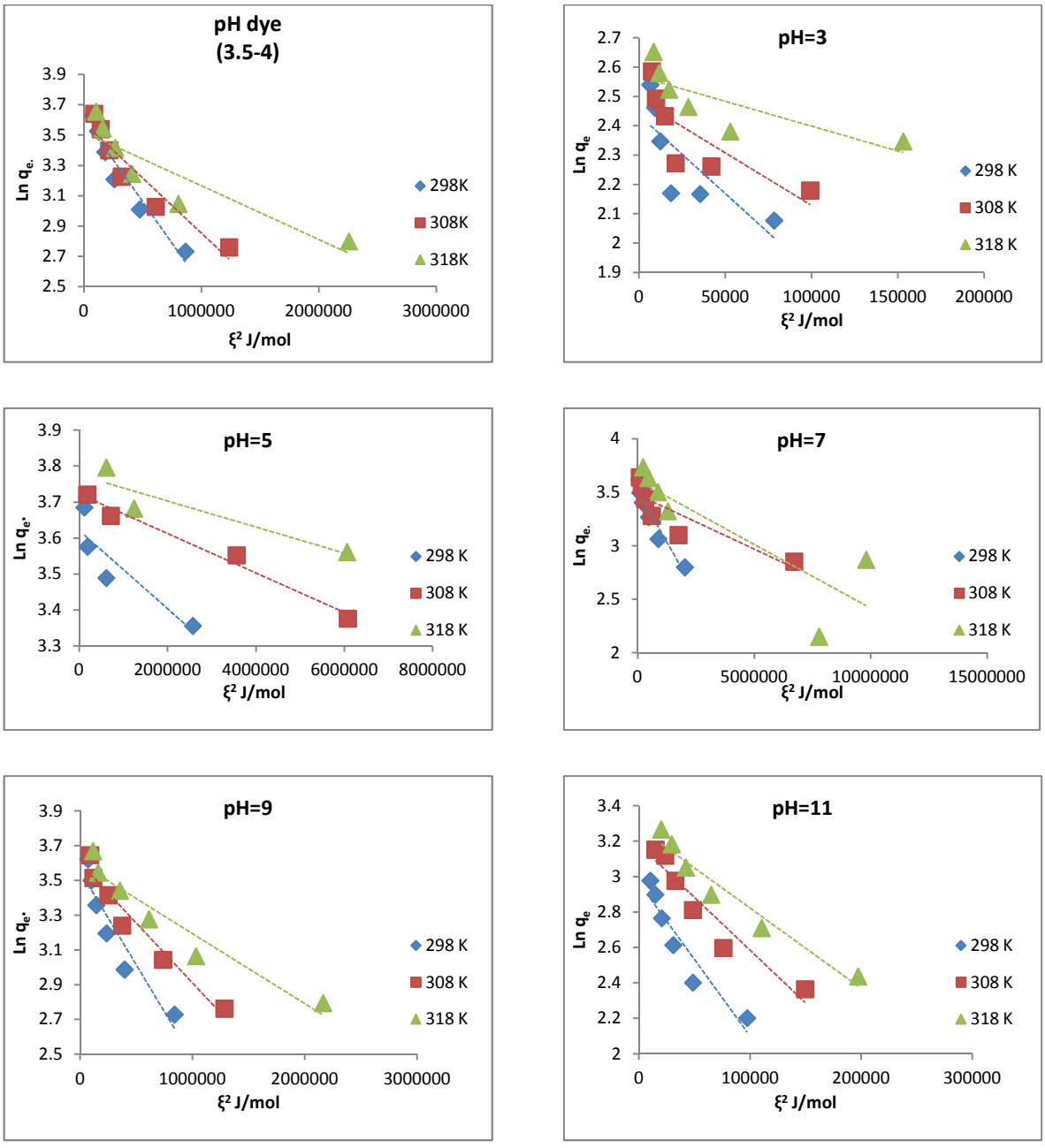

Figure (3.35): The D-R adsorption isotherm for the adsorption of MGox dye on SD surface at different temperatures and pH.

Table (3.23): Adsorption values of MGox on SD/PANI surface with D-R isotherm model calculations at different temperatures and pH.

pH	c_o	298K		308K		318K	
		ε^2 J/mol	Ln q_e.	ε^2 J/mol	Ln q_e.	ε^2 J/mol	Ln q_e.
pH dye (3.5-4)	15	47363	1.595	51952	1.620	58243	1.694
	20	25292	1.774	28024	1.830	30940	1.880
	25	14525	1.779	16501	1.898	18290	1.965
	30	9913	1.907	10730	1.936	11861	2.010
	35	7194	2.020	7582	2.032	8336	2.060
	40	5252	2.024	5699	2.065	6166	2.103
5	15	38319	1.202	45335	1.424	54691	1.614
	20	19948	1.312	24593	1.609	27937	1.725
	25	12461	1.376	14924	1.693	17663	1.905
	30	8351	1.401	9814	1.718	11941	2.023
	35	6075	1.492	7023	1.779	8282	2.045
	40	4476	1.530	5346	1.882	6134	2.090
9	15	34905	0.985	39904	1.145	45872	1.336
	20	19496	1.194	22098	1.366	25681	1.567
	25	11887	1.262	13282	1.405	15377	1.611
	30	8212	1.331	9192	1.513	10343	1.686
	35	5905	1.361	6535	1.522	7352	1.721
	40	4480	1.428	4781	1.534	5473	1.742

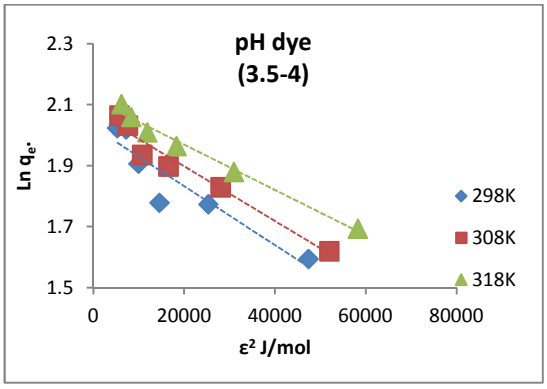

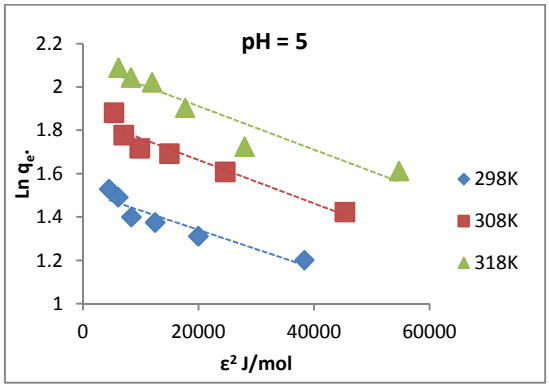

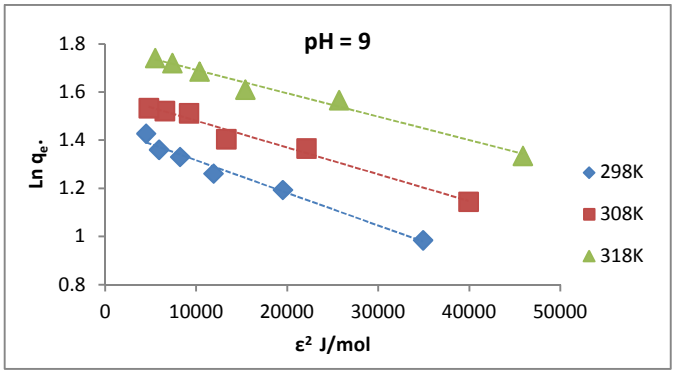

Figure (3.36): The D-R adsorption isotherm for the adsorption of MGox dye on SD/PANI surface at different temperatures and pH.

All the data of the three isotherm models for MGox on SD and SD/PANI surfaces are presented in tables (3.24) and (3.25), respectively. The correlation factor (R^2) values in the tables as shown below indicate that the Langmuir isotherm is the best for MGox dye than Freundlich isotherm and Debinin- Radushkevich isotherm. Values of R_L between 0 and 1 shown favorable adsorption of MGox on SD and SD/PANI surfaces in Langmuir isotherm. The Langmuir analysis shows the greatest monolayer capacity of MGox on SD and SD/PANI surfaces. The comparison of Langmuir isotherm constants for MGox dye on each of SD and SD/PANI surface indicates that SD is an effective adsorbent for the MGox dye compared to SD/PANI surface [112]. Values of n which are more than 1 in freundlich model explained that the type of interaction is chemical adsorption. The Freundlich isotherm gives an indication of surface heterogeneity of the adsorbent while Langmuir isotherm suggest towards surface homogeneity of the adsorbent. This leads to the indication that the surface of sawdust is made up of small heterogeneous adsorption patches which are very much similar to each other in respect of adsorption phenomenon [113].

Table (3.24): Adsorption isotherm constants of MGox dye on the SD surface at different pH and temperatures.

pH	T (K)	Langmuir constants				Freundlich constants			Dubinin and Radushkevich constants			
		q max	K_L	R_L	R^2	n	K_F	R^2	β	q max	E	R^2
3	298	17.036	0.082	0.289	0.900	2.733	3.471	0.861	$5*10^{-3}$	11.440	10	0.627
	308	16.313	0.117	0.222	0.936	3.385	4.629	0.842	$4*10^{-3}$	12.029	11.236	0.638
	318	15.873	0.219	0.312	0.986	4.936	6.928	0.920	$2*10^{-3}$	13.037	15.873	0.633
pH dye (3.5-4)	298	79.365	0.109	0.234	0.982	1.485	9.256	0.993	$1*10^{-3}$	36.925	22.222	0.932
	308	67.568	0.158	0.174	0.988	1.654	11.010	0.995	$7*10^{-4}$	35.913	27.027	0.904
	318	56.180	0.261	0.113	0.970	1.685	11.852	0.992	$4*10^{-4}$	33.778	35.714	0.815
	298	42.373	1.484	0.022	0.990	5.959	27.990	0.958	$1*10^{-4}$	37.382	71.429	0.811

5	308	43.103	3.937	0.008	0.999	7.018	33.220	0.875	$5*10^{-5}$	41.364	100	0.989
	318	45.045	8.547	0.004	0.991	9.823	38.159	0.945	$6*10^{-6}$	40.459	333.333	0.767
7	298	45.045	0.428	0.072	0.992	2.532	15.642	0.975	$4*10^{-4}$	33.623	35.714	0.919
	308	43.290	0.743	0.043	0.987	3.272	20.105	0.992	$1*10^{-4}$	32.314	71.429	0.772
	318	45.872	1.372	0.024	0.973	3.463	25.722	0.962	$1*10^{-4}$	36.911	71.429	0.714
9	298	75.758	0.106	0.239	0.971	1.529	8.950	0.999	$1*10^{-3}$	34.939	22.222	0.887
	308	59.524	0.209	0.138	0.978	1.802	12.131	0.974	$7*10^{-4}$	36.573	27.027	0.950
	318	54.945	0.375	0.082	0.989	2.002	2.340	0.977	$4*10^{-4}$	36.503	35.714	0.928
11	298	48.309	0.029	0.535	0.948	1.416	2.145	0.993	$9*10^{-3}$	19.401	7.463	0.892
	308	55.866	0.038	0.467	0.905	1.418	2.994	0.974	$6*10^{-3}$	24.059	9.091	0.919
	318	59.880	0.044	0.431	0.989	1.419	3.559	0.994	$5*10^{-3}$	26.478	10	0.951

Table (3.25): Adsorption Isotherm Constants of MGox dye on the SD/PANI surface at different pH and Temperatures.

pH	T (K)	Langmuir constants				Freundlich constants			Dubinin and Radushkevich constants			
		q max	K_L	R_L	R^2	n	K_F	R^2	B	q max	E	R^2
pH dye (3.5-4)	298	10.449	0.078	0.299	0.969	2.613	1.996	0.944	$1*10^{-2}$	7.588	7.092	0.862
	308	10.460	0.090	0.270	0.991	2.687	2.170	0.956	$9*10^{-3}$	7.980	7.463	0.960
	318	10.395	0.111	0.231	0.998	2.988	2.581	0.961	$7*10^{-3}$	8.315	8.475	0.984
5	298	5.721	0.107	0.238	0.991	3.421	1.605	0.980	$9*10^{-3}$	4.564	7.463	0.893
	308	8.584	0.082	0.289	0.981	2.680	1.716	0.958	$1*10^{-2}$	6.438	7.092	0.932
	318	12.034	0.064	0.343	0.980	2.202	1.699	0.964	$1*10^{-2}$	8.266	7.092	0.905
9	298	5.659	0.075	0.308	0.993	2.561	1.035	0.958	$1*10^{-2}$	4.270	7.092	0.980
	308	6.083	0.097	0.256	0.986	2.257	1.366	0.902	$1*10^{-2}$	4.910	7.092	0.977
	318	7.418	0.100	0.250	0.991	2.866	1.707	0.909	$1*10^{-2}$	5.983	7.092	0.985

3.4. Thermodynamic parameters:

The adsorption studies for both BTB and MGox dyes solutions were carried out at different temperatures (298, 308, & 318) K and at initial concentration of 30 ppm for BTB and 25 ppm for MGox dyes solutions. Thermodynamic data for adsorption of BTB and MGox dyes solutions on SD and SD/PANI composite are presented in tables (3.26), (3.27), (3.28) and (3.29), respectively. From equation (1.9), the equilibrium constant K for both dyes at different temperature was calculated. The standard enthalpy change (ΔH^o) and entropy change (ΔS^o) values for the adsorption of BTB and MGox

dyes solutions on SD and SD/PANI composite surfaces were determined from the slope and intercept of linear regression between lnK and 1000/Taccording eq. (1.8) as shown in figures (3.37–3.40). Also, the spontaneously of the adsorption process (ΔG^o) was calculated using equation (1.10). The results are given in tables (3.30–3.33). Thermodynamically parameters showed that the adsorption of both dyes is endothermic in nature because the positive value of ΔH^o indicates that adsorption was favorable at higher temperature (318K). The increase in adsorption with increase the temperature may be due to the increase in available active sites on the surface which leads to an enhanced rate of intraparticle diffusion of dyes [114].

Table (3.26): Effect of temperature on thermodynamic equilibrium constant for the adsorption of BTB on SD surface at different pH.

pH	T/K	1000/T	c_o (mg/g)	BTB on SD		
				c_e (mg/g)	K	Ln K
pH dye (3.5-4)	298	3.356	30	11.086	3.412	1.227
	308	3.247	30	10.871	1.258	1.258
	318	3.145	30	10.489	1.314	1.314
3	298	3.356	30	6.224	7.640	2.033
	308	3.247	30	6.161	7.738	2.046
	318	3.145	30	5.538	8.834	2.178
5	298	3.356	30	16.717	1.589	0.463
	308	3.247	30	16.473	1.642	0.495
	318	3.145	30	16.437	1.650	0.501
7	298	3.356	30	20.614	0.910	-0.094
	308	3.247	30	20.506	0.925	-0.077
	318	3.145	30	20.322	0.952	-0.049
9	298	3.356	30	19.668	1.051	0.049
	308	3.247	30	19.586	1.063	0.061
	318	3.145	30	19.553	1.068	0.065
11	298	3.356	30	19.235	1.119	0.112
	308	3.247	30	19.200	1.125	0.117
	318	3.145	30	19.077	1.145	0.135

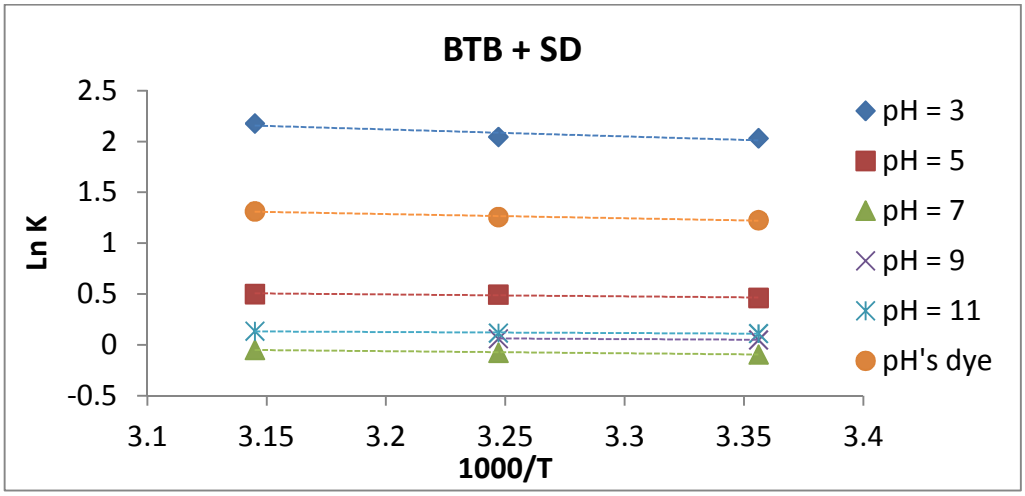

Figure (3.37): The Van't Hoff plot for adsorption of BTB dye on the SD surface at different pH.

Table (3.27): Effect of temperature on thermodynamic equilibrium constant for the adsorption of BTB on SD/PANI surface at different pH.

pH	T/K	1000/T	c_o (mg/g)	BTB on SD/PAN		
				c_e (mg/g)	K	Ln K
pH dye (3.5-4)	298	3.356	30	0.804	72.627	4.285
	308	3.247	30	0.655	89.603	4.495
	318	3.145	30	0.556	105.914	4.663
3	298	3.356	30	4.885	10.282	2.330
	308	3.247	30	4.822	10.443	2.346
	318	3.145	30	4.667	10.856	2.385
5	298	3.356	30	4.496	11.345	2.429
	308	3.247	30	4.142	12.486	2.525
	318	3.145	30	3.971	13.110	2.573
7	298	3.356	30	4.869	10.323	2.334
	308	3.247	30	4.608	11.021	2.400
	318	3.145	30	4.316	11.902	2.477
9	298	3.356	30	8.949	4.705	1.549
	308	3.247	30	8.263	5.261	1.660
	318	3.145	30	7.789	5.703	1.741

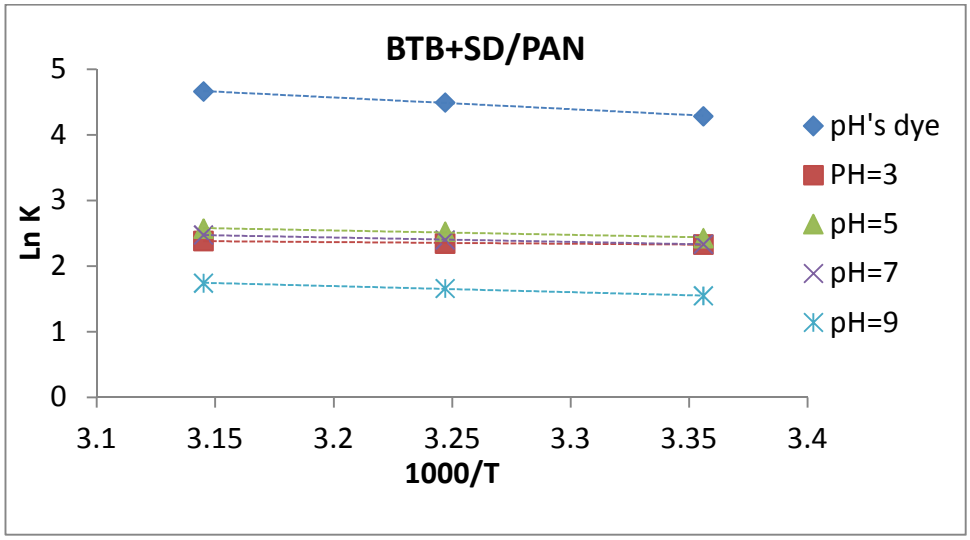

Figure (3.38): The Van't Hoff plot for adsorption of BTB dye on the SD/PANI surface at different pH.

Table (3.28): Effect of temperature on thermodynamic equilibrium constant for the adsorption of MGox on SD surface at different pH.

pH	T/K	1000/T	c_o (mg/g)	MGox + SD		
				c_e (mg/g)	K	Ln K
3	298	3.356	25	17.698	0.495	-0.703
	308	3.247	25	16.917	0.573	-0.557
	318	3.145	25	15.202	0.773	-0.257
pH dye (3.5-4)	298	3.356	25	4.390	5.634	1.729
	308	3.247	25	4.034	6.237	1.830
	318	3.145	25	3.649	7.021	1.949
5	298	3.356	25	1.099	26.097	3.262
	308	3.247	25	0.618	47.343	3.857
	318	3.145	25	0.076	393.526	5.975
7	298	3.356	25	3.091	8.506	2.141
	308	3.247	25	2.825	9.419	2.243
	318	3.145	25	1.859	14.938	2.704
9	298	3.356	25	4.629	5.281	1.664
	308	3.247	25	3.707	6.893	1.931
	318	3.145	25	2.898	9.152	2.214
11	298	3.356	25	13.625	1.002	0.002
	308	3.247	25	11.125	1.497	0.403
	318	3.145	25	9.875	1.838	0.609

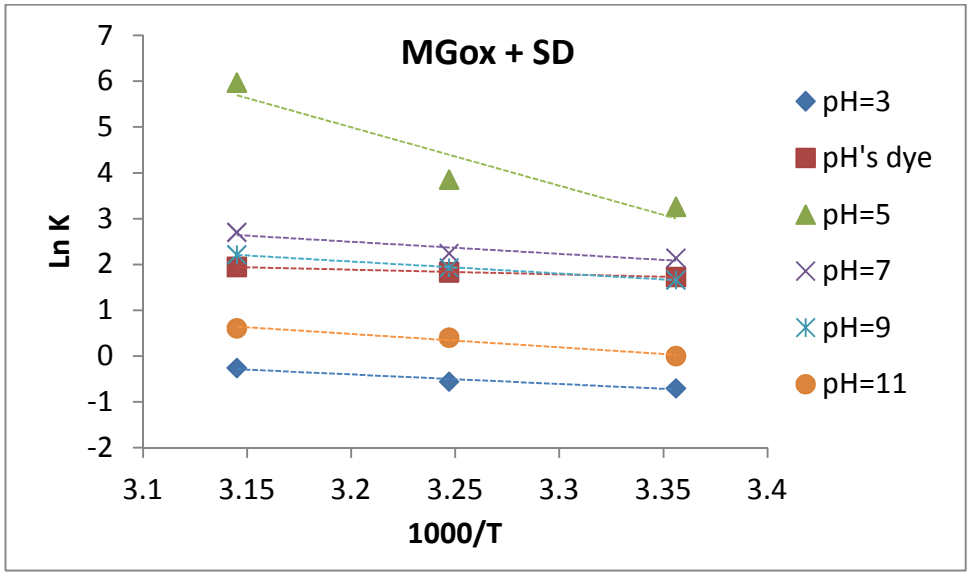

Figure (3.39): The Van't Hoff plot for adsorption of MGox dye on the SD surface at different pH.

Table (3.29): Effect of temperature on thermodynamic equilibrium constant for the adsorption of MGox on SD/PANI surface at different pH.

pH	T/K	1000/T	c_o (mg/g)	MGox + SD/PAN.		
				c_e (mg/g)	K	Ln K
pH dye (3.5-4)	298	3.356	25	20.064	0.295	-1.221
	308	3.247	25	19.441	0.343	-1.070
	318	3.145	25	19.056	0.374	-0.983
5	298	3.356	25	21.701	0.182	-1.704
	308	3.247	25	20.468	0.266	-1.324
	318	3.145	25	19.400	0.346	-1.061
9	298	3.356	25	22.057	0.160	-1.833
	308	3.247	25	21.604	0.189	-1.666
	318	3.145	25	20.827	0.240	-1.427

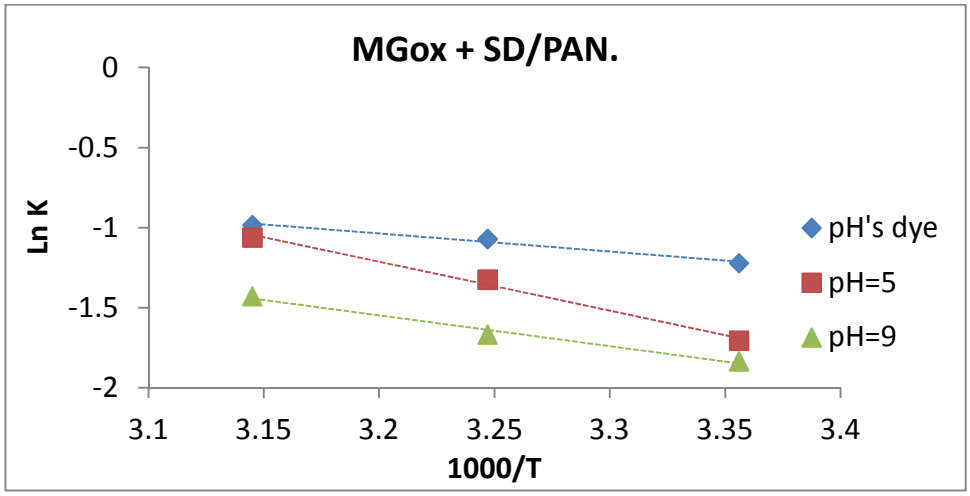

Figure (3.40): The Van't Hoff plot for adsorption of MGox dye on the SD/PANI surface at different pH.

Table (3.30): Thermodynamics parameters for adsorption of BTB dye on SD surface at different pH.

pH	T (K)	ΔH kJ/mol	ΔS J/mol	R^2	ΔG kJ/mol
pH dye (3.5-4)	298	3.417	21.631	0.9667	-3.029
	308				-3.245
	318				-3.462
3	298	5.660	35.733	0.8016	-4.988
	308				-5.346
	318				-5.703
5	298	1.508	8.944	0.8778	-1.157
	308				-1.247
	318				-1.336
7	298	1.767	5.134	0.9748	0.237
	308				0.186
	318				0.134
9	298	0.915	3.479	0.999	-0.122
	308				-0.157
	318				-0.191
11	298	0.900	3.934	0.8922	-0.272
	308				-0.312
	318				-0.351

Table (3.31): Thermodynamics parameters for adsorption of BTB dye on SD/PANI surface at different pH.

pH	T (K)	ΔH kJ/mol	ΔS J/mol	R^2	ΔG kJ/mol
pH dye (3.5-4)	298	14.909	85.703	0.998	-10.63
	308				-11.488
	318				-12.345
3	298	2.157	26.578	0.936	-5.763
	308				-6.029
	318				-6.295
5	298	5.693	39.362	0.971	-6.037
	308				-6.43
	318				-6.824
7	298	5.628	38.275	0.996	-5.778
	308				-6.161
	318				-6.543
9	298	7.577	38.339	0.995	-3.848
	308				-4.231
	318				-4.615

Data presented in tables (3.30) and (3.31) show the calculated values of standard thermodynamic quantities for the BTB dye adsorption on SD and SD/PANI surfaces. Values of ΔH° in the range of 2.1–20.9 kJ mol^{-1} indicate the favorability of physisorption, while when the values within the range 20.9–418.4 kJ mol^{-1} indicate chemisorption [115]. It is very clear from the results of tables that physical adsorption of BTB dye solution on SD and SD/PANI composite surfaces is much more possible. The positive values of ΔH^o indicate the endothermic nature of adsorption process [116]. The negative values of the Gibbs free energy change ΔG^o explained that the adsorption process was spontaneous. Also, the positive values of the entropy ΔS^o refers that the increased randomness at the solid-solute during adsorption process and it may also indicate that ion exchange reactions take place and create steric hindrances [117].

Table (3.32): Thermodynamics parameters for adsorption of MGox dye on SD surface at different pH.

pH	T (K)	ΔH kJ/mol	ΔS J/mol.k	R^2	ΔG kJ/mol
3	298	17.502	52.666	0.954	1.808
	308				1.281
	318				0.754
pH dye (3.5-4)	298	8.658	43.401	0.996	-4.275
	308				-4.710
	318				-5.144
5	298	106.207	381.401	0.893	-7.450
	308				-11.265
	318				-15.079
7	298	22.022	91.199	0.868	-5.155
	308				-6.067
	318				-6.979
9	298	21.659	86.476	0.999	-4.111
	308				-4.976
	318				-5.840
11	298	23.996	80.784	0.973	-0.078
	308				-0.885
	318				-1.693

In table (3.32), the values of ΔG^o (a change of Gibbs free energy) for adsorption of MGox dye solution on SD adsorbent at pH 5 were negative and this indicate the spontaneous nature of adsorption. Increasing the negative values of ΔG^o with an increase in temperature gives better adsorption and a more energetically favorable adsorption. This might be because of the faster movement of solute molecules in the aqueous solution at higher temperatures that increases their absorptivity processed toward the adsorbent surface [118]. The value of ΔH^o was positive referring to the endothermic nature of adsorption and it is greater than 20.9 $kJmol^{-1}$ which means the type of adsorption is chemisorption.

Table (3.33): Thermodynamics parameters for adsorption of MGox dye on SD/PANI surface at different pH.

pH	T (K)	ΔH kJ/mol	ΔS J/mol.k	R^2	ΔG kJ/mol
pH dye (3.5-4)	298	9.403	21.480	0.982	3.002
	308				2.787
	318				2.572
5	298	19.560	54.488	0.993	3.323
	308				2.778
	318				2.233
9	298	15.962	38.213	0.985	4.575
	308				4.192
	318				3.810

Table (3.33) represents the thermodynamic functions for the adsorption of MGox dye solution on SD/PANI composite surface. The positive values of ΔG^o refer to nonspontaneous adsorption process. The small and positive values of ΔH^o indicates the endothermic nature of physisorption process. The positive values of ΔS° presented in the table (3.33) show the increased disorder and randomness of MGox dye adsorbed on SD/PANI adsorbent [119].

3.5. Adsorption kinetics:

The determination of efficiency of adsorption process requires an understanding the kinetic of uptake dyes by adsorbents or the time dependence of the concentration distribution in the solution and identification of the rate determining step. From the studies of contact time effect of BTB and MGox dyes solutions, the adsorption reaches equilibrium after 15 and 20 minutes, respectively. The adsorption kinetics data were evaluated by using pseudo-first, pseudo-second order and intraparticle diffusion model to determine the controlling mechanism of BTB and MGox dyes adsorption from aqueous solution using SD and SD/PANI composite surfaces were shown in tables (3.34) and (3.35) respectively.

Table (3.34): The Adsorption data of q_t and q_e for BTB dye on the SD and SD/PANI surfaces at 298 K.

	t (min)	√time	q_t	q_e	(q_e-q_t)	$Log(q_e-q_t)$	t/q_e
SD	5	2.236	7.986	14.900	6.914	0.840	0.626
	10	3.162	12.778		2.122	0.327	0.783
	15	3.873	14.785		0.115	-0.939	1.015
	20	4.472	14.818		0.082	-1.086	1.350
	25	5	14.835		0.065	-1.187	1.685
SD/PANI	5	2.236	51.858	59.918	8.060	0.906	0.096
	10	3.162	54.776		5.142	0.711	0.183
	15	3.873	57.694		2.224	0.347	0.260
	20	4.472	58.49		1.428	0.155	0.342
	25	5	59.884		0.034	-1.469	0.417

Table (3.35): The Adsorption data of q_t and q_e for MGox dye on the SD and SD/PANI surfaces at 298 K.

	t (min)	√time	q_t	q_e	(q_e-q_t)	$Log(q_e-q_t)$	t/q_t
SD	5	2.236	20.129	26.410	6.281	0.798	0.248
	10	3.162	24.87		1.540	0.188	0.402
	15	3.873	25.596		0.814	-0.089	0.586
	20	4.472	26.366		0.044	-1.357	0.759
	25	5	26.381		0.029	-1.538	0.948
	30	5.477	26.396		0.014	-1.854	1.137
	35	5.916	26.396		0.014	-1.854	1.326
SD/PANI	5	2.236	1.151	7.391	6.240	0.795	4.344
	10	3.162	2.603		4.788	0.680	3.842
	15	3.873	4.721		2.670	0.427	3.177
	20	4.472	6.04		1.351	0.131	3.311
	25	5	6.099		1.292	0.111	4.099
	30	5.477	6.114		1.277	0.106	4.907
	35	5.916	7.355		0.036	-1.444	4.759

3.5.1. Pseudo first order model:

From The Lagergren pseudo-first order equation (1.11) t is the contact time. The adsorption rate constant (k_1) and q_e values were calculated from the plot of log (q_e-q_t) against t as shown in figures (3.41) and (3.42) for

adsorption of BTB and MGox dyes solutions, respectively on SD and SD/PANI composite surfaces.

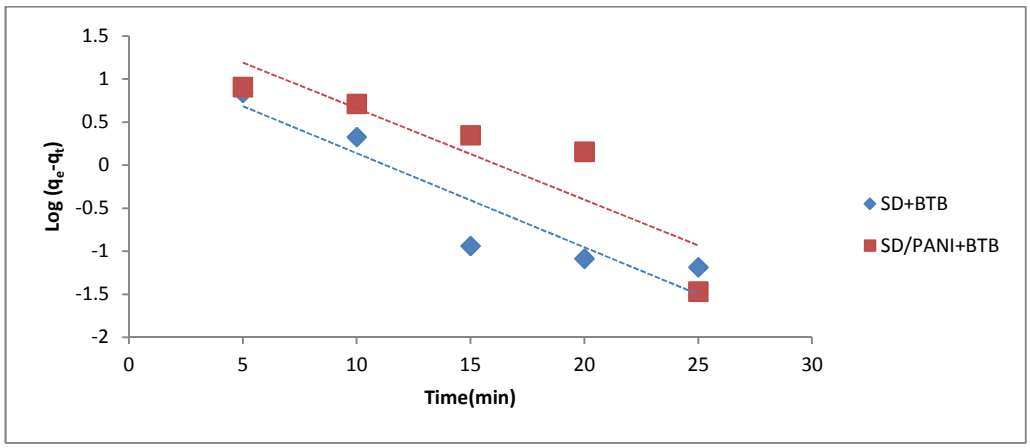

Figure (4.41): The pseudo first order kinetic model to BTB dye on the SD and SD/PANI surfaces.

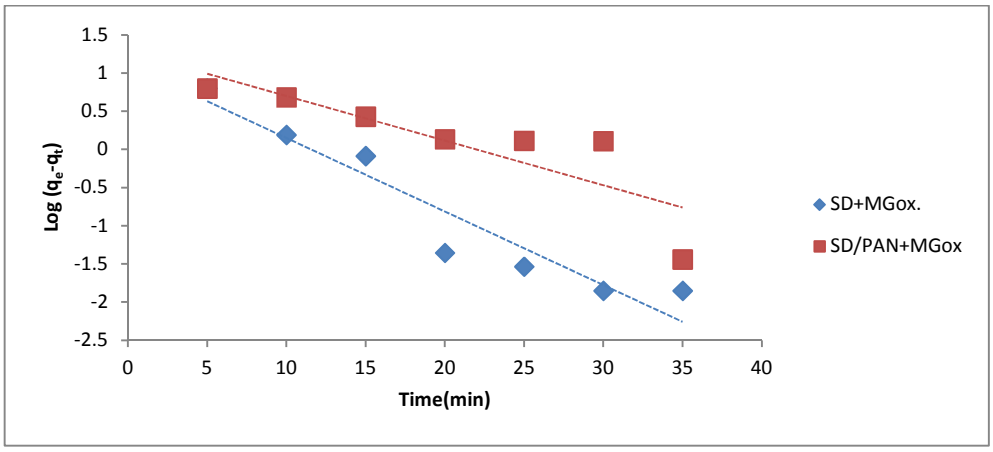

Figure (3.42): The pseudo first order kinetic model to MGox dye on the SD and SD/PANI surfaces.

3.5.2. Pseudo second order model:

The pseudo second order equation (1.15) that clarified previously was used to study the adsorption of both dyes on SD and SD/PANI composite surfaces. Values of q_e and k_2 were estimated from the slope and intercept of the linear plot of t/q_t against t and the corresponding

graphs on both adsorbents are presented in figures (3.43) and (3.44) for BTB and MGox dyes, respectively.

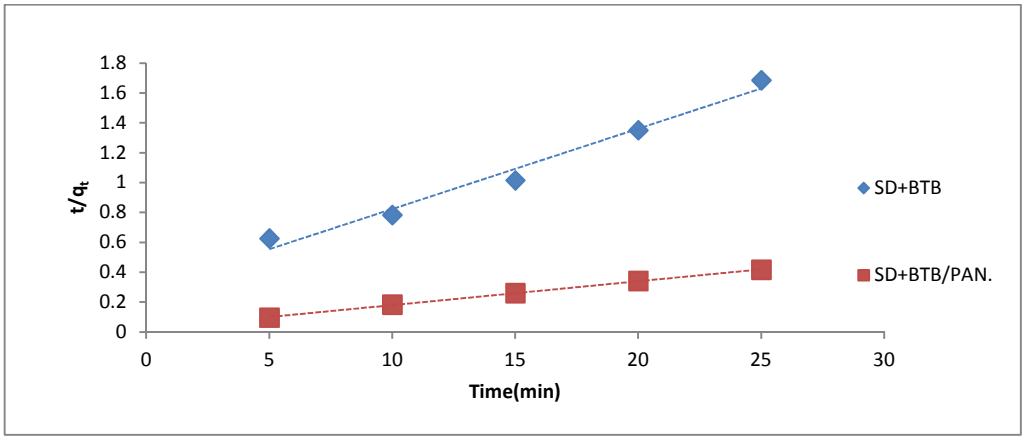

Figure (3.43): The pseudo second order kinetic model to BTB dye on the SD and SD/PANI surfaces.

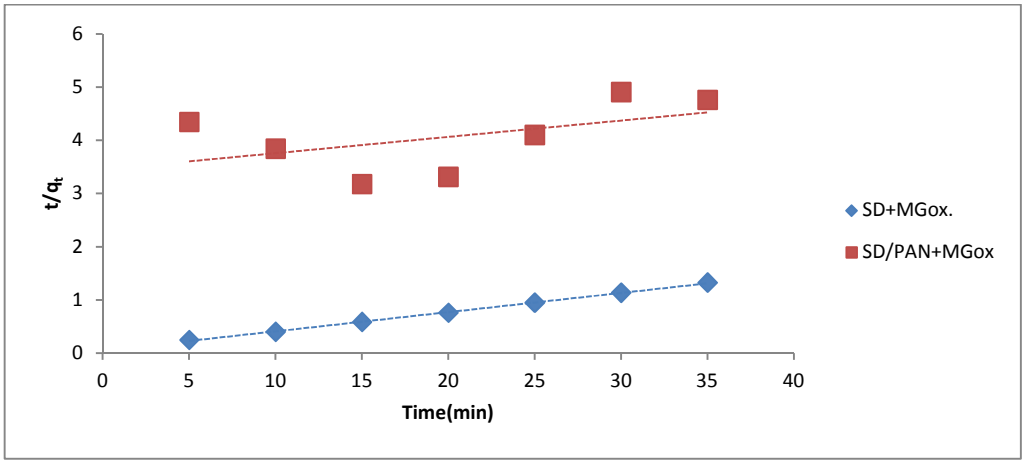

Figure (3.44): The pseudo second order kinetic model to MGox dye on the SD and SD/PANI surfaces.

3.5.3. Intraparticle diffusion model:

The effect of intraparticle diffusion resistance on adsorption of both dyes on SD and SD/PANI surfaces were calculated by using equation (1.16) where C is the intercept and k_D is the diffusion constant of intraparticle diffusion which are determined from the linear plot of q_t versus $t^{1/2}$ as shown in figures

(3.45) and (3.46) for BTB and MGox dyes, respectively. All the data of kinetic studies are presented in table (3.36).

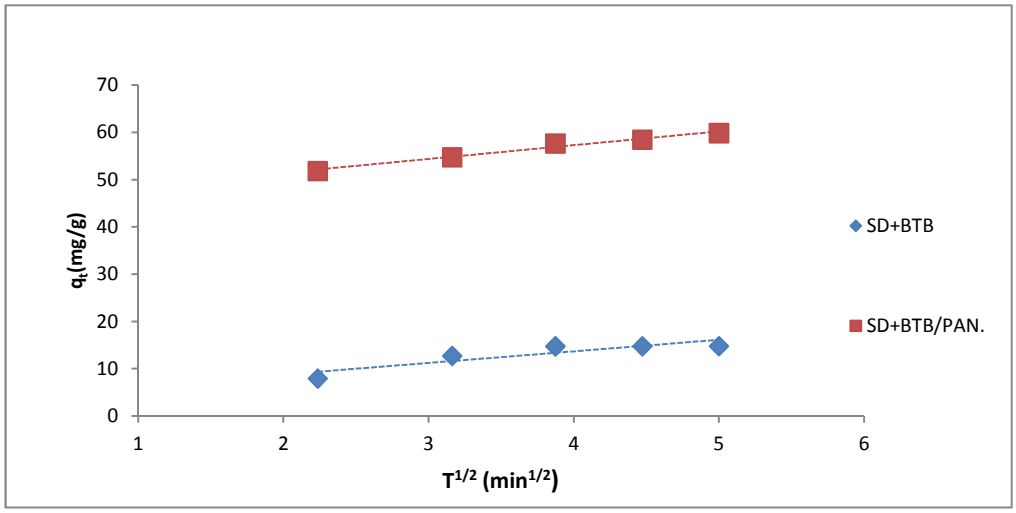

Figure (3.45): The Intraparticle diffusion model to BTB dye on the SD and SD/PANI surfaces.

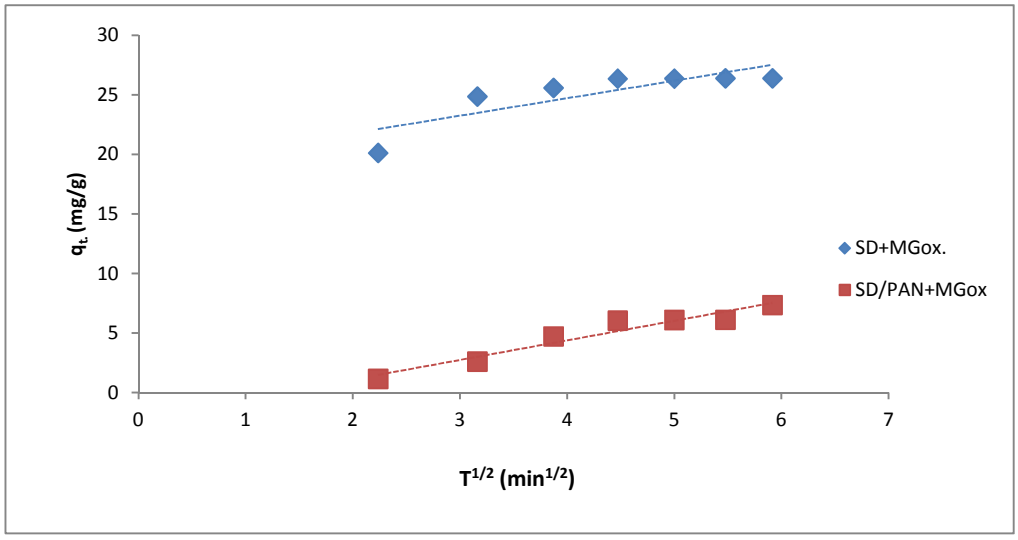

Figure (3.46): The Intraparticle diffusion model to MGox dye on the SD and SD/PANI surfaces.

Table (3.36): Adsorption kinetics constants of BTB (30ppm) & MGox (25ppm) dyes on the SD and SD/PANI surfaces at 298 K.

	Pseudo-first order			Pseudo-second order			Intrapartical diffusion		
	k_1 (L/min)	q_e (mg/g)	R^2	k_2 (mg/g.min)	q_e (mg/g)	R^2	k_D (mg/g.min$^{1/2}$)	C	R^2
BTB									
SD	-0.252	17.026	0.867	0.010	18.622	0.979	2.438	3.902	0.803
SD/PANI	-0.244	52.699	0.794	0.013	62.500	0.999	2.925	45.575	0.980
MGox									
SD	-0.222	12.939	0.914	0.027	27.624	0.999	1.467	18.846	0.6986
SD/PANI	-0.134	19.226	0.722	0.00027	32.573	0.246	1.644	-2.210	0.9369

Examining the results in table (3.36) it can be seen that the adsorption of BTB dye solution on SD and SD/PANI surfaces and the adsorption of MGox dye solution on SD surface, the correlation coefficients (R^2) are much greater fitting with the pseudo second order model which are in the range of 0.979 to 0.999 confirming a very good agreement with experimental data. The best fit to the pseudo second order kinetic indicates that the adsorption mechanism depends on both of the adsorbate and adsorbents [120, 121]. On the other hand, the correlation coefficients (R^2) of the adsorption of MGox dye solution on SD/PANI is fitting with the pseudo first order model. For intraparticular diffusion kinetic study of BTB dye adsorption, the value of C increase from 3.902 to 45.575 and this change in C value attributed to increase in thickness of the boundary layer and decrease the chance of the external mass transfer and subsequently prominent increase in the amount of internal mass transfer [122]. Generally, the adsorption process can pass through three stages: the outer diffusion that is an instantaneous adsorption and is probably due to a strong electrostatic attraction between dye and the external surface of adsorbent. The inner diffusion is a gradual adsorption stage, which can be attributed to diffusion of dye molecules through the pores of adsorbent. The final stage corresponds to the equilibrium adsorption when dye molecules occupy all active sites of the adsorbent so the adsorption process may be

controlled by outer and/or inner diffusion [123]. If the plot of q_t versus $t^{1/2}$ was linear and the straight line passed through the origin then the adsorption rate was controlled by intra-particle diffusion only. Otherwise, the other diffusion mechanism will be joined by intra-particle diffusion [124]. It is clear from figures (3.45) and (3.46) that plots gave straight lines for the dyes on each adsorbent but did not pass through the origin so intra-particle diffusion was not the unique rate-controlling step for the adsorption of BTB and MGox dyes.

4.1. Conclusion:

1. Results proved that SD and SD/PANI adsorbents are very effective in the removal of dyes from aqueous solutions. The effectiveness of SD/PANI greater than the effectiveness of the SD in the removal of BTB dyes from aqueous solutions. On the other hand, the effectiveness of the SD in the removal of MGox dyes from aqueous solution greater than the effectiveness of the SD/PANI adsorbent.
2. The effect of pH investigated for values ranging from 3 to 11, showed maximum removal of BTB on the SD was at pH=3 and on SD/PANI was at pH dye (3.5-4) but the maximum adsorption of MGox on the SD was at pH=5, and on SD/PANI at pH dye (3.5-4).
3. The results of the isotherm adsorption study of the BTB on the surface of SD and SD/PANI showed that the adsorption is subject to the Freundlich isotherm which indicates that the surface of the adsorbent is heterogeneous leads to physical forces (Vander Waals & H-bonding) that occur between the active functional groups in the BTB and adsorbent surface. On the other hand, the adsorption of MGox obeyed to Langmuir isotherm which indicates that the surface of adsorbent is homogeneous leads to chemical bonds between adsorbent and adsorbate.
4. Through thermodynamic functions values (ΔH^o, ΔS^o, ΔG^o) obtained, It is very clear that the positive values of ΔH^o indicate the endothermic nature of adsorption and the negative values of the Gibbs free energy change ΔG^o explained that the adsorption process was spontaneous. Also, the positive values of the entropy ΔS^o refers that the increased randomness at the solid-solute during adsorption process.

5. The kinetic study of the dyes adsorption on the surfaces of SD and SD/PANI showed that the adsorption is obeyed to pseudo second order equation.

Contents

Chapter Two: Materials & Methods

-Table of Abbreviations-

Abbreviations	*Full Name*
AFM	Atomic Force Microscopy
BTB	Bromothymol Blue
B	Dubinin-Radushkevich isotherm constant
C_o	Initial Concentration
C_e	Equilibrium Concentration
ε	Polanyi potential
E	mean free energy
FT-IR	Fourier Transform-Infra Red
ΔG	Gibbs free energy Change
ΔH	Enthalpy change
K	Equilibrium Constant
k_1	Pseudo-First Order Constant
k_2	Pseudo-Second Order Constant
k_D	Diffusion Constant
k_F	Freundlich Constant
k_L	Langmuir constant
λmax	Maximum Absorbance
MGox	Malachite Green oxalate
N	Intensity of adsorption
q_e	Quantity of adsorbate at equilibrium
q_t	Quantity of adsorbate at any time
q_{max}	Maximum monolayer Adsorption Capacity
R^2	Correlation Coefficient
%R	Percentage Removal of adsorbate

R_L	equilibrium parameter or separation factor
R	gas constant
ΔS	Entropy change
SD	Sawdust
SD/PANI	Sawdust coated polyaniline
SEM	Scanning Electron Microscope
T	absolute temperature

-Table of Figures-

-List of Tables-

5.1. References:

1. M. K. Hill, 2004, Understanding Environmental Pollution, the United States of America by Cambridge University Press, New York, P: 239-240.
2. A. Shukla, Y. Zhang, P. Dubey, J.L. Margrave, S. S. Shukla, 2002, The role of sawdust in the removal of unwanted materials from water, Journal of Hazardous Materials, **95**, P: 137-152.
3. M. Rafatullah, O. Sulaiman, R. Hashim, A. Ahmad, 2009, Adsorption of copper (II), chromium (III), nickel (II) and lead (II) ions from aqueous solutions by meranti sawdust, Journal of Hazardous Materials, **170**, P: 969-977.
4. S. Dashamiri, M. Ghaedi, K. Dashtian, M. R. Rahimi, A. Goudarzi, R. Jannesar, 2016, Ultrasonic enhancement of the simultaneous removal of quaternary toxic organic dyes by CuO nanoparticles loaded on activated carbon: Central composite design, kinetic and isotherm study, Ultrasonics Sonochemistry, **31**, P: 546–557.
5. C. Srilakshmi, R. Saraf, 2016, Ag-doped hydroxyapatite as efficient adsorbent for removal of Congo red dye from aqueous solution: Synthesis, kinetic and equilibrium adsorption isotherm analysis, Microporous and Mesoporous Materials, **219**, P: 134-144.
6. M. S. Alam, R. Khanom, M. A. Rahman, 2015, Removal of Congo Red Dye from Industrial Wastewater by Untreated Sawdust, American Journal of Environmental Protection, **4**(5), P: 207-213.
7. F. B. AbdurRahman, M. Akter, M. Z. Abedin, 2013, Dyes Removal from Textile Wastewater Using Orange Peels, International journal of scientific & technology research, **2**(9) P: 47-50.
8. H. Chen, J. Zheo, 2009, Adsorption study for removal of cango red anionic dye using organo-attapulgite, Adsorption, **15**, P: 381-389.

9. B. H. Hameed, A. T. M. Din, A. L. Ahmad, 2006, Adsorption of methylene blue onto bamboo-based activated carbon: Kinetics and equilibrium studies, Journal of Hazardous Materials, **7**(49), P: 1.

10. G. Z. Kyzas, J. F. and K. A. Matis, 2013, The Change from Past to Future for Adsorbent Materials in Treatment of Dyeing Wastewaters, Materials, **6**, P: 5131-5158.

11. J. R. Aspland, 1997, Textile Dyeing and Coloration, 1st addition, Association of Textile Chemists and Colorists, P: 3-310.

12. M. C. Costa, F. B. Mota, A. D. Santos, 2012, Effect of dye structure and redox mediators on anaerobic azo and anthraquinone dye reduction, Quim. Nova, **35**(3), P: 482-486.

13. E. D. Głowacki, G. Voss, L. Leonat, M. I. Vladu, S. Bauer and N. S. Sariciftci, 2012, Indigo and Tyrian Purple – From Ancient Natural Dyes to Modern Organic Semiconductors, Israel Journal Chem. **52**, P: 1 – 12.

14. R. S. Lepkowicz, C. M. Cirloganu, O. V. Przhonska, D. J. Hagan, E. W. V. Stryland, M. V. Bondar, Y. L. Slominsky, A. D. Kachkovski, E. I. Mayboroda, 2004, Absorption anisotropy studies of polymethine dyes, Chemical Physics, **306**, P: 171–183.

15. K. Hunger, 2007, Industrial dyes: chemistry, properties, applications, John Wiley & Sons.

16. R.Christie, 2014, Colour chemistry, 2nd addition, Royal Society of Chemistry.

17. M. Adachi, T. Bredow, K. Jug, 2004, what is the origin of color on metal complex dyes? Theoretical analysis of a Ni-coordinate azo dye, Dyes and Pigments, **63**, P: 225–230.

18. J. Hoffmann, A. Puszynski, Chemical engineering and chemical process technology, Pigments and dyestuffs, Encyclopedia of Life Support Systems (EOLSS).

19. H. Zollinger, 1987, Color Chemistry: Synthesis, Properties and Applications of Organic Dyes and Pigments, 2nd addition, VCH Publishers, New York.

20. K. E. Cheong, 2012, Removal of basic dyes using sugarcane bagasse, M.Sc. thesis, Department of Science, Faculty of Engineering and Science, University Tunku Abdul Rahman.

21. A. Dabrowski, 2001, Adsorption from theory to practice, Advances in Colloid and Interface Science, **93**, P: 135_224.

22. I. Ali, M. Asim, T. A. Khan, 2012, Low cost adsorbents for the removal of organic pollutants from wastewater, Journal of Environmental Management, **113**, P: 170-183.

23. E. Worch, 2012, Adsorption Technology in Water Treatment, Deutsche Nationalbibliothek, P: 1.

24. D. J. Horner, 1999, Adsorption of Selected Herbicides from Water using Activated Carbon and Polymeric Adsorbents, Doctoral Thesis, Philosophy of Loughborough University.

25. C. H. Giles, 1983, Adsorption from Solution at the Solid liquid Interface, Parfitt and Rochester, London.

26. O. Bolland, 2013, TEP03 CO2 capture in power plants Part 4 Absorption, Department of Energy and Process Engineering, Norwegian University of Science and Technology.

27. J. M. Saleh, 1980, Surface Chemistry and Catalyst, 1st addition, Baghdad University Press.

28. A. Bahl, B.S. Bahl, G.D. Tuli, 2015, Essentials of physical chemistry, Multicolour edition, P: 844.

29. E. Qada, E. N, 2008, Adsorption of basic dyes from aqueous solution onto activated carbons, Chemical engineering journal, **135**(3), P: 174-184.

30. S. Brunauer, 1943, the adsorption of gases and vapors, chemist, Bureau of plant Industry United States Department of Agriculture oxford University press, London, P: 4-6.

31. P. A. Webb, 2003, Introduction to Chemical Adsorption Analytical Techniques and their Applications to Catalysis, MIC Technical Publications, Micromeritics Instrument Corp, Norcross, Georgia, P: 1.

32. M.C. John and R.C. Fay, 2001, Chemistry, 3rd addition, Prentice-Hall. Inc. New Jersey, P: 433,511.

33. R. L. Yeh, A. Thomas, 1995, Color difference measurement and color removal from dye wastewaters using different adsorbents, Journal of chemical technology and biotechnology, **63**, P: 55-59.

34. S. N. A. Abas, M. H. S. Ismail, M. L. Kamal and S. Izhar, 2013, Adsorption Process of Heavy Metals by Low-Cost Adsorbent: A Review, World Applied Sciences Journal, **28** (11), P: 1518-1530.

35. N. C. Martinez, J. A. Dumesic, 1992, Applications of Adsorption Microcalorimetry to the Study of Heterogeneous Catalysis, Advances in catalysis, **38**, P: 149.

36. M. R. Rigi, M. Farahbakhsh, and K. Rezaei, 2015, Adsorption and Desorption Behavior of Herbicide Metribuzin in Different Soils of Iran, Journal. Agriculture Science Tech., **17**, P: 777-787.

37. R. E. Majors, D. E. Wilmington, 2013, Sample Preparation fundamentals for chromatography, Agilant technology, P: 160.

38. Y. J. Chan, M. F. Chong, C. L. Law, D. G. Hasse, 2009, A review on anaerobic-aerobic treatment of industrial and municipal wastewater, Chemical engineering journal, **155**, P:1-15.

39. J. Kandasamy, S. Vigneswaran, T.T.L. Hoang, D.N.S.Chaudhary, Adsorption and biological filtration in wastewater treatment, Encyclopedia of Life Support Systems (EOLSS), P: 2.

40. Z. Melichov, L. Hromada, 2013, Adsorption of Pb^{2+} and Cu^{2+} Ions from Aqueous Solutions on Natural Bentonite, Pollution Journal Environmental Study, **22**(2), P: 457-464.

41. A. D. Marczewsk, A. W. Marczewski, 2002, Effect of adsorbate structure on adsorption from solutions, Applied Surface Science, **196**, P: 264–272.

42. A. D. Site, 2001, Factors Affecting Sorption of Organic Compounds in Natural Sorbent/Water Systems and Sorption Coefficients for Selected Pollutants. A Review, Journal Physical Chemistry, **30**, P: 194.

43. S. Mukherjee, A. M. Vannice, 2006, Solvent effects in liquid-phase reactions II. Kinetic modeling for citral hydrogenation, Journal of Catalysis, **243**, P: 131–148.

44. M. A. Fox and M. Dulay, 1993, Heterogeneous Photocatalysis, Chemical Reviews, **93** (1), P: 341-357.

45. S. Agarwal, I. Tyagi, V. K. Gupta, F. Golbaz, A. N. Golikand, O. Moradi, 2016, Synthesis and characteristics of polyaniline/zirconium oxide conductive nanocomposite for dye adsorption application, Journal of Molecular Liquids, **218**, P: 494-498.

46. Y.K. Kumar, H. B. Muralidhara, Y. A. Nayaka, J. Balasubramanyam, H. Hanumanthappa, 2013, Low-cost synthesis of metal oxide nanoparticles and their application in adsorption of commercial dye and heavy metal ion in aqueous solution, Powder Technology, **246**, P: 125-136.

47. S.D. Khattri, M.K. Singh, 2009, Removal of malachite green from dye wastewater using neem sawdust by adsorption, Journal of Hazardous Materials, **167**, P: 1089–1094.

48. D.M. Borrok, J.B. Fein, 2005, The impact of ionic strength on the adsorption of protons, Pb, Cd, and Sr onto the surfaces of Gram

negative bacteria: testing non-electrostatic, diffuse, and triple-layer models, Journal of Colloid and Interface Science, **286**, P: 110-126.

49. D.A. Skoog and D.M. west, 1969, Fundamentals of Analytical Chemistry, 2nd addition, Rinehart and Winstone, Inc., California.

50. L.I Antropov, 1975, Theoretical Electro Chemistry, Mir Publishers, 2nd addition, Moscow.

51. J.C. Kuriacose and J. Rajaram, 1984, Chemistry in Engineering and Technology, **1**, TATA Mcgraw – Hill Pulishing Co. LTD., New Delhi.

52. C. L. Mangun, M. A. Daley, R. D. Braatz and J. Economy, 1998, Effect of pore size on adsorption of hydrocarbons in phenolic-based activated carbon fibers, Carbon, **36** (1-2), P: 123-131.

53. C. H. Giles, D. Smith and A. Hultson, 1973, A general treatment and classification of the solute adsorption isotherm, Journal of colloid and interface science, **47** (3), P: 755-765.

54. C. H. Giles, T. H. Macewans, N. Nakhwa and D. Smith, 1958, Studies in Adsorption Part XI. A System of Classification of Solution Adsorption Isotherms and its Use in Diagnosis of Adsorption Mechanisms and in Measurement of Specific Surface Areas of Solids, Journal Society Dyers Colorists, **74**, P: 846.

55. N. Muhammad et al, 1998, Adsorption of Heavy Metals in Slow Sand Filters, 24th addition, WEDC Conference, Water Treatment. Islamabad, Pakistan, P: 346-349.

56. Dunicz, B. Ludwik, 1961, Surface Area of Activated Charcoal by Langmuir Adsorption Isotherm, Journal Chemical Education, **38**, P: 357.

57. S. Benyoucef, M. Amrani, 2011, Adsorption of phosphate ions onto low cost Aleppo pine adsorbent, Desalination, **275**, P: 231-236.

58. M. Rahimi , M. Vadi, 2014, Langmuir, Freundlich and Temkin Adsorption Isotherms of Propranolol on Multi-Wall Carbon Nanotube,

Journal of modern drug discovery and drug delivery research, **1**, P: 1-3.

59. Y. F. Lam, L. Y. Lee, S. J. Chua, S. S. Lim, S. Gan, 2016, Insights in to the equilibrium, kinetic and thermodynamics of nickel removal by environmental friendly Lansium domesticum peel biosorbent, Ecotoxicology and Environmental Safety, **127**, P: 61-70.

60. S. Tiwari, V. K. Gupta, P.C. Pandey, H. Singh, P.K.Mishra, 2009, Adsorption Chemistry of Oil-in-Water Emulsion from Spent Oil Based Cutting Fluids Using Sawdust of Mangifera indica, Journal International Environmental Application & Science, **4** (1), P: 99-107.

61. S. A. Ahmed, 2011, Batch and fixed-bed column techniques for removal of Cu(II) and Fe(III) using carbohydrate natural polymer modified complexing agents, Carbohydrate Polymers, **83**, P: 1470–1478.

62. J.C Igwe, A.A. Abia, 2007, Adsorption isotherm studies of Cd (II), Pb (II) and Zn (II) ions bioremediation from aqueous solution using unmodified and EDTA-modified maize cob, Ecl. Quím, São Paulo, **32**(1), P: 33-42, 2007.

63. G. Neeraj, S. Krishnan, S. P. Kumar, K. R. Shriaishvarya, V. V. Kumar, 2016, Performance study on sequestration of copper ions from contaminated water using newly synthesized high effective chitosan coated magnetic nanoparticles, Journal of Molecular Liquids, **214**, P: 335–346.

64. A.O Dada, A.P Olalekan, A.M. Olatunya, O. Dada, 2012, Langmuir, Freundlich, Temkin and Dubinin–Radushkevich Isotherms Studies of Equilibrium Sorption of Zn2+ Unto Phosphoric Acid Modified Rice Husk, Journal of Applied Chemistry, **3** (1), P: 38-45.

65. Z. Bekc, Y. Sekia, L. Cavas, 2009, Removal of malachite green by using an invasive marine alga Caulerpa racemosa var. cylindracea, Journal of Hazardous Materials, **161**, P: 1454-1460.

66. V. Gopalakannan, N. Viswanathan, 2016, One pot synthesis of metal ion anchored alginate–gelatin binarybiocomposite for efficient Cr (VI) removal, International Journal of Biological Macromolecules, **83**, P: 450–459.

67. M. V. Subbaiah, D. S. Kim, 2016, Adsorption of methyl orange from aqueous solution by aminated pumpkin seed powder: Kinetics, isotherms, and thermodynamic studies, Ecotoxicology and Environmental Safety, **128**, P: 109–117.

68. R. Acosta, V. Fierro, A. M. Yuso, D. Nabarlatz, A. Celzard, 2016, Tetracycline adsorption onto activated carbons produced by KOH activation of tyre pyrolysis char, Chemosphere, **149**, P: 168-176.

69. A. K. Agarwal, M. S. Kadu, C. P. Pandhurnekar, I. L. Muthreja, 2015, Kinetics study on the adsorption of Ni^{2+} ions onto fly ash, Journal of Chemical Technology and Metallurgy, **50** (5), P: 601-605.

70. M. Bhaumik, R. I. Crindle, A. Maity, S. Agarwal, V. K. Gupta, 2016, Polyaniline nanofibers as highly effective re-usable adsorbent for removal of reactive black 5 from aqueous solutions, Journal of Colloid and Interface Science, **466**, P: 442–451.

71. K.G. Sreejalekshmi, K. A. Krishnanb, T. S. Anirudhan, 2009, Adsorption of Pb(II) and Pb(II)-citric acid on sawdust activated carbon: Kinetic and equilibrium isotherm studies, Journal of Hazardous Materials, **161**, P: 1506–1513.

72. Y. S. Ho, G. M. Kay, 1999, Pseudo-second order model for sorption processes, Process Biochemistry, **34**, P: 451–465.

73. S. Agarwal, H. Sadegh, M. Monajjemi, A. S. Hamdy, G. A. M. Ali, A. O. H. Memar, R. S. ghoshekandi, I. Tyagi, V. K. Gupta, 2016,

Efficient removal of toxic bromothymol blue and methylene blue from wastewater by polyvinyl alcohol, Journal of Molecular Liquids, **218**, P: 191-197.

74. M. H. Dehghani, G. A. Haghighat, K. Yetilmezsoy, G. McKay, B. Heibati, I. Tyagi, S. Agarwal, V. K. Gupta, 2016, Adsorptive removal of fluoride from aqueous solution using single- and multi-walled carbon nanotubes, Journal of Molecular Liquids, **216**, P: 401–410.

75. M. Ghaedi, N. Taghavimoghadam, S. Naderi, R. Sahraei, A. Daneshfar, 2013, Comparison of removal of bromothymol blue from aqueous solution by multiwalled carbon nanotube and Zn(OH)2 nanoparticles loaded on activated carbon: A thermodynamic study, Journal of Industrial and Engineering Chemistry, **19**, P: 1493-1500.

76. M.M. Haque, M. Muneer, 2007, TiO2-mediated photocatalytic degradation of a textile dye derivative, bromothymol blue, in aqueous suspensions, Dyes and Pigments, **75**, P: 443-448.

77. S. S. Tahir, N. Rauf, 2006, Removal of a cationic dye from aqueous solutions by adsorption onto bentonite clay, Chemosphere, **63**, P: 1842-1848.

78. S. Banerjee, M.C. Chattopadhyaya, 2013, Adsorption characteristics for the removal of a toxic dye, tartrazine from aqueous solutions by a low cost agricultural by-product, Arabian Journal of Chemistry, P: 1-9.

79. M. B. Keivani, K. Zare, H. Aghaie and R. Ansari, 2009, Removal of methylene blue dye by application of polyaniline nano composite from aqueous solutions, Journal of Physical and Theoretical Chemistry of Islamic Azad University of Iran, **6** (1), P: 50-56.

80. J. Stejskal, 2002, Polyaniline praperation of a conducting polymer, Pure Appl. Chem., **74** (5), P: 857–867.

81. A. Green, A. E. Woodhead, 1912, Journal Chemical Society, Trans., **101**, P: 1117-1123.

82. S. Shreepathi, 2006, Dodecyl benzene sulfonic Acid: A Surfactant and Dopant for the Synthesis of Processable Polyaniline and its Copolymers, M.Sc. thesis, von der Fakultät für Naturwissenschaften der Technischen Universität Chemnitz.

83. A. Geetha and P. N. Palanisamy, 2015, Kinetics and Equilibrium Studies on The Removal of Anionic Dyes using Polyaniline Coated Sawdust Composite, International Journal of Chem. Tech. Research, **7** (5), P: 2439-2447.

84. A. Geetha, N. Palanisamy, 2015, Advanced Non-Conventional Activated Carbon and Sawdust Coated with Polymers for the remediation of Dye House Effluent, International Journal of Innovative Research in Science, Engineering and Technology, **4**, P: 8335-8338.

85. M. A. K. Hanafiah, S. W. Ngah, S. H. Zolkafly, L. C. Teong, Z. A. Abdul Majid, 2012, Acid Blue 25 adsorption on base treated Shorea dasyphylla sawdust: Kinetic, isotherm, thermodynamic and spectroscopic analysis, Journal of Environmental Sciences, **24**(2), P: 261-268.

86. M. Badu, I. W. Boateng and N. O. Boadi, 2014, Evaluation of adsorption of textile dyes by wood Sawdust, Research Journal of Physical and Applied Sciences, **3** (1), P: 006-014.

87. G. Z. Kyzas, and M. Kostoglou, 2014, Green Adsorbents for Wastewaters: A Critical Review, Materials, **7**, P: 333-364.

88. A. Agalya, P.N. Palanisamy and P. Sivakumar, 2012, Kinetics, Equilibrium studies on removal of ionic dyes using a novel non-conventional activated carbon, International Journal of Chemistry Research, **3** (1), P: 62-68 .

89. R. Gong, M. Feng, J. Zhao, W. Cai, L. Liu, 2009, Functionalization of sawdust with monosodium glutamate for enhancing its malachite green removal capacity, Bio resource Technology, **100**, P: 975–978.

90. J. R. Baseri, P.N.Palanisamy and P.Sivakumar, 2012, Application of Polyaniline Nano Composite for the Adsorption of Acid Dye from Aqueous Solutions, E-Journal of Chemistry, **9** (3), P: 1266-1275.

91. M. R. Patil, V. S. Shrivastava, 2015, Adsorption of malachite green by polyaniline–nickel ferrite magnetic nanocomposite: an isotherm and kinetic study, Appl Nanosci, **5**, P: 809–816.

92. P. K. Baskaran, B. R Venkatraman and S. Arivoli, 2011, Adsorption of Malachite Green Dye by Acid Activated Carbon - Kinetic, Thermodynamic and Equilibrium Studies, E-Journal of Chemistry, **8**(1), P: 9-18.

93. S. D. Khattri, M. K. Singh, 2009, Removal of malachite green from dye wastewater using neem sawdust by adsorption, Journal of Hazardous Materials, **167**, P: 1089-1094.

94. E. Karada, D. Saraydin and O. Guven, 1998, Removal of some cationic dyes from aqueous solution by acrylamide/itaconic acid hydrogels, Water, Air, and Soil Pollution, **106**, P: 369-378.

95. K. Binod, K. Upendra, 2014, Removal of Malachite Green and Crystal Violet Dyes from Aqueous Solution with Bio-Materials: A Review, Global Journal of Researches in Engineering: E Civil And Structural Engineering, **14** (1), P: 51-60.

96. C. Brasquet, B. Rousseau, H. E. Szwarckopf, P. L. Cloirec, 2000, Observation of activated carbon fibers with SEM and AFM correlation with adsorption data in aqueous solution, Carbon, **38**, P: 407-422.

97. J. Singh, N.S. Mishra, U. S. Banerjee, and Y. C. Sharma, 2011, Comparative studies of physical characteristics of raw and modified

sawdust for their use as adsorbents for removal of acid dye, Bio Resoures, **6** (3), P: 2732-2743.

98. D. L. Pavia, G. M. L. George, S. Kriz, 2001, Introduction to spectroscopy, 3rd addition, development of chemistry Western Washington University Bellingham, Washington.

99. P. R. Anizelli, J. P. T. Baú, D. F. Valezi, L. C. Canton, C. E.A. Carneiro, E. Di Mauro, A. C.S. da Costa, D. Galante, A. H. Braga, F. Rodrigues, J. Coronas, C. C. Coterillo, C. T.B.V. Zaia, D. A.M. Zaia, 2016, Adenine interaction with and adsorption on Fe-ZSM-5 zeolites: A prebiotic chemistry study using different techniques, Microporous and Mesoporous Materials, **226**, P: 493-504.

100. A. Geetha and P. N. Palanisamy, 2015, Adsorption of acidic and basic dyes from aqueous solutions using polyaniline coated sawdust as an adsorbent, Journal of Chemical and Pharmaceutical Research, **7**(2), P: 268-274.

101. M. Ghorbani, H. Esfandian, N. Taghipour, R. Katal, 2010, Application of polyaniline and polypyrrole composites for paper mill wastewater treatment, Desalination, **263**, P: 279–284.

102. M.S. Mansour, M.E. Ossman, H.A. Farag, 2011, Removal of Cd (II) ion from waste water by adsorption onto polyaniline coated on sawdust, Desalination, **272**, P: 301–305.

103. J. Vivekanandan, V. Ponnusamy, A. Mahudeswaran and P. S. Vijayanand, 2011, Synthesis, characterization and conductivity study of polyaniline prepared by chemical oxidative and electrochemical methods, Archives of Applied Science Research, **3** (6):147-153.

104. A. E. Ofomaja, E. I. Unuabonah, 2011, Adsorption kinetics of 4-nitrophenol onto a cellulosic material, mansonia wood sawdust and multistage batch adsorption process optimization, Carbohydrate Polymers, **83**, P: 1192-1200.

105. H. Akrout, S. Jellali, L. Bousselmi, 2015, Enhancement of methylene blue removal by anodic oxidation using BDD electrode combined with adsorption onto sawdust, Comptes Rendus Chimie, **18**, P: 110-120.

106. O. Pezoti, A. L. Cazetta, K. C. Bedin, L. S. Souza, A. C. Martins, T. L. Silva, O. S. Júnior, J. V. Visentainer, V. C. Almeida, 2016, NaOH-activated carbon of high surface area produced from guava seeds as a high-efficiency adsorbent for amoxicillin removal: Kinetic, isotherm and thermodynamic studies, Chemical Engineering Journal, **288**, P: 778–788.

107. A. Shamsizadeh, M. Ghaedi, A. Ansari, S. Azizian, M. K. Purkait, 2014, Tin oxide nanoparticle loaded on activated carbon as new adsorbent for efficient removal of malachite green-oxalate: Non-linear kinetics and isotherm study, Journal of Molecular Liquids, **195**, P: 212–218.

108. K. Banerjee, S. T. Ramesh, R. Gandhimathi, P. V. Nidheesh and K. S. Bharathi, 2012, A Novel Agricultural Waste Adsorbent, Watermelon Shell for the Removal of Copper from Aqueous Solutions, Iranica Journal of Energy & Environment, **3** (2), P: 143-156.

109. D. Sud, G. Mahajan, M. P. Kaur, 2008, Agricultural waste material as potential adsorbent for sequestering heavy metal ions from aqueous solutions – A review, Bioresource Technology, **99**, P: 6017–6027.

110. H. Zhang, Y. Tang, X. Liu, Z. Ke, X. Su, D. Cai, X. Wang, Y. Liu, Q. Huang, Z. Yu, 2011, Improved adsorptive capacity of pine wood decayed by fungi Poria cocos for removal of malachite green from aqueous solutions, Desalination, **274**, P: 97–104.

111. M. Lambri, R. Dordoni, A. Silva, D. M. De Faveri, 2013, Odor-active Compound Adsorption onto Bentonite in a Model White Wine Solution, chemical engineering transactions, **32**, P: 1741-1746.

112. V. Dulman, S. M. C. Man, 2006, Sorption of some textile dyes by beech wood sawdust, Journal of Hazardous Materials, **162**, P: 1457–1464.

113. M. Rafatullaha, O. Sulaimana, R. Hashima, A. Ahmad, 2009, Adsorption of copper (II), chromium (III), nickel (II) and lead (II) ions from aqueous solutions by meranti sawdust, Journal of Hazardous Materials, **170**, P: 969–977.

114. H. Kalavathy, B. Karthik, L. R. Miranda, 2010, Removal and recovery of Ni and Zn from aqueous solution using activated carbon from Hevea brasiliensis: Batch and column studies, Colloids and Surfaces B: Biointerfaces, **78**, P: 291–302.

115. A. W. Krowiak, 2011, Analysis of influence of process conditions on kinetics of malachite green biosorption onto beech sawdust, Chemical Engineering Journal,**171**, P: 976– 985.

116. P. K. Baskaran, B. R. Venkatraman, M. Hema and S. Arivoli, 2010, Adsorption studies of copper ion by low cost activated carbon, Journal of Chemical and Pharmaceutical Research, **2** (5), P: 642-655.

117. B.A. Fil, K. Karakasz, R. Boncukuoglu, A. E. Yilmaz, 2013, Removal of cationic dye (basic Red 18) from aqueous solution using natural Turkish clay, Global NEST Journal, **15** (4), P: 529-541.

118. D. Alipoura, A. R. Keshtkarb, M. A. Moosavian, 2016, Adsorption of thorium (IV) from simulated radioactive solutions usinga novel electrospun PVA/TiO2/ZnO nanofiber adsorbent functionalizedwith mercapto groups: Study in single and multi-component systems, Applied Surface Science, **366**, P: 19-29.

119. R. Prabakaran, S. Arivoli, 2012, Adsorption kinetics, equilibrium and thermodynamic studies of Nickel adsorption onto Thespesia Populnea bark as biosorbent from aqueous Solutions, European Journal of Applied Engineering and Scientific Research, **1** (4), P: 134-142.

120. C. Srilakshmi, R. Saraf, 2016, Ag-doped hydroxyapatite as efficient adsorbent for removal of Congo red dye from aqueous solution: Synthesis, kinetic and equilibrium adsorption isotherm analysis, Microporous and Mesoporous Materials, **219**, P: 134-144.

121. S. M. Sayyah, A. A. Essawy, A. M. El-Nggar, 2015, Kinetic studies and grafting mechanism for methyl aniline derivatives onto chitosan: Highly adsorptive copolymers for dye removal from aqueous solutions, Reactive and Functional Polymers, **96**, P: 50-60.

122. M. Ghaedi, H. Z. Khafri, A. Asfaram, A. Goudarzi, 2016, Response surface methodology approach for optimization of adsorption of Janus Green B from aqueous solution onto ZnO/Zn(OH)2-NP-AC: Kinetic and isotherm study, Spectrochimica Acta Part A: Molecular and Biomolecular Spectroscopy, **152**, P: 233-240.

123. A. Ahmada, M. Rafatullahb, O. Sulaimanb, M. H. Ibrahima, R. Hashim, 2009, Scavenging behaviour of meranti sawdust in the removal of methylene blue from aqueous solution, Journal of Hazardous Materials, **170**, P: 357-365.

124. F. Yu, S. Sun, S. Han, J. Zheng, M. Jie, 2016, Adsorption removal of ciprofloxacin by multi-walled carbon nanotubes with different oxygen contents from aqueous solutions, Chemical Engineering Journal, **285**, P: 588-595.

Summary

In this research the effectiveness of sawdust SD and Sawdust coated polyaniline SD/PANI composite, which is one of the environmentally friendly materials, cheap and available in very large quantities were testing to remove the bromothymol blue BTB and malachite green oxalate MGox dyes as chemical contaminants for industrial bio-waste water using Batch Adsorption technique. The adsorbents surfaces were diagnosed by using Fourier Transmission Infrared Spectroscopy (FTIR), Scanning Electron Microscopy (SEM), Atomic Force Microscopy (AFM), and UV-visible Spectroscopy to measure the adsorption capacity. The particle size of SD and SD/PANI composite surfaces were measured by particle size analyzer and the results of surface area of SD (0.8164) and SD/PANI (2.7325) m^2 /g. This was due to the addition of polyaniline that led to increase the surface area of the sawdust and thus to increase their efficiency in the removal of the dyes.

The adsorption properties of both adsorbents in the removal of dyes include the study of several factors on the adsorption process, which are contact time, the quantity of adsorbent, pH and temperature. It was found that the maximum removal of BTB is 49% and 99% at 15 minute on the surface of each of SD and SD/PANI composite, respectively while the maximum removal of MGox dye at 20 minute is 88% and 20% on the surface of each of the SD and SD/PANI composite, respectively. The rate of removal of dyes increases with increasing the adsorption time until reaches to the equilibrium time. The obtained results represented that the appropriate weight to remove BTB is (0.015)g and the percentage removal reaches to (69% and 97%) for each of SD and SD/PANI composite respectively. On the other hand, the suitable weight to remove

the MGox is (0.025)g and the percentage removal reaches to (84% and 18%) for each of SD and SD/PANI composite, respectively.

By studying the pH (3, 5, 7, 9, 11) effect at different temperatures (298, 308, 318)K, it was found that the highest percentage removal of BTB on the surface of SD reaches to 81% when pH = 3 and on the surface of SD/PANI composite the maximum percentage removal of dye reaches to 98% at the original pH of dye (3.5-4), and found a higher percentage removal of MGox dye on the surface of SD reaches to 99% at pH = 5 and on the surface of SD/PANI composite the percentage removal does not exceed 30% at the original pH of dye (3.5-4).

From the analysis of the results of adsorption both BTB and MGox dyes on surfaces each of SD and SD/PANI composite by using Langmuir, Freundlich and Dubinin-Radushkevich isotherms, the results showed that Freundlich isotherm model is best suited to represent the adsorption of BTB dye and Langmuir isotherm model to represent the adsorption of MGox dye.

In addition, the thermodynamics parameters (ΔH^o, ΔS^o, ΔG^o) represented that the percentage removal increase with increase the temperature which indicate that the adsorption is endothermic process. The negative values of ΔG^o show that the process is spontaneous. Positive values of ΔH^o indicate an endothermic process in nature and indicating that the process occurs is physical adsorption in the adsorption of BTB because the values of ΔH^o less than 20.9 kJ / mol but the process is chemical adsorption in the adsorption of MGox because the values of ΔH^o more than 20.9 kJ/mol. The positive values of ΔS^o indicate an increase randomly system and from the negative values of ΔG^o found that spontaneous interaction where increases with increasing temperatures. Adsorption Kinetic study was found to follow a pseudo-second order rate expression for BTB dye on the surface of SD and SD/PANI composite

and for MGox dye on SD. On the other hand, the adsorption kinetic study was found to follow a pseudo-first order rate for MGox on SD/PANI composite.

Supervisor Certification

I certify that this thesis was prepared by “Abeer Erfan Adnan” under my supervision at the College of science/ Al-Nahrain University, as a partial fulfillment of the requirement for the Degree of Master of Science in chemistry.

Signature:

Name: **Dr. Taghried A. Salman**

Scientific Degree: **Assistant Professor**

Date: / /2017

****

In view of the available recommendation, it forwards this **thesis** for debate by the examining committee.

Signature:

Name: **Dr. Emad Al-Sarraj**

Scientific Degree: **Professor**

Title: **Head of Chemistry Department**

Date: / / 2017

Committee Certification

We, the examining committee certify that we have read this thesis entitled "**Adsorption of Dyes from Aqueous Solution Using Sawdust Coated with Polymers**" and examined the student " **Abeer Erfan Adnan** " in its contents and that in our opinion, it is accepted for the Degree of Master of Science, in Physical Chemistry.

Signature:
Name: **Dr. Taki A. Himdan**
Scientific Degree: Professor
Date: / /
(Chairman)

Signature:
Name: **Dr. Souad Abd Mousa**
Scientific Degree: Assistant Professor
Date: / /
(Member)

Signature:
Name: **Dr. Shatha Fadil AL-Saidi**
Scientific Degree: Assistant Professor
Data: / /
(Member)

Signature:
Name: **Dr. Taghried A. Salman**
Scientific Degree: Assistant Professor
Date: / /
(Member/**Supervised**)

****

I, hereby certify upon the decision of the examining committee.
Signature:
Name: **Dr. Hadi M.A. Abood**
Scientific Degree: Professor
Title: Dean of College of Science
Date: / /

إهداء

إلى النور الذي ينير لي درب النجاح... أبي

ويا من علمتني الصمود مهما تبدلت الظروف... أمي

إلى من كانوا يضيئون لي الطريق ويساندوني ويتنازلون عن حقوقهم لإرضائي

والعيش في هناء... إخوتي

الى اساتذتي وكل من أضاء بعلمه عقل غيره أو هدى بالجواب الصحيح حيرة سائليه

فأظهر بسماحته تواضع العلماء وبرحابته سماحة العارفين.

الى من وقف بجانبي زميلاتي (مياسة عصام، الاء بدر، الاء رزاق).

عبير

Acknowledgment

First and before anything, I want to thank Allah for standing by my side. And I would like also to express my deepest thanks and appreciation to my supervisor, **Dr. Taghried Ali Salman** for suggesting the project, her guidelines and advice during the development of this work.

I want to express my thanks and appreciation to the staff of the Department of Chemistry in Colloge of Science / Al-Nahrain University especially of **Dr. Nasreen Raheem Jber** for their help in supporting this project.

-الخلاصه-

أختبرت فعالية نشارة الخشب الطبيعية و المحسنة بواسطة البولي انلين و التي تعتبر من المواد الصديقة للبيئه ورخيصة الثمن ومتوفرة بكميات كبيرة جدا لازالة صبغه البروموثيمول الزرقاء والمالكيت اوكزالات الخضراء كملوثات كيميائية لمياه الصرف الصناعي والحيوي باستخدام تقنية الامتزاز بالوجبة (Batch Adsorption) . تم تشخيص السطوح المازة باستخدام تقنيات طيف الاشعة تحت الحمراء (FTIR)، المجهر الالكتروني الماسح (SEM)، و مجهر القوة الذرية (AFM) وجهاز مطيافية الاشعة الفوق البنفسجية – المرئية (UV-visible) لمتابعة سعة الامتزاز من خلال قياس الامتصاصيه. ومن خلال جهاز قياس المساحه السطحيه تم حساب المساحه السطحيه لنشارة الخشب المعالجه والمحسنة بالبولي انلين وكانت النتائج كما يأتي, (0.8164) م2/غم لنشارة الخشب المعالجه اما لنشارة الخشب المحسنة بالبولي انلين (2.7325) م2/غم ويعزى ذلك الى ان اضافة البولي انلين ادت الى زيادة المساحة السطحية لنشارة الخشب وبالتالي الى زيادة كفائتها في ازالة الصبغة. كما تم دراسة تأثير عدة عوامل على عملية الامتزاز والتي تشمل زمن الاتزان، كمية الماده المازة، الدالة الحامضية للمحاليل و درجة الحراره.

و لقد وجد ان اقصى نسبة ازالة لصبغة البروموثايمول الزرقاء عند زمن الاتزان 15 دقيقة هي 49% و 99% على سطح كل من نشارة الخشب المعالجه ونشارة الخشب المحسنة بالبولي انلين على التوالي, اما اقصى نسبة ازاله لصبغة المالكيت اوكزالات الخضراء عند زمن الاتزان 20 دقيقه هي 88% و 20% على سطح كل من نشارة الخشب المعالجه ونشارة الخشب المحسنة بالبولي انلين على التوالي. ووجد ان نسبة الازاله تزداد مع زيادة زمن الامتزاز الى حين وصوله الى زمن الاتزان. من جهة اخرى تم ايجاد الوزن المناسب لكل من نشارة الخشب المعالجه والمحسنة بالبولي انلين حيث وجد ان الوزن المناسب لازاله صبغة البروموثايمول الزرقاء هي (0.015) غم بنسبه تصل الى (69% و 97%) لكل من نشارة الخشب المعالجه والمحسنة بالبولي انلين على التوالي, ولازالة صبغة المالكيت اوكزالات الخضراء هي (0.025) غم بنسبه تصل الى (84% و 18%) لكل من نشارة الخشب المعالجه والمحسنة بالبولي انلين على التوالي.

من خلال دراسة الداله الحامضيه (3, 5, 7, 9, 11) وباختلاف درجات الحرارة (298, 308, 318) كلفن وجد ان اعلى نسبة مئوية لازالة صبغه البروموثيمول الزرقاء على سطح نشارة

الخشب المعالجه بنسبة 81% عند الدالة الحامضية PH=3 وعلى سطح نشارة الخشب المحسنة بالبولي انلين بنسبة 98% عند الدالة الحامضية الاصلية للصبغة (3.5-4), ووجد اعلى نسبة ازاله لصبغة المالكيت اوكزالات الخضراء على سطح نشارة الخشب المعالجه بنسبة 99% عند داله الحامضيه pH=5 وعلى سطح نشارة الخشب المحسنة بالبولي انلين بنسبة لا تتجاوز 30% عند داله الحامضيه الاصليه للصبغه (3.5-4).

تم تحليل نتائج امتزاز صبغة البروموثيمول الزرقاء على سطوح نشارة الخشب المحسنة و المعالجة باستخدام ايزوثيرمات لانكماير فريندلج ودبنن واظهرت النتائج ان ايزوثيرم فريندلج هو الانسب لتمثيل عملية الامتزاز لصبغة البروموثايمول الزرقاء وايزوثيرم لانكموير لتمثيل عملية الامتزاز لصبغة المالكيت اوكزالات الخضراء.

بالاضافة الى ذلك تم حساب الدوال الثرموديناميكية المتمثلة بقيم ΔH^o و ΔS^o من خلال تطبيق معادلة فانت-هوف والتغير بالطاقة الحرة ΔG^o من خلال تطبيق معادلة جبس وقد وجد ان زيادة نسبة امتزاز الصبغه تزداد مع زيادة درجات الحراره اي ان التفاعل ماص للحراره. وتم معرفة نوع تفاعل الامتزاز من خلال قيم ΔH^o حيث انه اذا كانت القيم ضمن المدى من 2.1 الى 20.9 كيلوجول/ المول فهذا يدل على ان الامتزاز فيزيائي كما في صبغة البروموثايمول الزرقاء اما اذا كانت القيم تتراوح بين 20.9 الى 418.4 كيلوجول/ المول مما يدل على ان الامتزاز كيميائي كما في صبغة المالكيت اوكزالات الخضراء اما قيم ΔS^o الموجبه فتشير الى زيادة بعشوائية النظام ومن خلال قيم ΔG^o السالبة وجد ان التفاعل تلقائي حيث التلقائية تزداد مع زيادة درجات الحرارة. ومن خلال الدراسة الحركية لعملية الامتزاز وجد ان امتزاز كلا الصبغتين على سطح نشارة الخشب المعالج والمحسن يخضع لمعادلة المرتبة الثانية الكاذبة.

جمهورية العراق
وزارة التعليم العالي والبحث العلمي
جامعة النهرين
كلية العلوم
قسم الكيمياء

دراسة امتزاز بعض الصبغات باستخدام نشارة الخشب المغطاة بالبوليمر

رساله

مقدمة الى كلية العلوم / جامعة النهرين

كجزء من متطلبات نيل درجة الماجستير في علوم الكيمياء

من قبل

عبير عرفان عدنان

بكالوريوس ٢٠١٢

باشراف

الاستاذ المساعد الدكتوره

تغريد علي سلمان

جمادى الثاني
١٤٣٨ هـ

اذار
٢٠١٧م

Republic of Iraq
Ministry of Higher Education
and Scientific Research
Al-Nahrain University
College of Science
Department of Chemistry

Adsorption of Dyes from Aqueous Solution Using Sawdust Coated with Polymers

AThesis

Submitted to the College of Science Al- Nahrain University as a partial fulfillment of the requirement For the Degree of Master of Science in Chemistry.

By

Abeer Erfan Adnan

B.Sc.Chemistry/ College Science/Al.Nahrain University

Supervised by

Dr.Taghried Ali Salman.

(Asst. Prof.)

March 2017 1438